EPHRIN-B SIGNALING IN CALVARIAL BONE FORMATION

A Dissertation

by

RAJAY A. D. KAMATH

Submitted to the Graduate and Professional School of
Texas A&M University
in partial fulfillment of the requirements for the degree of

DOCTOR OF PHILOSOPHY

Chair of Committee,	M. Douglas Benson
Committee Members,	Lynne A. Opperman
	Jian (Jerry) Q. Feng
	Hu Zhao
	Xiaohua Liu
	Reginal W. Taylor
Head of Department,	Lynne A. Opperman

August 2021

Major Subject: Oral Biology

ABSTRACT

Skeletal growth deficiencies arising from birth defects, injury or disease exist despite advances in therapy; as a public health imperative, this reflects the need for a deeper understanding of its causes. The molecular mechanisms underlying bone growth are complex, however, the exact mechanism remains unclear. It is well known that the craniofacial skeleton forms from the neural crest, with the parietal bones forming from paraxial mesoderm. The cranial vault consists of the frontal and paired parietal bones, and interposed between them are sutures that, together with the periosteum, serve as active sites of osteogenesis during skull growth and repair. Interactions between the cranial sutures and periosteum are complex and involve a network of signaling pathways that determine mesenchymal lineage fate specification. Ephrins and their Eph-kinases constitute a unique signaling system in calvarial growth and morphogenesis, and mutations in genes encoding these proteins frequently result in craniosynostosis. First reported in 1987, Eph kinases total 14 and their ligands or 'ephrins' total 8 in the mammalian vertebrate. Of interest to us are the transmembrane B-ephrins that mediate diverse cell-cell contact-dependent events such as cell migration, tissue boundary formation during osteogenesis and axon guidance through 'forward' signaling into Eph-kinases; ephrins also act as 'receptors' to which Eph-kinases bind in a process termed 'reverse' signaling. Ephrin-B1 is crucial in mouse development, as its ablation causes skeletal defects arising from defective migration of neural crest and mesenchymal precursors, findings consistent with human CFN syndrome caused by mutations in

ephrin-B1. This ligand is also critical in BMSC differentiation into osteoblasts via upregulation of Osterix. Ephrin-B2 forward signaling promotes osteoblast differentiation and, via hormone-mediated effects, promotes OB maturation and bone formation through ephrin-B2 upregulation in OBs themselves. We observed ephrin-B2 in the cranial sutures/ periosteum and its upregulation at sites of injury to the adult parietal calvaria; further, recombinant ephrin-B2 dramatically increased bone mass in embryonic calvaria, implying anabolic roles for this ligand in bone. Moreover, in the developing embryonic calvaria, the combined ablation of ephrin-B1/B2 in Axin2 suture stem cell niche dramatically impaired calvarial bone growth suggesting that these ephrins work together in regulating the niche.

DEDICATION

I'd like to dedicate this work to my Mum and Dad who have given me all the encouragement, love and support I needed to get to this stage in my life. I owe it all to them!

My heartfelt gratitude to my older brothers Ajay, Vijay and Sujay Kamath and their wives Sunithi, Anne and Jyotsna for their moral support, guidance and love during my 7-year journey as a PhD graduate student at Texas A&M University College of Dentistry.

Most of all, I express my wholehearted appreciation and gratitude to my wife, Annie, for her love and support and extreme resilience during these 7 years while we were apart; to my son, Ashwin, who's been a source of inspiration and strength to me and without whom this would never have been possible. I attribute my success to him!

I'm sincerely appreciative and thankful to my Mother-in-law, Mrs. Valsa A. Anthony for her ardent support and patience all along, and to my Father-in-law, Mr. Anthony Francis, for believing in me even when times were difficult; without them, this important milestone would never have come about. I'm most grateful!

Finally, my gratitude to all my Aunts and Uncles on both my Mum's and Dad's side for the encouragement, love and support given to me since my arrival in the United States and beyond.

ACKNOWLEDGEMENTS

I would like to thank my Committee Chair and Mentor, Dr. M. D. Benson, for his unconditional support and guidance during the 7 years that I worked in his lab, and for the numerous chances given to me to prove myself throughout the course of my research, owing to the belief he had in me. I personally wish to thank my Regents Professor and Interim Dean, Dr. Lynne A. Opperman, for her encouragement and unwavering support, and impetus in preparing me especially during the last year of my research. I also wish to express my gratitude to my Graduate Faculty Member, Dr. Jerry Q. Feng, for his immense patience, support and dedication right through my project. He instilled in me the belief that "Project data are your best teachers; they speak to you!" My heartfelt appreciation to my Co-mentor, Dr. Hu Zhao, for his knowledge and guidance, especially during the final year of my PhD, to my Associate Professor of Orthodontics, Dr. Reginald W. Taylor, for taking time off his busy schedule to guide me on my project, and to my First Teacher, Dr. Xiaohua Liu, for his patience, support and commitment to my work.

I wish to thank Dr. Chunlin Qin and M/s. Suzhen Wang for their moral support during my 7-year stay at Texas A&M University College of Dentistry. A word of sincere appreciation to Dr. Hua Zhang for her prompt and timely assistance with H/E microscopy in preparation for all my lab and committee meetings. My heartfelt gratitude to Dr. Philip Kramer for his unconditional support in my project, and timely assistance with epifluorescence microscopy during the performance of my immunofluorescence

experiments. A note of appreciation to Dr. L. Bruno Ruest for imparting a few 'tricks' of the trade; those were of great help to me! A word of gratitude to Dr. Allen Honeyman who made me understand that there's more to life than research, though its equally important to be focused and motivated in one's profession, and to Connie Tilburg for her kind assistance with histology. A special note of appreciation and gratitude to my senior colleague and friend, Dr. Shaun. M. Logan, for being there every step of the way, especially during my lows! She helped me understand that "Failure will always be a part of science but let not the fear of failure defeat you. Believe in yourself; that's what makes a great scientist!" My appreciation and gratitude go out to Dr. Larry Ballinger for introducing me to the PhD curriculum, to Dr. Paul Dechow for sharing insights into the basics of bone biology, and to Dr. Peter Buschang and Dr. Emmet Schneiderman for assisting me with my research statistics.

Research cannot advance without friends and colleagues who play a huge role in its success. My special thanks and gratitude to my best friend and philosopher, Dr. Priyam H. Jani for his encouragement, timely help and valuable support along the way. My sincere appreciation goes out to each of my colleagues – seniors and juniors – especially – Dr. Chi Ma, Dr. Yan Jing, Dr. Yinshi Rene, Dr. Jun Wang, Dr. Yating Yi, Dr. Chunmei Xu, Dr. Leslie Pryor, M/s. Isra Ibrahim, Dr. Maria Serrano, Dr. Jaya Aseervatham, Dr. Gokul Gopinath and Dr. Crystal P. Stinson, Taha Azimai, Dr. Tian Liang (Mickey), Dr. Mirali Pandya, Dr. Neelam Ahuja, Dr. Pavani V. K., Dr. Hui Shui, Mr. Jason, and Mr. Mahesh, and last but definitely not the least Dian Jing, Zexi Chen, Dr. Ke Wang, Dr. Wenjing Lui (Abbey), Dr. Bei Chang and Yeuija Deng – for making

my stay at Texas A&M University College of Dentistry one of the most rewarding and liberating experiences of my life.

My appreciation and gratitude to the Department Faculty and Staff, especially M/s. Nancy Anthony, M/s. Jean, M/s. Darla Benson, and M/s. Marge Palma for their timely assistance in getting me prepared for this important moment in my life – June 11, 2021 – the day I defended my PhD thesis. I also wish to thank M/s. Sophie and Meghann for assisting me on the administrative front, seeing to it that things went smoothly right till the end. I personally wish to thank M/s. Lilin Xiang for her guidance and support during the initial years of my research in the lab – she did teach me the basics and that helped me churn out the massive body of data needed for my thesis defense. My appreciation goes out to M/s. Yiqing Zhang for her assistance during the primary phases of my research and for tolerating my many mistakes in the lab; she helped me become a better person. How could I forget – M/s. Mary and M/s. Ying – for their tremendous patience in taking me through microCT and Scanning Electron Microscopy during the initial phase of my research, and Mary for assisting me with the VLS Scanner in preparation for my thesis proposal. Last but definitely not the least, a big thank you to M/s. Priscilla Hall and Mr. Gerald Hill for assisting me with my mice and taking care of them while I was away on work or vacation, and to M/s. Willie May for giving me a safe lab environment to work in every day. Lastly, I thank Mr. Richard Cardenas who has been of great help to me, especially during the period of lapse in my immigration status.

A word of appreciation and gratitude to my International Student Advisor, M/s. Kimberly Luttman, for her steadfast guidance and vigilance in student immigration

affairs before and during my period as a research trainee at Texas A&M University College of Dentistry, especially when I risked deportation from the USA in 2020 Fall when my employment and legal visitor status expired due to oversight. Without her prompt and timely assistance, I would never have been able to complete my PhD.

Above all, and with profound humility, I thank God for blessing me with the opportunity to study in one of America's most prestigious universities – Texas A&M University, College Station, Texas, and for giving me all the wonderful people who made a tremendous difference to my life!

CONTRIBUTORS AND FUNDING SOURCES

This work was supervised by a dissertation committee consisting of Committee Chair, Dr. M. Douglas Benson and Committee Members, Dr. Lynne A. Opperman, Dr. Jian (Jerry) Q. Feng, Dr. Hu Zhao and Dr. Xiaohua Liu of the Department of Biomedical Sciences and Dr. Reginald W. Taylor, Associate professor of the Department of Orthodontics.

The data analyzed for Chapter 3 was provided by Dr. M. D. Benson. The analyses depicted in Chapter 4 were conducted in part by Dr. Lynne A. Opperman, Dr. Jian Q. Feng, Dr. Hu Zhao and Dr. Xiaohua Liu of the Department of Biomedical Science and Dr. Reginald W. Taylor.

All other work conducted for the dissertation was completed by the student independently.

Graduate study was supported by the Office of Research and Graduate Studies Texas A&M University and a dissertation research fellowship from the Baylor Oral Health Foundation.

This work was also made possible in part by the National Institute of Dental and Craniofacial Research, a branch of the National Institutes of Health, under Grant Number R01DE022804. Its contents are solely the responsibility of the authors and do not necessarily represent the official views of the National Institutes of Health or the National Institute of Dental and Craniofacial Research.

NOMENCLATURE

FB	Frontal Bone
PB	Parietal Bone
CS	Coronal Suture
SS	Sagittal Suture
LS	Lambdoid Suture
SOB	Supra-Occipital Bone
IFS	Inter-Frontal Suture
EB1/EB2	Ephrin-B1/ Ephrin-B2
LoxP	Locus of X(cross)-over in P1
CFNS	Craniofrontonasal Syndrome
Ob	Osteoblast
Oc	Osteoclast
IF	Immunofluorescence
GFP	Green Fluorescent Protein
MAR	Mineral Apposition Rate
μCT	Micro Computerized Tomography
sEB2/EphB4	soluble clustered ephrin-B2/EphB4
rtta	reverse tetracycline trans activator
CKO	conditional knockout

TABLE OF CONTENTS

Page

LIST OF FIGURES

Page

CHAPTER I

INTRODUCTION

1.1 Cranial development and suture biology

Skeletal growth deficiencies arising from birth defects, injury, or disease exist despite advances in therapy and, as a public health imperative, this reflects the need for a deeper understanding of its causes before more effective therapies can be applied in the setting of defective bone growth. The morbidity associated with defective or deficient bone growth is considerable and affects the majority of the American population, with high management costs that inevitably burden the economy (Poenaru et al., 2016; Williams et al., 2020; Wu et al., 2013). The molecular underpinnings controlling bone growth are complex, however, the exact mechanism remains unclear. It is well known that the craniofacial skeleton forms from the neural crest mesenchyme, with the parietal bones forming from paraxial mesoderm. The cranial vault or calvaria that encases the brain forms by intramembranous ossification (Chai and Maxson, 2006; Jiang et al., 2002). Developmentally, the mesenchyme undergoes condensation and patterning to form presumptive cranial bones. As condensation progresses, the cells in the center begin to commit to an osteoprogenitor fate under Runx2, the master regulator of both osteoprogenitor commitment and osteoblast differentiation. Osteoblasts then begin to lay down osteoid (type1 collagen matrix) and, through interactions with cell-surface integrin $\alpha 2\beta 1$ (Xiao et al., 1998), begin to secrete bone mineralizing proteins that convert the mature matrix to bone. The widely separated cranial bones then begin to expand

commensurate with growth of the underlying brain, and as the bone fronts approach each other they meet to form presumptive sutures. The mature cranium thus formed is a composite of paired frontal and parietal bones along with the supraoccipital bone with sutures interposed between them; the sutures and periosteum together serve as active sites of osteogenesis during skull growth and repair (Benson and Opperman, 2011). Notably, the transversely oriented coronal and lambdoid sutures are overlap type, and the midline metopic and sagittal sutures are butt type, the major sutures of the cranium that remain patent for much of postnatal life and thereafter gradually fuse in late adulthood (Fig. 1A) (Opperman, 2000). On the other hand, the proliferative chondrocyte layer of the growth plate in the appendicular skeleton is a growth center that contributes to trabecular bone (Ransom et al., 2016; Shi et al., 2017).

Interactions between the cranial sutures and periosteum are complex and involves a network of signaling pathways including growth factors such as PDGF, PTH and TGF-β1, and extensive 'crosstalk' between TGF-β/BMP, Wnt/β-catenin, FGFs, and Hedgehog pathways that ultimately specify mesenchymal lineage fate, the mutations of which frequently result in craniosynostosis (Fig. 1B) (Doro et al., 2017). Briefly, FGFs are a family of 18 soluble ligands that guide skeletal patterning through their activation of the four FGF receptor (FGFR) tyrosine kinases. To date, 22 highly conserved FGF ligands and 5 FGF receptors have been identified in mammals (Ornitz, 2000). The extracellular domain of the FGFRs features 3 immunoglobulin (Ig)-like domains, in addition to a single hydrophobic membrane-spanning segment and a split cytoplasmic

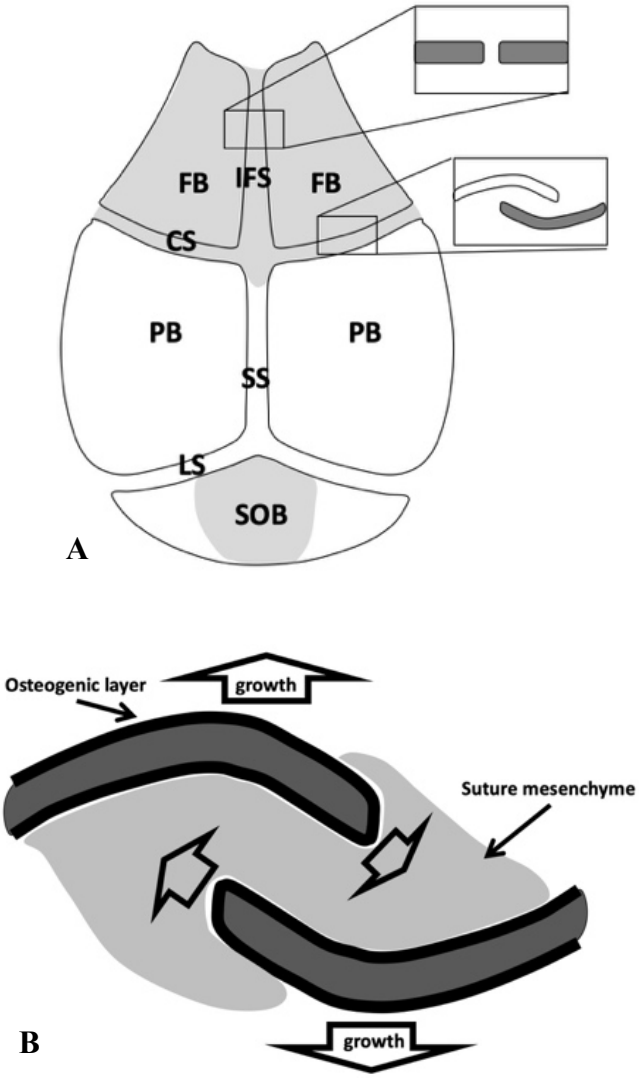

Figure 1 – Anatomical origins of the cranial bones (A). Gray denotes cranial neural crest derived tissue. Insets show the interfrontal and coronal sutures. Bone growth in the calvaria (B). The 2 opposing bones are buffered by the suture mesenchyme. The osteogenic layer contains osteoprogenitors that increase bone thickness, and cells that migrate to the leading edge of the bone promote lateral bone growth.

tyrosine kinase domain. Alternative splicing of the Ig III domain into ‘b’ and ‘c’ variants influences binding specificity for the subsets of FGFs, with the IIIc variant preferentially expressed in the mesenchyme. FGFR1 and 2 are predominantly expressed in the cranial sutures and mutations of these receptors in or near their IgIII domains are associated

with syndromic craniosynostoses, thus emphasizing their importance in cranial growth (Ornitz et al., 1996). Approximately, 20% cases of cranio-synostoses are due to mutations in FGFR1, R2 or R3 which are found in at least 6 commonly known craniosynostosis syndromes such as Apert, Crouzon, Pfeiffer, Muenke, Jackson-Weiss and Beare-Stevenson syndromes, most often characterized by bicoronal craniosynostosis or cloverleaf skull, distinctive facial features and limb abnormalities (Passos-Bueno et al., 2008). Point mutations in FGFR1 and R2 are linked to Pfeiffer syndrome, while FGFR2 mutations are associated with Apert and Crouzon syndromes – all gain-of-function/activating mutations characterized by increased ligand binding, receptor dimerization or tyrosine kinase activity (Wilkie, 2005; Zhang et al., 2006). The majority of the activating mutations (90%) are missense, and approximately 20% of these create unpaired cysteine residues that form intermolecular disulfide bonds between receptor dimers leading to constitutive activation, as seen in Pfeiffer and Crouzon syndrome. Mutations in splicing of exons encoding the IgIII domain account for 10% of Pfeiffer syndrome cases. However, two of the most common mutations – Ser252Trp and Pro253Arg – occur in the IgII-IgIII linker region and account for the majority of Apert syndrome cases. The Ser252Trp mutation accounts for 66% of Apert cases and is associated with a more severe phenotype that often includes cleft palate. Homologous mutations to the FGFR2 (Pro253Arg) mutation are also found in FGFR1 and FGFR3; the FGFR1(Pro252Arg) mutation accounts for 5% of Pfeiffer syndrome cases that exhibit a milder phenotype compared to that caused by FGFR2 mutations, while the FGFR3 (Pro250Arg) mutation accounts for 6-8% of all craniosynostosis patients with

Muenke syndrome (Passos-Bueno et al., 2008). FGFR5, also known as FGFRL1, lacks a split cytoplasmic tyrosine kinase domain and hence its function is still unclear, although a mutation within this gene has been implicated in craniosynostosis (Rieckmann et al., 2009).

The TGFβ superfamily is grouped into three sub families based on structure and receptor binding – the TGFβs, the activins, and the Bone Morphogenetic Proteins (BMPs). Expressed in mammals, TGFβ1, β2, and β3 are highly homologous secreted peptides and in dimerized active forms control a variety of developmental processes including growth, differentiation and apoptosis. The precise expression patterns of each during various stages of suture morphogenesis only reflects their dynamic but distinct roles in suture formation and stability; while all three are expressed in the bone fronts of patent sutures, TGFβ3 is absent in fused sutures where high levels of TGFβ1, 2 are found, suggesting that β1and β2 promote suture ossification while β3 maintains patency (Opperman et al., 1997; Roth et al., 1997). All three TGFβ proteins confer their effects on target cells through a signaling complex tetramer comprising type I and type II dimer receptors. Heterozygosity of either receptor causes craniosynostosis in Marfan syndrome related disorders, while conditional deletion of the type II receptor in the cranial NCCs in mice leads to agenesis of cranial bones, thus, punctuating the requirement of intact TGFβ signaling in cranial development (Ito et al., 2003; Mizuguchi and Matsumoto, 2007).

BMPs can promote osteogenic differentiation but only in the right context, however, their role in regulation of suture formation and patency is still unclear. There

are no mutations to the BMP pathway that result in craniosynostosis but that may be due to the requirement of these morphogens early on in development, as indicated by loss of viability of mice with mutations in the BMP pathway. Evidence has indicated that inhibition of bmp signaling inhibits osteogenic differentiation. Furthermore, addition of BMP inhibitor noggin to either naturally fusing or pathologically fusing futures can prevent synostosis (Wan et al., 2008). However, BMP beads placed on osteogenic fronts on the mid-suture did not promote suture closure in ex vivo calvaria as observed when FGF beads were placed, suggesting that BMP signaling is necessary but not sufficient to promote suture closure (Kim et al., 1998).

Haploinsufficiency of *TWIST1* is associated with Saethre-Chotzen syndrome (SCS), one of the most common autosomal dominant disorders of craniosynostosis with an incidence of 1 in 25000 to 1 in 50000 live births (el Ghouzzi et al., 1997). The most frequent clinical phenotypes of this disorder include misshapen skulls due to coronal suture synostosis, and hypertelorism associated with mid face hypoplasia. Typical limb abnormalities include soft-tissue syndactyly (Passos-Bueno et al., 2008). More than 100 different mutations have been identified within the *TWIST1* gene, suggesting SCS is due to haploinsufficiency of *TWIST1*. Moreover, *Twist1*$^{+/-}$ mice exhibit phenotypes similar to those in humans (Carver et al., 2002). Also, mutations in FGFR2 and FGFR3 have been reported in patients manifesting phenotypes consistent with SCS, indicating that haplo-insufficiency of *TWIST1* produces similar phenotypes as activation of FGFR signaling (Passos-Bueno et al., 2008).

MSX2 is a highly conserved homeobox gene located on the long arm of chromosome5, the mutations of which result in Boston-type craniosynostosis in humans. This is an autosomal dominant disorder characterized by coronal suture synostosis, associated with variable phenotypes that include fronto-orbital recession, frontal bossing and turribrachycephaly, resulting from a Pro148His mutation in the DNA-binding region of the protein. This increases the DNA-binding affinity of the protein resulting in enhanced protein activity (Lenton et al., 2005). Patients with craniosynostosis have been identified to have an extra copy of *MSX2*, further supporting that *MSX2* gain-of-function promotes craniosynostosis; associated phenotypes include microcephaly, developmental delay and dysmorphic features. Chromosomal studies of the proband showed 46,XY,add(2) (q37) dn, while those of the parents are normal. Moreover, comparative genomic hybridization (CGH) on the patient's rearranged material revealed loss of 2Mb distal to 2q37.3 and duplication of 15Mb from 5q34 →qter. It has been proposed that the extra copy of *MSX2* maps to 5q35.2 causing premature synostosis of the sutures via an MSX2-mediated pathway of calvarial osteogenesis (Kariminejad et al., 2009), suggesting *MSX2* duplication in the etiology of craniosynostosis. Conversely, mutations resulting in MSX2 haploinsufficiency cause ossification deficiencies and parietal foramina (Lenton et al., 2005).

1.2 B-ephrins (B1 and B2) in calvarial bone growth and homeostatic maintenance

Ephrins and their Eph-kinase receptors constitute a unique signaling system in calvarial growth and morphogenesis, and mutations in genes encoding these proteins result in

synostosis of the cranial bones. First reported in 1987, these cell-surface proteins were isolated from an *E*rythropoietin-*P*roducing *H*epatocellular carcinoma cell line and were termed *Eph*s, and the proteins that specifically interacted with these kinases were called *Ephrin*s – the abbreviated form of *EPH R*eceptor-*IN*teracting proteins (Hirai et al., 1987). Eph kinases constitute the largest subfamily of Receptor Tyrosine

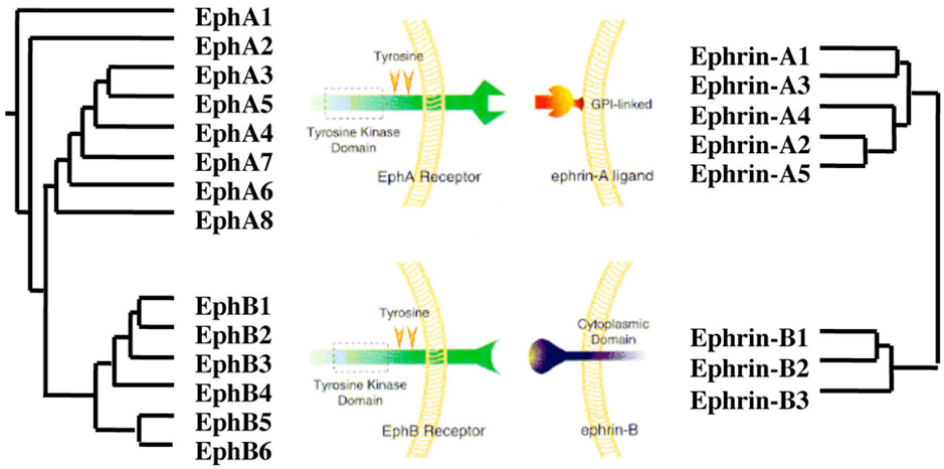

Figure 2 – Classification of Eph kinases and ephrins, based on sequence of homology and receptor or ligand binding affinity.

Kinases, totaling 16 [EphA1-A10 and EphB1-B6] but only 14 exist in the mammalian vertebrate – EphB5 and EphA9 are avian – and are classified into EphA and EphB kinases, based on sequence of homology and ligand binding affinity (Rundle et al., 2016). The ligands or 'ephrins' total 9 (ephrinA1-A6, and ephrin-B1-B3) and are classified in a similar manner into A-ephrins and B-ephrins, but only 8 exist in the mammalian genome (Fig. 2). Typically, an Eph kinase, from the extracellular N-terminus, features an ephrin-binding domain, a cysteine-rich region, a domain comprising two fibronectin type III repeats, a juxtamembrane region, a tyrosine kinase

domain, a sterile α-motif (SAM), and a C-terminal PDZ-domain binding motif. While the A-ephrins tether to the cell membrane via a GPI anchor, the B-ephrins are transmembrane molecules that feature a highly conserved cytoplasmic tail and a C-terminal PDZ-domain binding motif (Kawabe et al., 2009). Receptor-ligand interactions are preferential for the most part, i.e. A-ephrins interact with Eph-A kinases and B-ephrins with the Eph-Bs, with EphA4 and EphB2 being notable exceptions that further exhibit binding between classes (Himanen et al., 2004; Kania and Klein, 2016). The unique feature of this signaling system lies in its ability to initiate a two-way signaling event, i.e., while the ligand binds to the kinase causing signal transmission into the cell, termed 'forward' signaling, the ligand itself can act as a 'receptor' to which the kinase binds in a process termed 'reverse' signaling. Also, teasing out the exact function of each receptor and/or ligand constitutes a challenge, as functional redundancy exists among this large family of receptor tyrosine kinases and their cognate ligands (Kullander and Klein, 2002; Pasquale, 2010). For biologically relevant signaling to occur, an Eph-bearing cell must contact an ephrin-bearing cell; following receptor-ligand dimerization, oligomerization and clustering ensue resulting in a two-way signaling event (Tonna and Sims, 2014).

Over the last two decades, the transmembrane B-ephrins – ephrin-B1 and ephrin-B2 – have gained attention, as mounting evidence implicates these ephrins as key players in bone; ephrin-B3 expression is rather restricted, with high levels only in the brain and heart (Zhou, 1998). These molecules mediate diverse cell-cell contact-dependent biological events such as cell migration and sorting via repulsion and

adhesion, tissue boundary formation during embryogenesis, osteogenesis, angiogenesis and vascularization, and rewiring of neurons via axon guidance through 'reverse' signaling via their transmembrane domain (Kullander and Klein, 2002). Though functionally diverse, all the three B-ephrins (B1, B2, B3) possess a highly conserved cytoplasmic domain, of which the last 33 amino acids (in the C-terminal region) are 100% identical between all three proteins (Davy et al., 2004). To elucidate the roles of ephrin-B1 in the developmental context, mouse lines carrying mutations in *efnb1* gene were generated. While the conditional deletion of ephrin-B1 demonstrated its control over NCC migration autonomously (via reverse signaling, induced by a mutation in its PDZ binding domain), the ablation of ephrin-B1 resulted in perinatal lethality caused by a range of phenotypes including defects in Neural Crest Cell (NCC)-derived tissues, incomplete body wall closure, and abnormal skeletal patterning (Compagni et al., 2003) – findings consistent with human Cranio-Fronto-Nasal Syndrome (CFNS) caused by mutations in ephrin-B1 (Twigg et al., 2004).

CFN syndrome, a subgroup of FND first described by Cohen, is an X-linked develop-mental malformation syndrome with an unusual pattern of inheritance since females are more severely affected than males. Proposed explanations for the genetic basis of CFNS include disruptive interaction between wild type and mutant alleles – termed 'metabolic interference', aberrant functional disomy of the X-chromosome, and compensation by a Y-linked homologue (Feldman et al., 1997; Rollnick et al., 1981). This syndrome is caused by heterozygous mutations or deletions in the ephrin-B1encoding gene, *EFNB1,* located on chromosome X12/13, and is associated with a

sporadic and familial incidence. Though this syndrome presents with a spectrum of clinical signs and symptoms, synostosis of coronal suture is a typical manifestation. Thus far, 129 *EFNB1* mutations including 87 distinct missense, frameshift, nonsense, and splice site mutations as well as 8 gene deletions exist in humans (Wieland, 2011). The severe manifestations of CFNS in heterozygous females have been regarded a consequence of the random X-inactivation of the wild-type and mutant *EFNB1*-carrying X-chromosomes (Migeon, 2007; Wieland et al., 2004), which results in a cellular mosaic consisting of two ephrin-B1-expressing cell populations – one that expresses the wild type ephrin-B1, and the other dysfunctional ephrin-B1 protein. Since loss-of function rather than a dominant negative mutation in *EFNB1* more likely causes CFNS, bidirectional signaling will only be mediated by ephrin-B1-expressing cells upon cell-cell contact with opposing Eph-expressing cells. In the mosaic females, cellular interference (from mutant ephrin-B1-expressing cells) presumably leads to divergent cell sorting and migration, ultimately causing loss of tissue boundary sharpness and premature fusion of the coronal suture (Merrill et al., 2006). However, in hemizygous males, all cells are unable to produce functional ephrin-B1 protein and so the syndrome does not manifest in the manner it does in mosaic females. In males, normal boundaries are probably maintained through alternative mechanisms such as ephrin redundancy or promiscuity of the ephrin-kinase system (van den Elzen et al., 2014). Other pathogenic mechanisms of CFNS include cellular interference combined with impaired signaling capacity of ephrin-B1 and pleiotropic defects due to improper regulation of gap junctional communication (GJC) (Davy et al., 2006; Makarov et al., 2010). Also, a

genotypic-phenotypic correlation in CFNS has been proven, however, studies suggest that it is unlikely (Davy et al., 2006; Makarov et al., 2010; Wieland et al., 2008). However, recent evidence in support of ephrin-B1 mosaicism, as observed in CFNS, suggests that the syndrome-associated craniofacial dysmorphology is the direct result of aberrant segregation of post-migratory NCC-derived mesenchymal precursors in the craniofacial primordia causing local dysmorphogenesis of craniofacial structures, and not by neural tissue-specific disruption of ephrin-B1; further, EphB2 and EphB3, signaling partners for ephrin-B1, appear to influence cell segregation in the craniofacial region, while EphB1 is more critical for cell segregation in the brain in the ephrin-B1 heterozygous triple receptor knockout state (Niethamer et al., 2020).

The association of human CFNS with mutations in ephrin-B1 implies a defect in NCC migration, sorting, and differentiation of mesenchymal precursors into bone forming cells, owing to presence of deficient functional ephrin-B1 in the precursors (Twigg et al., 2013). Analyzing the function of osteoblast-produced ephrin-B1 *in vivo* revealed a complex mechanism by which ephrin B1 reverse signaling regulates bone formation. Targeting ephrin-B1 in type1α2 collagen-producing cells resulted in severe calvarial defects with decreased bone size, bone mineral density (BMD) and trabecular bone volume (BV), caused by impaired Osterix expression and consequent osteoblast differentiation. It is known that the cytoplasmic domain of eprhinB1 contains a PDZ-binding motif that interacts with PTPN13, NHERF1/2 (Lu et al., 2001) and the transcriptional coactivator TAZ, as they all contain that motif. Coimmunoprecipitation, using TAZ/PTPN13-specific antibodies, revealed a protein complex containing ephrin-

B1, PTPN13, NHERF1 and TAZ in BMS cells; further, activation of ephrin-B1 reverse signaling with soluble clustered EphB2-Fc led to time-dependent increase in TAZ dephosphorylation and shuttling from the cytoplasm to nucleus. Moreover, Western blotting revealed a 4-fold increase in Osterix expression in BMS cells treated with exogenous EphB2-Fc. However, a more conclusive approach included silencing TAZ by specific lentivirus small-hairpin RNA (shRNA) that decreased TAZ mRNA by 78%, and ephrin-B1 reverse signaling-induced Osterix mRNA levels by 75% in BMS cells. Similarly, knockdown of NHERF1 expression reduced basal levels of Osterix expression by 90% and abolished ephrin-B1-mediated induction of Osterix expression (Xing et al., 2010). Thus, ephrin-B1 via reverse signaling promotes osteoblast differentiation in BMS cells by regulating Osterix expression, thereby assuming crucial roles in bone homeostasis.

Bone marrow-derived mesenchymal stem cells (MSC), through self-renewal, contribute to skeletal tissue formation and the regulation of hematopoiesis (Sacchetti et al., 2007). To that end, the Eph/ephrin family of receptor tyrosine kinases, in addition to bone, assume important roles in maintaining the stem cell niche within neural (Picco et al., 2007), intestinal (Sancho et al., 2003) and dental tissues (Arthur et al., 2009). In determining the molecular expression profile in human MSC and bone marrow-derived populations using *ex vivo* expansion and RT-PCR, Eph-B (EphB2/B4) and ephrin-B (ephrin-B1/B2) were found to be highly expressed in these cells. To further elucidate the contribution of these molecules in MSC recruitment, functional spreading and migration assays, using soluble clustered EphB2-Fc/EphB4-Fc, and ephrin-B1-Fc/ephrin-B2-Fc,

showed that ephrin-B reverse signaling inhibited MSC attachment and spreading, as indicated by cell contraction and rounding caused by activation of Src-kinase, PI3-Kinase- and JNK-dependent signaling pathways. By contrast, EphB2 forward signaling promoted MSC migration by activating the Src kinase- and Abl-dependent signaling pathways. Furthermore, activation of ephrin-B1 and/or ephrin-B2 increased osteogenic differentiation (indicated by increased mineralization), while ephrin-B1 activation promoted chondrogenic differentiation, as indicated by increased GAG production in MSC treated with sEphB2-Fc. Thus, EphB/ephrin-B interactions possibly mediate MSC recruitment, migration and differentiation, and assume potential roles in fracture repair of endochondral bone (Arthur et al., 2011).

Cleft palate is one of the many clinical manifestations of CFNS caused by mutations in ephrin-B1, with females exhibiting far more severe phenotypic manifestations than obligate hemizygous males (Niethamer et al., 2020). Further, EphB2/B3 kinases work together in palate development (Orioli et al., 1996). Specifically, ephrin-B1 plays an intrinsic role in palatal shelf outgrowth in mice by regulating cell proliferation in the anterior palatal shelf mesenchyme. In ephrin-B1 heterozygous mutants, owing to random X-inactivation, the mosaic expression of ephrin-B1 caused disruption of cell proliferation, with post-transcriptional up-regulation of EphB receptor expression, mainly EphB3, through relief of endocytosis and degradation. The alteration in proliferation rates resulting from ectopic Eph–ephrin expression boundaries correlated with the more severe dysmorphogenesis in ephrin-B1 heterozygotes. Also, by integrating phospho-proteomic and transcriptomic approaches, it

was demonstrated that ephrin-B1 controls proliferation in the anterior palate by regulating the ERK/MAPK signal transduction pathway (Bush and Soriano, 2010).

Several lines of evidence ascribe EpB2 as a high-affinity receptor for ephrin-B1 (Arthur et al., 2011; Xing et al., 2010). Because expression of EphB2 was strongly induced in response to locally-applied mechanical strain i.e. 2-week four-point bending in mouse tibia, and because ephrin-B1 reverse signaling – with sEphB2-Fc – induced osteoblast differentiation through upregulation of Osterix in BMS cells, transgenic mice overexpressing ephrin-B1 [(under the control of a 3.6kb rat collagen1α1 promoter (Col3.6-Tg^{efnb1})] were generated to increase the interaction of the ligand with the receptor *in vivo* to induce bone formation. It was observed that Col3.6-Tg^{efnb1} mice express 6-, 12-, and 14-fold greater levels of full-length ephrin-B1 protein in osteoclasts (Oc), calvarial osteoblasts (Ob), and BMS cells, respectively. The long bones of both genders of Col3.6-Tg*efnb1* mice exhibited increased trabecular bone volume (32%), trabecular number (10%), and trabecular thickness (10%) and decreased trabecular separation (8.5%). Enhanced bone formation (indicated by a 39% increase in MAR) and decreased bone resorption (indicated by a 23% decrease in TRAP+ Oc) contributed to increased trabecular bone mass in Col3.6-Tg*efnb1* mice. Consistent with these findings, *in vitro* analysis revealed that over-expression of ephrin-B1 increased osteoblast differentiation and mineralization in BMS cells, as indicated by Osterix and collagen1α1 expression. Interaction of ephrin-B1 with sEphB2-Fc decreased Oc precursor differentiation into multinucleated cells. Furthermore, the mechanical loading-induced expression of ephrin-B1/EphB2, and new bone formation, were significantly greater in

the Col3.6-Tg^{efnb1} mice than in WT littermate controls. Thus, manipulating ephrin-B1 signaling may provide a means to stimulate new bone formation in the skeleton under mechanical strain (Cheng et al., 2013).

Bidirectional signaling has important roles in many developmental contexts such as in angiogenesis, axon guidance, cell sorting, and boundary formation (Davy and Soriano, 2007). While ephrin-B2 and its cognate receptor EphB4 are reciprocally expressed in arterial and venous endothelial cells, mice deficient in ephrin-B2 or EphB4 exhibit phenotypes of early embryonic lethality due to disorganized arteriovenous formation (Adams et al., 1999; Gerety et al., 1999; Wang et al., 1998). However, removing the C-terminal cytoplasmic domain of ephrin-B2 revealed that ephrin-B2 reverse signaling through the cytoplasmic domain is not required for early vascular development but required for axon pathfinding and cardiac valve formation (Cowan et al., 2004). Furthermore, ephrin-Eph interactions regulate embryonic stem-cell differentiation (Wang et al., 2004) including the immune response (Sharfe et al., 2002; Yu et al., 2003), intestinal epithelial cell migration (Batlle et al., 2002), and skeletal patterning (Compagni et al., 2003; Davy et al., 2004)). It is well known that bone homeostasis requires a precise functional balance between bone-resorbing osteoclasts and bone-forming osteoblasts. In identifying various EphB/ephrin-B molecules that coordinate osteoblast and osteoclast function, it was shown that osteoclasts express ephrin-B2 (an NFATc1 target) while osteoblasts express EphB4. Gain- and loss-of-function studies have demonstrated that reverse signaling through ephrin-B2 on osteoclast precursors suppressed their differentiation by inhibiting the osteoclasto-genic

c-Fos-NFATc1 cascade. In addition, forward signaling through EphB4 on osteoblasts enhanced their differentiation, possibly via ERK1/2 pathway activation and RhoA activity attenuation. To that end, transgenic mice overexpressing EphB4 showed a strong bone phenotype, but conditional KO mice lacking ephrin-B2 in the myeloid lineage did not, suggesting that ephrin-B1 may functionally compensate for ephrin-B2 in the osteoclast lineage *in vivo*. Thus, ephrin-Eph bidirectional signaling links two major molecular mechanisms for the differentiation of cells concerned with bone homeostasis (Zhao et al., 2006).

Ephrin-B2 is one of several mediators implicated in bone remodeling, a process that couples bone formation and resorption in the Bone Multicellular Unit (BMU). So, its intuitively obvious that ephrin-B2 may assume a dual role in bone homeostasis by balancing the activity between osteoblasts and osteoclasts. In that regard, hormones, through autocrine or paracrine effects, influence bone cells that ultimately regulate skeletal bone mass through local bone remodeling pathways. A hormone critical to bone homeostasis is PTH that mobilizes calcium from bone – by increasing bone resorption – when serum calcium levels drop. However, exogenously administered PTH has potent anabolic effects on bone caused by locally produced PTH-related protein (PTHrP), which also binds to the common PTH/PTHrP receptor (PTHR1) found in osteoblasts (Miao et al., 2005). It is well-understood that osteoclast formation and activation function is regulated by osteoblastic RANK-L expression in linking the cellular phases of bone formation to resorption (Suda et al., 1999; Teitelbaum and Ross, 2003). Other proposed mediators include matrix-derived TGF-β (Centrella et al., 1991), IGF-I and -II

(Crane and Cao, 2014; Smith, 2020), released by osteoclast action and, more recently, the osteoclast-derived ephrin-B2 that suppresses osteoclast differentiation via reverse signaling through EphB4 (Zhao et al., 2006). To compare the anabolic effects of PTH/PTHrP treatment on PTHR1-expressing mouse Kusa4b10 cells, and whether such effects are ephrin-B2-mediated, mouse whole genome cDNA microarray identified production of ephrin-B2, EphB2 and EphB4 in these cells. Moreover, in a dose-dependent manner, PTH/PTHrP stimulated ephrin-B2 production within the PTHR1+ cells causing them to differentiate into osteoblasts, while promoting osteoblast maturation in other precursor cells, thus, exerting autocrine and paracrine effects respectively (Allan et al., 2008).

It is well known that interactions between ephrin-B2 and EphB4 within the osteoblast lineage play key roles in regulating osteoblast maturation (Zhao et al., 2006). In determining the role of the ephrin-B2/EphB4 signaling in the skeleton, sEphB4 treatment of cultured osteoblasts specifically inhibited EphB4 and ephrin-B2 phosphorylation and reduced mRNA levels of late markers of osteoblast/osteocyte differentiation (i.e., osteocalcin, DMP-1, sclerostin, MEPE), while substantially increasing RANK-L. Though sEphB4 treatment *in vivo*, with or without PTH, substantially increased osteoblast formation and mRNA levels of early osteoblast markers (i.e., Runx2, ALP, Collagen1α1, and PTHR1), there was no significant change in bone formation rate or expression of late markers of osteoblast/osteocyte differentiation. Instead, sEphB4 treatment with PTH significantly increased osteoclast formation, causing a decrease in trabecular number, an effect that may have dampened

the anabolic effect of PTH. This effect was also reproduced in cultured osteoblasts treated with sEphB4, significantly impairing mineralizing ability. Clearly, ephrin-B2/EphB4 signaling within the osteoblast lineage is required for late-stage osteoblast differentiation and, to restrict osteoblast-mediated osteoclastogenic support by partly limiting RANKL production (Takyar et al., 2013).

Ephrin-B2 on osteoclasts activates the EphB4 receptor on osteoblasts to promote bone formation as part of homeostasis (Zhao et al., 2006). To define the role of ephrin-B signaling in developmental bone formation, ephrin-B2/LacZ chimeric mice were generated in which the coding region of the cytoplasmic domain of ephrin-B2 is replaced by that of β-galactosidase that turns eprhin-B2-expressing cells blue in the presence of the chromogenic substrate x-gal. While Ephrin-B2 was strongly expressed in the periosteum, sutural bone fronts, and dura mater of embryonic and neonatal mice, in the adult its expression was largely confined to sutures but was strongly upregulated at sites of bone injury. Complimenting this was treatment of *ex vivo* embryonic calvariae with soluble clustered ephrin-B2-Fc, which doubled their bone content without alteration in suture width or overall calvarial morphology. More importantly, even without Ascorbate addition, ephrin-B2-Fc stimulated expression of osteoblastic markers, osteocalcin and BSP, in cultured MC3T3 preosteoblasts. *In vivo* analysis also indicated that EphB4 kinase was strongly expressed in blood vessels (Gerety et al., 1999) but not in embryonic or adult calvaria; while EphB2 was expressed at sites of osteogenesis in both embryonic and postnatal calvaria, EphB1 was detected in the calvaria only after birth, implying crucial roles for these kinases early on in development. However, in adult mice, only

EphB1 knockout exhibited significant reduction in calvarial bone content compared to littermate control mice, not EphB2 knockout. Thus, evidence implicates ephrin-B2 in developmental and regenerative bone growth via activation of osteoblast-specific gene expression; further, though EphB1/B2 appear likely candidate receptors for ephrin-B2 early on in development, there may yet be other ligands for EphB1 in the adult (Benson et al., 2012).

1.3 Stem cells in suture patency and skeletal bone growth including homeostatic maintenance

It was only recently that stem cell populations were characterized in terms of expression and function during skeletal development. Bone formation in mammals requires the continuous supply of osteoblasts throughout life – first during modeling that begins in the embryo, and later during bone remodeling that occurs in the mature skeleton (Matsuo and Otaki, 2012). Using lineage-tracing, Gli1 has been identified as a common molecular marker for all osteogenic mesenchymal progenitors in fetal or postnatal skeletal growth in mice – while osteoblasts in the cortical shaft and secondary ossification center arise from embryonic Gli1+ cells, the cancellous bone osteoblasts in the primary ossification center are descendants of the Gli1+ cells that reside immediately beneath the growth plate (in the metaphysis) and are essential for cancellous bone formation during postnatal growth. Besides osteoblasts, these Gli1+ progenitors also give rise to bone marrow adipocytes and stromal cells *in vivo*. To that end, RNA profiling of the Gli1+ progenitors revealed a molecular signature resembling that of

MSC, as they expressed several marker genes, including CD146/Mcam, CD44, CD106/Vcam1, PDGFR-α/β, αSma/Acta2, and LepR previously identified in MSCs and were, thus, termed "metaphyseal mesenchymal progenitors" (MMPs). Besides being a marker, Gli1 expression in MMPs could indicate a physiological role for HH signaling in those cells. As suggested, HH signaling is necessary for normal proliferation and osteoblast differentiation of MMPs in cancellous bone, as disruption of Hh signaling in *Gli1-cre^{ERT2}; Ai9; Smo$^{c/c}$* mice, impaired their proliferation and differentiation.

Previous reports have indicated that Wnt/β-catenin functions downstream of HH to regulate osteoblastogenesis in the mouse embryo (Rodda and McMahon, 2006). Additionally, the postnatal deletion of β-catenin in Osterix+ cells not only reduced bone mass but also increased bone marrow adiposity (Chen and Long, 2013). In a similar vein, removing β-catenin in *Gli1-cre^{ERT2}; Ai9; β-catenin$^{c/c}$* mice caused MMPs to switch to an adipogenic fate, resulting in osteopenic cancellous bone with increased marrow adiposity. However, in both situations, decreased cancellous bone mass was not attributed to increased bone resorption but to decreased bone formation, as serum levels of CTX-1 levels in both the knockout and control mice were similar. While Gli1 marks MMPs critical for normal bone formation in postnatal mice, it was also demonstrated that Gli1+ identifies skeletal progenitors that contribute chondrocytes and osteoblasts during bone fracture healing. Thus, Gli1 labels metaphyseal progenitors for developmental and reparative bone growth (Shi et al., 2017).

Bone turnover in the skeleton is constant and is supported by mesenchymal stem cells that reside in diverse niches such as the periosteum, sutures of the craniofacial

region, and the long bone growth plate. Recent studies have shown that Nestin and Gremlin label a subset of perivascular mesenchymal stem cells (MSC) in the long bones that contribute to their turnover (Méndez-Ferrer et al., 2010; Worthley et al., 2015). However, in the craniofacial sutures, Gli1 has been shown to mark the major MSC population within the suture mesenchyme. At birth, the Gli1+ cells are present throughout the periosteum, duramater and suture mesenchyme but gradually restrict to the sutures where they lie in the mid-suture region, not associated with vasculature; these cells no longer become detectable in the periosteum, duramater, and bones abutting the sutures (in 1-3month old mice). Previously it was proposed that progenitor cells supporting craniofacial bone repair mainly reside in the periosteum, however, calvarial suture-transplant studies have indicated otherwise in that only sutures possess intrinsic bone regenerative ability and not the calvarial bone, periosteum or duramater, as the transplanted suture devoid of these tissues generated new periosteum, duramater and bone with a significant number of Gli1-derived cells in them (Slater et al., 2008). In characterizing stem cell behavior of Gli1+ suture cells, culture and clonal assays revealed in these cells a high expression of typical MSC markers including CD44, CD90, Sca-1, CD146 and CD73 (not CD34) and clone-forming ability, and clone sub-cultures were capable of osteogenic, chondrogenic and adipogenic differentiation and were all Gli1-derived (Xu et al., 2007); however, immunohistochemical assays on tissues failed to recapitulate the *in vitro* molecular profile of the Gli1+ suture cells, suggesting that while these cells have the ability to behave like MSCs under controlled conditions, they are not bonafide stem cells. Gli1 is a critical regulator in early growth

and morphogenesis of the skull, as ablation of Gli1+ cells leads to skull suture synostosis and growth arrest, compromised injury repair, and osteoporosis. Further, *Twist-1+/-* mice with cranio-synostosis demonstrated reduced Gli1+ cells in the sutures, suggesting this phenotype may result in part from a diminished Gli1+ population in the sutures. Thus, craniofacial sutures provide a unique niche for MSCs in craniofacial bone growth, homeostasis, and repair (Zhao et al., 2015).

Gli1+ suture cells have been characterized in terms of molecular profile, expression, and function in the craniofacial region (Zhao et al., 2015) and, while these cells exhibited strong regenerative capacity in response to calvarial suture injury, such a response was tested in the calvaria bone at varying distances from the suture in mice. It was concluded that the calvarial sutures possess much stronger regenerative capacity than the non-suture bony areas of the calvaria, as supplemented by microCT and histology including Gli1 cell proliferation assays. Moreover, the healing rate of the calvarial bone was inversely proportional to the distance between the suture and injury site. i.e., injuries closer to the suture healed faster. Because the majority of the stem cell population of the calvarial bone resides within the suture, the ability of these cells to respond and migrate into an injury area in sufficient numbers for repair is dependent upon the distance of the injury site from the suture. Further, following complete removal of the (sagittal) suture, regeneration and restoration of normal organization occurred within 6-8 weeks, with possible contribution from the coronal and lambdoid sutures (Park et al., 2016). Thus, from available evidence, though Gli+ cells within the calvarial suture mesenchyme are the cellular source for bone injury repair and regeneration, bone

healing is not an evenly distributed event in the calvaria, a finding attributable to its diverse embryological origins (Li et al., 2010; Quarto et al., 2010).

The bone marrow has long been shown to contain the osteogenic stem cell population for the skeleton; similarly, in the calvaria there is every likelihood that the osteogenic suture mesenchyme would regulate calvarial bone development. While the search continues for a cell population that satisfies the cardinal criteria for stem cells, evidence indicates that Gli1+ suture cells contribute to calvarial maintenance and injury repair (Zhao et al., 2015), suggesting that the identity and characteristics of suture stem cells responsible for calvarial bone maintenance and healing is yet limited. That Axin2 is critical in early growth and morphogenesis of the cranium by regulating suture patency, in addition to marking the basal cell layer of the skin, implies requirement of Axin2 for the maintenance of cell 'stemness' in diverse ecological niches of complex tissue systems (Lim et al., 2013; Yu et al., 2005). Further, as a transcriptional target of β-catenin, Axin2 is essential in orchestrating the signaling interplay of Wnt, BMP and FGF in mesenchymal fate determination during cranial development (Maruyama et al., 2010). Other evidence indicates that Axin2-expressing cells are capable of long-term self-renewal and differentiation into mature skeletal cell types during skeletal development and homeostasis. Moreover, like Gli1+ cells, Axin2-expressing suture cells are also highly responsive to injury and improve bone healing through direct engraftment. Gene-profiling analysis has shown that Axin-2 expressing cells express high levels of Gli1, suggesting possible overlap of these two stem cell populations. However, while Gli1 labels the entire suture mesenchyme, Axin2 is expressed in only 15% of mesenchymal

cells, is highly restricted to the suture midline, and colocalizes with slow-cycling cells. *In vivo* clonal analysis of Axin2-expressing suture cells further demonstrated their ability to clonally expand as a patch of cells sharing a common origin, or as a patched pattern with clear boundaries between them when generating ectopic bone as well as switch from one lineage fate to another in the presence of a bioactive cue such as BMP2, while having limited contribution to the maintenance of the body skeleton as Axin2-expressing cells are not bone marrow-associated (Maruyama et al., 2016).

Recently, Rap1b has been identified as a signaling effector of Axin2 in skeletal development (Maruyama et al., 2017); initially identified as an antagonist of Ras-induced transformation, Rap1 belongs to the Ras-like family of small GTPases with similar effector-binding domains (Raaijmakers and Bos, 2009). Rap1a and Rap1b, found in the mammalian genome, are two highly homologous and evolutionary conserved genes shown to possess specific as well redundant functions (Maddala et al., 2015). Rap1 acts as a molecular switch by cycling inactive GDP-bound and active GTP-bound forms, a transition that is tightly controlled by specific Guanine nucleotide Exchange Factors (GEFs) and GTPase-Activating Proteins (GAPs) (Caron, 2003). Rap1b has been identified as a downstream target of Axin2 in skeletogenesis, as immunoblot analysis confirmed that protein levels of Rap1b is elevated in the P3 Axin2-/- mutants. Also, Rap1b-GTP pull down assays using protein extracts from P3 control and $Axin2^{-/-}$ calvarial bones revealed that active Rap1b-GTP (active form of Rap1b) is enhanced in the absence of Axin2. Furthermore, Liquid Chromatography Tandem Mass Spectrometry (LC-MS) on protein extracts of P3 control and Axin2-/- calvaria revealed Rap protein

signal transduction and cGMP-mediated signaling are significantly affected by loss of Axin2 in skeletogenic modulation. To that end, double labeling in P10 calvaria (using LacZ staining for Axin2 and immunostaining for Rap1b) revealed Rap1b expression in skeletogenic mesenchyme including Axin2+ suture cells (Maruyama et al., 2016), suggesting potential involvement of Rap1b in Axin2-mediated signaling effects on suture morphogenesis and craniosynostosis. Further, while Axin2-mediated regulation of Rap1b is independent of β-catenin signaling in skeletogenic mesenchyme during calvarial morphogenesis, simultaneous knockout of Axin2 and decreased activity of FGFR1 signaling together with high levels of BMP signaling induced ectopic chondrogenesis of mesenchymal precursors and ossification in mice calvarial sutures (Maruyama et al., 2010). Also, BMP signaling may regulate mesenchymal cell fate specification through modulation of Rap1b, because inducible expression of constitutively active (ca) BMPR1A enhanced phosphorylation of Smad1/5/8 effectors and stimulated Rap1b expression in Axin2+ skeletogenic mesenchyme in P3 caBMPR1A^{Ax2} calvaria. This caused a switch to chondrogenic fate, suggesting that Rap1b is modulated by BMP signaling in mesenchymal cell fate determination, and not by Wnt/β-catenin alone (Mirando et al., 2010). Rap1b controls intra-membranous ossification in the calvaria by regulating mesenchymal progenitor commitment to an osteogenic fate, as ablation of Rap1b resulted in aberrant ossification and synostosis of the cranial sutures, suggesting enhanced osteoblast differentiation, characterized by Osterix and Col1 expression, in the absence of Rap1b. However, in C3H10T1/2 cells, Rap1b antagonizes osteoblast differentiation through modulation of FGF signaling by

negatively regulating MAPK-mediated osteogenesis. Rap1b also promotes chondrocyte differentiation *in vivo*, as chondrogenesis essential for endochondral ossification in embryonic limb development was significantly impaired in Rap1b-/- mutants. A similar trend was observed in *in vitro* chondrogenic assays on e18.5 wild type and Rap1b -/- mutant primary cells that revealed significant reductions in Sox9, Col2 and Aggrecan chondrogenic markers. Further, the inhibition of Rap1b in caBMPR1A^{Ax2} cells resulted in decreased chondrogenic differentiation, thus implying a BMP-Rap1b signaling axis operational in chondrogenesis. Hence, Rap1b assumes a dual and fate-specifying role in the differentiation of skeletogenic cell types (Maruyama et al., 2017).

Wnt signaling is critical in bone development, however, the identity and functions of cells that produce Wnt ligands is still unclear. While the expression profiles of all 19 Wnt ligands and the Wnt target gene – Axin2 – were determined in the neonatal mouse skeleton using in situ hybridization (Wang et al., 2012), it was further demonstrated that Osterix-expressing cells coexpress Wnt and Axin2, implying a subset of bone lineage cells that can both produce Wnt ligands and respond to Wnt signals, thereby regulating Wnt signaling in bone. Moreover, lineage tracing of Axin2-expressing osteolineage cells showed that they can give rise to descendants capable of sustaining osteogenesis over the long term, in addition to contributing to bone injury repair likely through proliferation giving rise to more osteolineage cells in the adult, suggesting that Wnt-responding stromal population contains osteolineage progenitors. Because *Wntless* is required for Wnt secretion through endosomal transport of Wnts (Bänziger et al., 2006), the deletion of *Wntless* in Osterix-expressing cells (from neonatal

Osx-GFP-Cre; Wntless $^{fl/fl}$ mice) resulted in improper differentiation, impaired (decreased) proliferation, increased apoptosis, and diminished Wnt signaling response (as indicated by significantly lower Axin2 levels). The mutants exhibited multiple significantly shorter long bones with a mid-diaphyseal constriction and brittle ribs compared to the controls, a phenotype likely resulting from undifferentiated osteolineage progenitors rather than from differentiated derivatives and chondrocytes. Therefore, Osterix-expressing cells through Wnt signaling response regulate cell proliferation and differentiation in skeletal bone homeostasis (Tan et al., 2014).

The mammalian skeleton performs a diverse range of vital functions – aside from providing structural support and locomotion, the skeleton acts as a supportive niche for hematopoiesis (Ding and Morrison, 2013) and is an active regulator of endocrine homeostasis (Cheloha et al., 2015), for which the skeleton relies on mechanisms of regeneration that restore functional skeletal cell populations, even in injury. It has been suggested that the Wnt pathway specifies distinct functional subsets of skeletal cell types; lineage tracing of Axin2 in *Axin2*^{CreER}*; R26*^{mTmG} mice has identified Wnt-Responding Cells (WRC) as a population of long-lived skeletal cells in the periosteum of long bone. In evaluating the contribution of periosteum in long bone injury repair short-term, local induction using tamoxifen identified injury responsive Axin2+ periosteal progenitor cells that have the ability to form both cartilage and bone (in the superficial periosteal callus), while long-term evaluation revealed a molecular phenotype of long-lived WRCs within the intact periosteum distinct from their descendants that had a phenotype consistent with a progenitor characteristic. Further, the absence of endosteal

WRCs over the long-term and their lack of contribution to intra-membranous bone formation (in the deep marrow callus) suggests a skeletal phenotype that is more differentiated than its periosteal counterpart. Other evidence indicates that the neonatal skeleton contains Wnt-responsive osteoprogenitors that give rise to the post-natal skeleton and exhibit sustained Axin2-expression, owing to autocrine stimulation through secretion of Wnt (Tan et al., 2014). Ablation of these WRCs in *Axin2*^{CreER}*; R26*^{mTmG}*; R26* $^{tm1(HBEGF)Awai}$ mice disrupts bone healing after injury, characterized by hyper-cellularity and reduced collagen deposition in the callus, and sites of chondrogenesis observed in both superficial and deep callus regions with relatively less ossification in comparison to the control mice at 1-week post-injury. Three-dimensional finite element modeling (Frost, 2000) together with microCT analysis of the mineralized callus in these mice 2 weeks post-injury delineated the crucial role of WRCs in functional bone regeneration – both in terms of bony bridging and collagen deposition during bone repair. Thus, WRCs serve as a therapeutic target to increase and restore the regenerative capacity of bone in the context of impaired skeletal regeneration (Ransom et al., 2016).

As stated earlier, the frontal bone (FB) is a major craniofacial structure that is NCC-derived (Chai and Maxson, 2006). In mammals, patterning and morphogenesis of the frontal bone begins with the migration of the frontal bone precursors into the frontal bone primordium (Opperman, 2000); in the mouse this migration proceeds in a caudal-to-rostral direction beginning at e11.5, followed by apical migration at e13.5 (Yoshida et al., 2008). Sonic Hedge-Hog (SHH) is critical in craniofacial and limb development, as deletion of Shh in mice causes holoprosencephaly characterized by encephalodysplasia

and in extreme cases cyclopia accompanied by other facial abnormalities and cleft palate (St-Jacques et al., 1999). Similarly, Indian HedgeHog (IHH) is critical in endochondral ossification, as loss of IHH decreases the proliferation of preosteoblasts leading to a reduction in cranial bone size and widened cranial sutures (Jacob et al., 2007), or mutations in HedgeHog (HH) effectors, co-receptors or ciliary proteins result in skeletal and craniofacial deformities (Pan et al., 2013). However, all these *in vivo* genetic approaches do not pinpoint the period when HH signaling becomes most critical in mouse craniofacial/skeletal embryogenesis. To that end, FB dysplasia has been suggested to not only result from genetic disruption of the HH pathway but from chemical disruption as well (Pan et al., 2013). Evidence indicates that pregnant mice receiving GDC-0449 (a HH-signaling inhibitor) – a single oral dose of 150mg/kg body weight – between e9.5 and e10.5 caused FB dysplasia in the developing embryos in utero, with most pronounced effects seen at e10.5, suggesting that time-specific inhibition of HH signaling appears to affect NCC migration after e10.5 causing FB dysplasia, an effect attributable to a reduction in proliferation, migration and differentiation, and increased apoptosis, of the NCC-osteoblast precursors in the developing FB. This teratogenic effect suggests that even BMP signaling may be compromised at this developmental timepoint, suggesting potential crosstalk between BMP and HH signaling in FB genesis (Jiang et al., 2019).

The Eph-kinase ligand, ephrin-B1 is important for normal development of bone and cartilage during skeletogenesis. Following long bone (femur) fracture in C57Bl/6 wildtype mice, the expression of ephrin-B1 was increased significantly at 1- and 2-

weeks post fracture, coinciding with the hematoma, soft-to hard callus formation, and remodeling stages of fracture repair (Schindeler et al., 2008). However, in investigating the specific role of ephrin-B1 within the osteolineage during fracture repair, 7-8-week-old control mice and mice with deletion of ephrin-B1 under the *Osterix* promoter ($EfnB1_{OB}^{fl/O}$) were subject to a femoral fracture with internal fixation. Two weeks post-fracture, microCT analysis revealed that $EfnB1_{OB}^{fl/O}$ mice displayed a significant increase in callus size and decrease in bone volume relative to tissue volume, increased cartilaginous tissue with a disproportionate distribution of osteoclasts within the hard callus (Arthur et al., 2019; Jing et al., 2014) and a significant reduction in osteo-progenitors, osteoid, and calcein-labelled bone within the fracture site, compared to *Osx*:*Cre* control mice, though at 8 weeks there were no significant differences between the two groups. Complementary *in vitro* studies demonstrated that, under osteogenic conditions, cultured $EfnB1_{OB}^{fl/O}$ stromal cells derived from the 2-week fracture site exhibited a reduced capacity to produce mineral, as indicated by decreased Alizarin Red staining intensity and calcium quantitation relative to DNA, together with a significant decrease in Osterix expression compared to the controls, suggesting that the loss of ephrin-B1 delays fracture healing by impairing ability of stromal cells at migration and osteogenic commitment at the fracture site. While loss of ephrin-B1 within the osteogenic lineage inhibits osteoblast function it cannot be ruled out whether this ligand influences osteogenic proliferation and apoptosis – loss of ephrin-B1 within NCC perturbs craniofacial development but has no effect on NCC proliferation or apoptosis (Davy et al., 2006). Furthermore, similar to mice, treatment of human BMS cells with

sEphB2Fc resulted in a significant decrease in phosphorylated TAZ levels together with significant upregulation of Osterix downstream targets, Osteocalcin and Col1α1, thus, exhibiting similarities in ephrin-B1 signaling between human and mouse stromal cell populations (Xing et al., 2010). Overall, loss of ephrin-B in the osteogenic and chondrogenic lineages impairs callus formation and remodeling in long bone fracture repair (Arthur et al., 2018; Arthur et al., 2020).

It is well established that ephrin-B ligands, ephrin-B1/B2, and some EphB kinases such as EphB2/B4 and EphA4 are expressed in osteoblasts and in osteocytes (Pasquale, 2010). While eprhin-B2 forward signaling promotes osteoblast differentiation, reverse signaling inhibits osteoclast formation and maturation (Zhao et al., 2006), and pharmacological inhibition of ephrin-B2/EphB4 impairs osteoblast differentiation (Martin et al., 2010; Takyar et al., 2013). Furthermore, via hormone-mediated effects, ephrin-B2 stimulates osteoblast formation and bone production through autocrine or paracrine signaling (Allan et al., 2008). It has been suggested that direct interaction of ephrin-B2 on the osteoclast and EphB4 on the osteoblast couples bone formation to resorption. However, this is controversial since osteoclasts and osteoblasts appear at different times in the basic multicellular unit (BMU), implying these cells are rarely in contact *in vivo* (Zhao et al., 2006). To determine the effect of ephrin-B2 ablation in the osteoblastic lineage, *Osx1EfnB2*$^{\Delta/\Delta}$ mouse calvarial osteoblasts, in culture, exhibited delayed expression of early and late osteoblastic markers such as Runx2, Osterix, ALP, PTHR1 and Osteocalcin; to that end, siRNA knockdown of ephrin-B2 in Kusa4b10 osteoblasts impaired their mineralization

compared to control, a finding that was not reproduced by EphB4 interference, suggesting the effect is solely ephrin-B2 mediated. MicroCT, histomorphometry and biomechanical testing of femurs from *Osx1EfnB2*$^{\Delta/\Delta}$ adult mice revealed a 2-fold delay in bone mineralization, as indicated by increased osteoid thickness, a low MAR and a significant reduction in bone stiffness with greater flexibility and deformation compared to gender and age-matched controls; also, while PTH treatment had no effect on osteoclastogenesis, a 50% reduction in osteoblast differentiation was observed in the mutant mice, suggesting impairment in osteoblastic activity in the face of normal osteoclastogenesis in response to PTH. Furthermore, greater levels of osteoblast and osteocyte apoptosis were observed in the mutant bone samples, as indicated by TUNEL assay and Transmission Electron (TE) microscopy, together with a 2-fold increase in annexinV, and a 7-fold increase in caspase8 activity in cultured ephrin-B2 deficient osteoblasts, suggesting that ephrin-B2 deletion in osteoblasts results in caspase8 mediated apoptosis (Tonna et al., 2014).

Recently, postnatal skeletal stem cells expressing Pair-related Homebox1 (Prx1) have been identified in the calvaria and in the axial skeleton. In the calvaria of 8w *Prx1CreER-GFP+* transgenic mice, these stem cells reside exclusively in the suture niche of the posterior frontal, coronal, sagittal and lambdoid sutures, and unlike Gli1+ stem cells (Zhao et al., 2015), Prx1+ cells are not found in other craniofacial sutures, the periosteum, duramater or even in calvarial bone marrow, and expression of Prx1 decrease with age (from 2-16 weeks) in these mice. Further, they do not coexpress Osterix (Nakashima et al., 2002) and are not associated with post-natal Col1+

osteoblasts (Ouyang et al., 2014), suggesting that Prx1+ stem cells are distinct from osteoprogenitors of the calvarial sutures. Lineage tracing has indicated that Prx1 is critical for embryonic and post-natal development of the calvarial bones and sutures (Yen et al., 2010), and via heterotopic suture transplantation Prx1+ cells contribute to regeneration of critical sized calvarial defects. To that end, lineage ablation of Prx1+ cells in *Prx1CreER-GFP+; DTA+* mice, and suturectomy in *Prx1CreER-GFP+; Tomato+* mice, perturb bone regeneration, suggesting that Prx1+ cells and their progeny are required for healing of critical-sized calvarial defects. Moreover, suturectomy and orthotopic transplantation of cranial sutures with traceable Prx1+ cells into wild type calvarial defects have shown that Prx1+ cells and their progeny migrate only from the transplanted suture into the defect (and not from native intact sutures) and contribute to bone regeneration, suggesting that calvarial suture is the exclusive niche of Prx1+ cells. Further, Prx1+ cells respond to Wnt signaling *in vitro* and *in vivo* by differentiating into osteoblasts, indicating that Prx1+ suture stem cells represent a quiescent population that can exit in the undifferentiated state by expressing Wnt inhibitors – Dkk1 and Sost – and differentiate into osteoblasts, besides presenting characteristics of bonafide stem cells. Finally, lineage ablation of Prx1 in 4-week-old *Prx1CreER-GFP+; DTA+* mice, while affecting long bone length, does not interfere with calvarial development, suggesting that Prx1 is critical in assuming different roles in post-natal endochondral bone growth. However, unlike Gli1, Prx1 becomes dispensable in post-natal craniofacial bone development – being a subset of Gli1+ stem cell population, Prx1 expression in the calvarial sutures decreases and its distribution across craniofacial tissues becomes

limited and highly restricted. Secondly, preosteoblasts and osteoblasts represent a reservoir of cells able to form bone (Park et al., 2012) even in the absence of Prx1+ progenitors. Thus, Prx1 may influence craniofacial development only if ablation is performed early enough when a significant pool of skeletal stem cells is still required. Other evidence indicates that Prx1+ cells express low levels of Axin2 but are highly Wnt-responsive, thus, speculating that Prx1+ cells may yet be Axin2+ suture stem cells or a subset thereof since, in the long bones, the majority of Osx+ cells co-express Axin2 (Tan et al., 2014). Thus, Prx1+ cells being distinct from Osx+ cells in the sutures, does not interfere with post-natal calvarial development (Wilk et al., 2017).

Years of research on calvarial stem cells has led to the identification of three major subpopulations of stem cells and signaling networks that govern their fate in mice, using linage tracing together with *in vitro* gene expression analysis and clonogenic assays. Sutures and periosteum together serve as sites of osteogenesis in the calvaria (Benson and Opperman, 2011), and sutures even possess regenerative capacity following calvarial injury (Park et al., 2016). Thus far, Gli1, Axin2 and, more recently, Prx1 have been proposed as major calvarial stem cells regulating calvarial bone growth and homeostatic maintenance. To that end, genetic mutations and errors in signaling cause suture synostoses in the cranium leading to bizarre skull growth (Doro et al., 2017). Evidence accumulated thus far is exclusively derived from studies on mice and other animals (Park et al., 2016; Wilk et al., 2017), however, little is known about the molecular control of the human calvarial osteogenic niche, although comparative studies provide distinctions on osteogenic capacity and homeostatic function between BMS

niches depending on location *in vivo* (Aghaloo et al., 2010; Matsubara et al., 2005). To that end, the osteogenic stem cell niche has been widely studied in the appendicular skeleton that develops through endochondral ossification (Chan et al., 2013; Ransom et al., 2016; Shi et al., 2017). In the context of the human skull vault, a recent study evaluated the marker expression profile in mesenchymal stem cells (MSC) between pathologically fused sutures and physiologically patent sutures in non-syndromic cranio-synostosis (NSC) patients, using *in vitro* osteogenic differentiation assays. No appreciable differences were found in Gli1 and Axin2 expression in the periosteum and endosteum including the osteogenic niche between the two suture groups. However, the expression of these markers was higher in calvarial MSCs compared to those of the long bone. Specifically, Axin2 followed a reduced expression trend in fused sutures compared to patent sutures in the NSC calvaria, suggesting that Axin2 undergoes depletion during premature ossification. To that end, Axin2 knock-down/silencing in normal calvarial MSCs induced activation of genes that promoted in them osteogenic commitment and differentiation, an effect comparable to *in vitro* osteogenic induction of pathologic calvarial MSCs (Di Pietro et al., 2020). Further supporting evidence reports of a *de novo* loss-of function mutation in exon4 of the Axin2 gene that caused synostosis of the sagittal suture resulting in scaphocephaly in a 3y old Turkish-Caucasian male (Yilmaz et al., 2018).

Recently, several therapeutic targets for Eph-ephrin signaling in terms of molecular interactions and specific signaling modalities have been described in numerous pathological settings, leading to the development of multiple therapies

especially in the settings of musculo-skeletal diseases and carcinomas. These include kinase inhibitor, small molecules, monoclonal antibodies, antibody-drug conjugates, nanobodies and peptides that target either the tyrosine kinase or the ligand binding domain of the kinase. Examples include trametinib, a kinase inhibitor, used in treating osteosarcoma by downregulating EphA2 and IL-7R or silencing EphA2 to reduce cell proliferation and migration; the PEGylated blocking peptide TNYL-RAW selectively blocks EphB4 to inhibit the ephrin binding in endothelial and epicardial mesothelial cell co-cultures; a peptide with dual function, termed BIDEN-AP specifically targets EphB4/ ephrin-B2 interaction where ephrin-B2-mediated endothelial cell angiogenic signaling is inhibited, while activating EphB4-dependent tumor-suppressive signaling in ovarian tumor cells (Arthur and Gronthos, 2021).

1.4 Role of Ki67, a cell proliferation maker

First identified in Hodgkin Lymphoma (HL) cell nuclei, Ki67 is a nuclear antigen that is expressed in G1, S, G2 and Mitotic but not in G0 phases of the cell cycle (Gerdes et al., 1983). In G1 phase, Ki67 is predominantly localized in the perinucleolar region, in the later phases of the cell cycle, the antigen is also detected throughout the nuclear interior, being predominantly localized in the nuclear matrix (Schlüter et al., 1993). This antigen is highly expressed in proliferating cells such as germinal centers of lymphoid follicles, cortical thymocytes, neck cells of the gastrointestinal (GI) mucosa, undifferentiated spermatogonia or in a number of human cell lines like L428, HL-60, U937 etc., but is strongly downregulated or absent in quiescent cells such as in medullary thymus, kidney,

brain, and parietal/Paneth cells of the GI mucosa (Gerdes et al., 1991), making Ki67 a clinically important proliferation marker in studies focused on grading various cancer types such as Breast Cancer, Gastro-Intestinal Stromal Tumors (GIST) and Pancreatic Neuroendocrine Neoplasms (PNEN) with well-established prognostic value (Dowsett et al., 2011; Pezzilli et al., 2016; Pyo et al., 2016). Ki67 is one of the best markers to assess cell proliferation in several tumor types and is used as a reagent to aid in determining patient prognosis for two reasons: critically, Ki67 it is not detected in noncycling cells though otherwise highly abundant. Secondly, its epitope – being present on nine of the sixteen Ki67 repeats – is naturally amplified when recognized by Ki67 monoclonal antibody (FKELF) (Booth and Earnshaw, 2017) (Booth and Earnshaw, 2017). Found in vertebrates, Ki67 is encoded by *(Monoclonal antibody) MKI67* in humans, and the protein is a 3256 amino acid sequence that encompasses 15 exons and 14 introns; Ki67 has several major functional regions namely the N-terminal Forkhead-associated (FHA) domain, a Protein Phosphate1(PP1) binding domain, a large unstructured central region comprising 16 tandem repeats of 122 residues (in primates), and a C-terminal LR (leucine/ arginine-rich) chromatin-binding domain (Sun and Kaufman, 2018). Analysis of Ki67 cDNA has shown that the center of the Ki67 protein is formed by a large 6,845-bp exon harboring the 16 concatenated, direct repeats (called the Ki67 repeats) which themselves contain a highly conserved 66-bp element (called the Ki67 motif) that encodes the epitope recognized by Ki67 (Schlüter et al., 1993).

Evidence indicates the MKI67 primary transcript is alternatively spliced and exists in two major isoforms, α long – weighing 395kDa, and β short – weighing

345kDa, and are encoded by the two major transcript variants that differ by alternative inclusion of exon7 (Gerdes et al., 1991). The other three isoforms include the γ (lacking exon3,4,7), δ (lacking exons3-12) as well as ε (lacking parts of exon7) (Schmidt et al., 2004); despite having different N-termini, all five MKI67 splicing variants or isoforms contain identical central tandem repeats and C-terminal regions; notably, in stimulated peripheral blood lymphocytes, the splicing patterns changes after stimulation, with the long isoform (α) appearing more slowly. In addition, in HeLa cells, overexpression of alternative exon7 (present only in the long isoform) reduced cell proliferation, whereas overexpression of an N-terminal fragment had opposite effects, suggesting that Ki67 isoforms could differentially impact cell proliferation and cell-cycle progression (Sun and Kaufman, 2018). In addition, Ki67 has also been implicated in major nuclear structural transitions during mitotic entry and exit, as initiation of mitosis requires active import of cyclinB to the nucleus during G2/M transition (Moore et al., 1999), and the mitotic localization of Ki67 is regulated by the balance of CDK/cyclin phosphorylation and PP1 de-phosphorylation (Takagi et al., 2014).

The functions of each domain will now be summarized in brief. The N-terminus FHA domain specifically interacts with two phosphoproteins during mitosis: kinesin-like motor protein Hklp2/Kif15, and a putative nucleolar RNA-binding protein NIFK (Durocher and Jackson, 2002) which are responsible for maintaining spindle bipolarity and cell proliferation and cancer metastasis, respectively. Hklp2 is a kinesin that participates in the assembly and stabilization of the bipolar spindle by localizing to the mitotic microtubules in a TPX2-dependent manner and to the chromosomes through

ki67 (Vanneste et al., 2009). NIFK enhances Ki67-dependent proliferation and promotes migration invasion *in vitro*, and metastasis *in vivo* via downregulation of casein kinase1α (CK1α), a suppressor of prometastatic TC4/β-catenin signaling, while CK1α is upregulated upon NIFK knockdown. However, the silencing of CK1α expression in NIFK-silenced cells restores TC4/β-catenin transcriptional activity, cell migration and metastasis. Furthermore, RUNX1 is identified as a transcription factor of CSNK1A1 (CK1α) that is negatively regulated by NIFK (Lin et al., 2016). The PP1 family, as it relates to the PP1 interaction domain of Ki67, contains 3 major isoforms – α, β, γ – and catalyzes approximately 1/3rd of all eukaryotic protein dephosphorylation events, spanning a wide variety of cellular functions such as anaphase progression, exit from mitosis, and is responsible for the maintenance of cells in G1 or G2 cell cycle phases. In addition, PP1 can promote apoptosis when cells are damaged. All PP1 isoforms can be found in the nucleus with PP1γ and PP1β/δ showing additional accumulation in the nucleoli. The localization of PP1 isoforms is dynamic and changes throughout mitosis, with each isoform assuming specific locations during the cell cycle such as in centrosomes, chromosomes or in parts thereof, suggesting isoform-specific roles. Thus, the functional versatility in terms of specific locations of PP1 isoforms can be due to different affinities for regulatory subunits or proteins which themselves assume distinct subcellular distribution (Rebelo et al., 2015). Finally, the central region of Ki67 is comprised of tandem repeats that contain residues phosphorylated by CDK1 during mitosis, as indicated by loss of perichromosomal staining in siRNA-mediated Ki67-depletion in HeLa cells or upon treatment with RO3306, a CDK1 inhibitor further

supported by immunoblot assays that detected mitotic-specific protein bands that were sensitive to Ki67-siRNA, RO3306 and Purvalanol A, another CDK1 inhibitor. Further, PP1γ-Ki67 is responsible for the timely dephosphorylation of Ki67 itself in anaphase (Takagi et al., 2014).

Evidence indicates that, during interphase in human dermal fibroblasts, dephosphorylated Ki67 forms fiber-like structures surrounding nucleoli, over-lapping the perinuclear chromatin (Kill, 1996). At the onset of mitosis, Ki67 becomes hyperphosphorylated and binds less avidly to the DNA, making it highly mobile on the chromosome periphery until anaphase, suggesting that Ki67 dynamically alters the nature of the interaction with chromatin structure during the cell cycle, an event that's closely related to the reformation process of the interphase nucleolar chromatin (Saiwaki et al., 2005). De-phosphorylation of Ki67 during mitotic exit stimulates its dissociation from the perichromosomal layer. On the mitotic chromosome surface, the highly positive charge of Ki67 serves as an electrostatic barrier for preventing hyperaggregation of chromosome arms (Takagi et al., 2016; Takagi et al., 2014). Furthermore, the weakly conserved LR-rich C-terminal domain of Ki67 can bind to DNA *in vitro* (Scholzen et al., 2002) and is required for association with chromosomes in living cells, as Ki67 depletion immobilize mitotic chromosomes by increased adhesion rather than spatial confinement. Though not required for initial chromosome individualization and condensation during prophase, Ki67 is required for the maintenance of spatial separation after nuclear envelope breakdown; spatial separation of chromosomes is important for efficient access of spindle microtubules and progression to anaphase (Cuylen et al.,

2016). The C-terminal domain of human Ki67 binds to all three isoforms of mammalian heterochromatin protein 1 (HP1) *in vitro* and *in vivo*; with over expression of HP1 in living cells, Ki67 is nearly exclusively found in nuclear foci and is almost entirely absent from the nucleoli and the nucleoplasm where its predominantly present (Kametaka et al., 2002; Scholzen et al., 2002). Other evidence indicates that overexpression of human, marsupial or Xenopus Ki67 result in the accumulation of HP1 and H3K9me3 (hallmark of constitutive heterochromatin) at sites of high Ki67 concentration, thereby inducing chromatin impaction, as measured by DAPI staining intensity (Scholzen et al., 2002; Sobecki et al., 2017). As cells prepare for mitosis, the chromosomes undergo a series of structural changes through a process called chromosomal condensation. A proteinaceous sheath termed perichromosomal layer (PCL) exists on the outer surface of individual chromosomes and comprises 30%-47% of the entire chromosome volume and more than 33% of the protein mass of isolated mitotic chromosomes, as indicated by 3D-Correlative Light and serial block-face scanning Electron Microscopy (CLEM) (Booth et al., 2016). Ki67 is one of the earliest proteins associated with the PCL and remains on it until telophase (Van Hooser et al., 2005). Evidence has indicated that Ki67 is required for the formation of the human PCL as acute depletion of this protein causes dispersal of PCL components including nucleolar proteins nucleolin, nucleophosmin, NIFK, PES1, cPERP-B, C, D, F and pre-ribosomal RNAs. However, depletion of these components did not alter perichromosomal localization of Ki67 (Booth et al., 2014; Hayashi et al., 2017). Two findings assign Ki67 as the essential foundational component of the PCL: first, disruption of the PCL upon Ki67 depletion delocalizes nucleolar components

during mitosis which in turn leads to their asymmetric distribution in daughter cells (Booth et al., 2014); second, Ki67 prevents the aggregation of mitotic chromosomes through its ability to act as a 'surfactant' on the chromosome surface. However, after nuclear envelope breakdown, cells depleted of Ki67 increase mitotic chromosome association resulting in impaired spindle assembly and metaphase plate formation thereby prolonging progression from prometaphase to anaphase (Cuylen et al., 2016). Furthermore, upon rapid removal of Ki67 in HCT116-based cell lines, using the mini–Auxin Inducible Degron (mAID) system, resulted in aberrant swollen mitotic chromosomes (Takagi et al., 2016). In a recent study, it was shown that depletion of either Ki67 or SMC2 (a core subunit of condensins that plays a role in chromosome assembly) did not largely affect their localization and dynamic behavior, however, combined ablation of both proteins resulted in ball-like chromosome clusters devoid of any discernable thread-like structure, suggesting that Ki67 and condensins localize to the external surface and central axis of mitotic chromosomes thereby maintaining their structural integrity (Takagi et al., 2018). Another recent study has shown that p160 subunit of histone chaperone Chromatin Assembly Factor1 (CAF-1) regulates Ki67 localization and can modulate the phase transition properties of Ki67 (Sun and Kaufman, 2018).

In summary, several growth factors and signaling pathways regulate the development of the cranial bones and the patency of their sutures (Doro et al., 2017). The sutures are a rich source of (Gli1+ and Axin2+) stem cells capable of regenerating bone, and both populations participate in developmental cranial osteogenesis through

osteoblast differentiation, however, little is known of the molecular control of migration, differentiation and maintenance of Axin2+ or Gli1+ stem cell populations, either during development or in the mature sutures. This glaring gap in knowledge needs to be filled before stem cell-based therapies for bone repair can be developed. Of importance are the membrane-bound ephrin-B ligands because important roles for them have been described in osteogenesis and maintenance of bone homeostasis through bidirectional signaling (Xing et al., 2010; Zhao et al., 2006). Ephrin-B2, via hormone-mediated effects, promotes OB maturation and bone formation through upregulation of ephrin-B2 in OBs themselves (Allan et al., 2008). Ephrin-B1 mutations in humans are linked to craniosynostosis (Twigg et al., 2013) thus, demonstrating its importance in cranial development. Further, deletion of ephrin-B1 with an Osterix-driven cre greatly impaired long bone growth, likely also through reverse signaling into osteoblast precursors. At the same time, ephrin-B1 deletion in these cells caused an increase in TRAP+ osteoclasts, indicating that ephrin-B1 also regulates bone remodeling (Nguyen et al., 2016). In addition, using a LacZ-indicator, we observed ephrin-B2-expressing cells at sites of osteogenesis during cranial development, in the mature sutures, and at sites of injury to the parietal bone; furthermore, adding soluble clustered recombinant ephrin-B2 to *ex vivo* embryonic calvariae dramatically increased their bone mass, causing a generalized narrowing of the sutures without obliterating them (Benson et al., 2012). These data lead to hypothesis that ***ephrin-Bs control calvarial bone growth and repair by regulating functions of Axin2+ and Gli1+ (osteoblastic) suture stem cells***. The hypothesis will be tested by achieving the following specific aims.

Aim 1. Identify the expression of ephrin-B1/B2 in Axin2+ and Gli1+ suture stem cell populations.

Our working hypothesis is that ephrin-B1/B2 expression labels a subset of Axin2+ and Gli1+ stem cells. For ephrin-B2, will generate mice harboring the *Gli1- or Axin2-cre*^{ERT2} alleles and the *Rosa26-STOP-loxP-tdTomato* indicator allele along with an ephrin-B2/GFP marker allele. The cre enzyme is expressed under the control of Gli1 or Axin2 in a tamoxifen-inducible manner; an incorporated tomato allele produces a strong red fluorescence in the cell that also expresses the enzyme. The Green Fluorescent Protein (GFP) is expressed under the control of ephrin-B2 and is localized to the nucleus. For ephrin-B1, we will generate mice harboring the *Gli1-* or *Axin2-cre*^{ERT2} alleles and the *Rosa26-STOP-loxP-eGFP* indicator allele along with an *ephrin-B1rtta/TetOptdTomato* marker allele. The cre enzyme is expressed under the control of Gli1 or Axin2 promoter in a tamoxifen-inducible manner; an incorporated eGFP allele produces a strong green fluorescence in the cell that also expresses the enzyme. The tomato protein is expressed under the ephrin-B1 promoter in a doxycycline-inducible manner (called the Tet-On system) and is localized to the nucleus. Collectively, these aims will reveal the extent to which the two fluorescence patterns overlap and will define ephrin-B1 and ephrin-B2 as a feature of either or both stem cell populations, implying a subset of stem cells that is amenable to ephrin-B signaling.

Aim2. Identify the requirement for ephrin-B1/B2 signaling in calvarial bone development.

The association of these ephrins with the calvarial suture niche implies a role for ephrin-B signaling in the osteogenic suture mesenchyme. *Our working hypothesis is that these ephrins, alone or together, mediate calvarial bone growth and establishment of the suture niche by Axin2+ or Gli1+ stem cells*. We generated mice harboring a conditional ephrin-B1 or ephrin-B2 allele, or both, along with a tamoxifen-inducible *Gli1-* or *Axin2-cre^{ERT2}*. We will use these mouse lines to examine the effects of ablating ephrin-B1 and/or ephrin-B2 in Axin2+ stem cells on embryonic calvarial bone formation. An included *Rosa26-STOP-loxP-tdTomato* indicator allele will allow us to observe changes in the presence and migration of Gli1+ and/or Axin2+ ephrin-B-deficient stem cells. Collectively, ablating these ephrins will reveal their effects on stem cell behavior and their contributions to the establishment and maintenance osteogenic stem cell niche in the cranial sutures. Also, individual, or combined ephrin ablation will delineate relative contributions of each ephrin to the developing calvaria. This will add to our understanding of the osteogenic mechanism underlying calvarial bone formation and will pave the way for possible translational use to improve bone regeneration and healing.

We found ephrin-B1 and ephrin-B2 to colocalize with Axin2+ stem cells mainly in the transversely oriented cranial sutures and periosteum of late-stage embryonic skulls (e19.5), suggesting that a subset of the Axin2+ stem cell population is subject to ephrin-B signaling in calvarial bone growth through intimate associations with the osteogenic

suture mesenchyme. For Gli1, we observed ephrin-B2 to colocalize with Gli1 in the sutures and periosteum of the adult cranium; further, ablating ephrin-B2 or ephrin-B1/B2 in the Gli1+ sutures and periosteum in the injured adult cranium did not result in any significant differences in healing between the knockouts and controls, as analyzed on x-ray. Even so, in late-stage Gli1+ embryonic skulls (e19.5), ablation of ephrin-B2 alone or in combination with ephrin-B1 in the sutures and periosteum (at e13.5-e15.5) did not perturb cranial growth. Hence, colocalization analysis of both these ephrins with Gli1 in the embryonic sutures and periosteum was not pursued further.

To define the functional contribution of ephrin-B1 and ephrin-B2 in establishing and maintaining the osteoblastic suture stem cell niche during cranial development, we targeted these ephrins in the Axin2+ suture stem cells (at e13.5-e15.5) and looked for phenotypic consequences in late-stage embryonic skulls (e19.5). Ablating either ephrin-B in this stem cell population did not result in any observable phenotype, suggesting possible functional redundancy amongst these ephrins in calvarial bone growth. However, the combined ablation of ephrin-B1/B2 in this stem cell compartment resulted in exencephaly, characterized by agenesis of the calvaria with bones of the face being affected to varying degrees. The phenotype had a 20% penetrance with a greater predilection for females. Thus, both ephrin-B1 and ephrin-B2 may work in tandem in controlling the Axin2 osteoblastic stem cell function during calvarial bone growth.

1.5 REFERENCES

1. Adams, R.H., Wilkinson, G.A., Weiss, C., Diella, F., Gale, N.W., Deutsch, U., Risau, W., and Klein, R. (1999). Roles of ephrin-B ligands and EphB receptors in cardiovascular development: demarcation of arterial/venous domains, vascular morphogenesis, and sprouting angiogenesis. Genes & development *13*, 295-306.
2. Aghaloo, T.L., Chaichanasakul, T., Bezouglaia, O., Kang, B., Franco, R., Dry, S.M., Atti, E., and Tetradis, S. (2010). Osteogenic potential of mandibular vs. long-bone marrow stromal cells. J Dent Res *89*, 1293-1298.
3. Allan, E.H., Häusler, K.D., Wei, T., Gooi, J.H., Quinn, J.M., Crimeen-Irwin, B., Pompolo, S., Sims, N.A., Gillespie, M.T., Onyia, J.E.*, et al.* (2008). Ephrin-B2 Regulation by PTH and PTHrP Revealed by Molecular Profiling in Differentiating Osteoblasts. Journal of Bone and Mineral Research *23*, 1170-1181.
4. Arthur, A., and Gronthos, S. (2021). Eph-Ephrin Signaling Mediates Cross-Talk Within the Bone Microenvironment. Front Cell Dev Biol *9*, 598612.
5. Arthur, A., Koblar, S., Shi, S., and Gronthos, S. (2009). Eph/ephrin-B mediate dental pulp stem cell mobilization and function. J Dent Res *88*, 829-834.
6. Arthur, A., Nguyen, T.M., Paton, S., Klisuric, A., Zannettino, A.C.W., and Gronthos, S. (2018). The osteoprogenitor-specific loss of ephrin-B1 results in an osteoporotic phenotype affecting the balance between bone formation and resorption. Scientific Reports *8*, 12756.

7. Arthur, A., Nguyen, T.M., Paton, S., Zannettino, A.C.W., and Gronthos, S. (2019). Loss of EfnB1 in the osteogenic lineage compromises their capacity to support hematopoietic stem/progenitor cell maintenance. Exp Hematol *69*, 43-53.

8. Arthur, A., Paton, S., Zannettino, A.C.W., and Gronthos, S. (2020). Conditional knockout of ephrin-B1 in osteogenic progenitors delays the process of endochondral ossification during fracture repair. Bone *132*, 115189.

9. Arthur, A., Zannettino, A., Panagopoulos, R., Koblar, S.A., Sims, N.A., Stylianou, C., Matsuo, K., and Gronthos, S. (2011). EphB/ephrin-B interactions mediate human MSC attachment, migration and osteochondral differentiation. Bone *48*, 533-542.

10. Bänziger, C., Soldini, D., Schütt, C., Zipperlen, P., Hausmann, G., and Basler, K. (2006). Wntless, a conserved membrane protein dedicated to the secretion of Wnt proteins from signaling cells. Cell *125*, 509-522.

11. Batlle, E., Henderson, J.T., Beghtel, H., van den Born, M.M., Sancho, E., Huls, G., Meeldijk, J., Robertson, J., van de Wetering, M., Pawson, T.*, et al.* (2002). Beta-catenin and TCF mediate cell positioning in the intestinal epithelium by controlling the expression of EphB/ephrin-B. Cell *111*, 251-263.

12. Benson, M.D., and Opperman, L.A. (2011). Regulation of Calvarial Bone Growth by Molecules Involved in the Craniosynostoses.

13. Benson, M.D., Opperman, L.A., Westerlund, J., Fernandez, C.R., San Miguel, S., Henkemeyer, M., and Chenaux, G. (2012). Ephrin-B stimulation of calvarial bone formation. Dev Dyn *241*, 1901-1910.

14. Booth, D.G., Beckett, A.J., Molina, O., Samejima, I., Masumoto, H., Kouprina, N., Larionov, V., Prior, I.A., and Earnshaw, W.C. (2016). 3D-CLEM Reveals that a Major Portion of Mitotic Chromosomes Is Not Chromatin. Mol Cell *64*, 790-802.

15. Booth, D.G., and Earnshaw, W.C. (2017). Ki-67 and the Chromosome Periphery Compartment in Mitosis. Trends Cell Biol *27*, 906-916.

16. Booth, D.G., Takagi, M., Sanchez-Pulido, L., Petfalski, E., Vargiu, G., Samejima, K., Imamoto, N., Ponting, C.P., Tollervey, D., Earnshaw, W.C.*, et al.* (2014). Ki-67 is a PP1-interacting protein that organises the mitotic chromosome periphery. Elife *3*, e01641.

17. Bush, J.O., and Soriano, P. (2010). Ephrin-B1 forward signaling regulates craniofacial morphogenesis by controlling cell proliferation across Eph-ephrin boundaries. Genes Dev *24*, 2068-2080.

18. Caron, E. (2003). Cellular functions of the Rap1 GTP-binding protein: a pattern emerges. Journal of Cell Science *116*, 435-440.

19. Carver, E.A., Oram, K.F., and Gridley, T. (2002). Craniosynostosis in Twist heterozygous mice: a model for Saethre-Chotzen syndrome. Anat Rec *268*, 90-92.

20. Centrella, M., McCarthy, T.L., and Canalis, E. (1991). Transforming growth factor-beta and remodeling of bone. J Bone Joint Surg Am *73*, 1418-1428.

21. Chai, Y., and Maxson, R.E., Jr. (2006). Recent advances in craniofacial morphogenesis. Dev Dyn *235*, 2353-2375.

22. Chan, C.K.F., Lindau, P., Jiang, W., Chen, J.Y., Zhang, L.F., Chen, C.-C., Seita, J., Sahoo, D., Kim, J.-B., Lee, A.*, et al.* (2013). Clonal precursor of bone, cartilage, and hematopoietic niche stromal cells. Proceedings of the National Academy of Sciences of the United States of America *110*, 12643-12648.

23. Cheloha, R.W., Gellman, S.H., Vilardaga, J.P., and Gardella, T.J. (2015). PTH receptor-1 signalling-mechanistic insights and therapeutic prospects. Nat Rev Endocrinol *11*, 712-724.

24. Chen, J., and Long, F. (2013). β-catenin promotes bone formation and suppresses bone resorption in postnatal growing mice. J Bone Miner Res *28*, 1160-1169.

25. Cheng, S., Kesavan, C., Mohan, S., Qin, X., Alarcon, C.M., Wergedal, J., and Xing, W. (2013). Transgenic overexpression of ephrin b1 in bone cells promotes bone formation and an anabolic response to mechanical loading in mice. PLoS One *8*, e69051.

26. Compagni, A., Logan, M., Klein, R., and Adams, R.H. (2003). Control of skeletal patterning by ephrin-B1-EphB interactions. Dev Cell *5*, 217-230.

27. Cowan, C.A., Yokoyama, N., Saxena, A., Chumley, M.J., Silvany, R.E., Baker, L.A., Srivastava, D., and Henkemeyer, M. (2004). Ephrin-B2 reverse signaling is required for axon pathfinding and cardiac valve formation but not early vascular development. Developmental Biology *271*, 263-271.

28. Crane, J.L., and Cao, X. (2014). Function of matrix IGF-1 in coupling bone resorption and formation. J Mol Med (Berl) *92*, 107-115.

29. Cuylen, S., Blaukopf, C., Politi, A.Z., Müller-Reichert, T., Neumann, B., Poser, I., Ellenberg, J., Hyman, A.A., and Gerlich, D.W. (2016). Ki-67 acts as a biological surfactant to disperse mitotic chromosomes. Nature *535*, 308-312.

30. Davy, A., Aubin, J., and Soriano, P. (2004). Ephrin-B1 forward and reverse signaling are required during mouse development. Genes Dev *18*, 572-583.

31. Davy, A., Bush, J.O., and Soriano, P. (2006). Inhibition of gap junction communication at ectopic Eph/ephrin boundaries underlies craniofrontonasal syndrome. PLoS Biol *4*, e315.

32. Davy, A., and Soriano, P. (2007). Ephrin-B2 forward signaling regulates somite patterning and neural crest cell development. Dev Biol *304*, 182-193.

33. Di Pietro, L., Barba, M., Prampolini, C., Ceccariglia, S., Frassanito, P., Vita, A., Guadagni, E., Bonvissuto, D., Massimi, L., Tamburrini, G.*, et al.* (2020). GLI1 and AXIN2 Are Distinctive Markers of Human Calvarial Mesenchymal Stromal Cells in Nonsyndromic Craniosynostosis. Int J Mol Sci *21*, 4356.

34. Ding, L., and Morrison, S.J. (2013). Haematopoietic stem cells and early lymphoid progenitors occupy distinct bone marrow niches. Nature *495*, 231-235.

35. Doro, D.H., Grigoriadis, A.E., and Liu, K.J. (2017). Calvarial Suture-Derived Stem Cells and Their Contribution to Cranial Bone Repair. Frontiers in physiology *8*, 956-956.

36. Dowsett, M., Nielsen, T.O., A'Hern, R., Bartlett, J., Coombes, R.C., Cuzick, J., Ellis, M., Henry, N.L., Hugh, J.C., Lively, T.*, et al.* (2011). Assessment of Ki67 in breast cancer: recommendations from the International Ki67 in Breast Cancer working group. J Natl Cancer Inst *103*, 1656-1664.

37. Durocher, D., and Jackson, S.P. (2002). The FHA domain. FEBS Lett *513*, 58-66.

38. el Ghouzzi, V., Le Merrer, M., Perrin-Schmitt, F., Lajeunie, E., Benit, P., Renier, D., Bourgeois, P., Bolcato-Bellemin, A.L., Munnich, A., and Bonaventure, J. (1997). Mutations of the TWIST gene in the Saethre-Chotzen syndrome. Nat Genet *15*, 42-46.

39. Feldman, G.J., Ward, D.E., Lajeunie-Renier, E., Saavedra, D., Robin, N.H., Proud, V., Robb, L.J., Der Kaloustian, V., Carey, J.C., Cohen, M.M., Jr.*, et al.* (1997). A novel phenotypic pattern in X-linked inheritance: craniofrontonasal syndrome maps to Xp22. Hum Mol Genet *6*, 1937-1941.

40. Frost, H.M. (2000). The Utah paradigm of skeletal physiology: an overview of its insights for bone, cartilage and collagenous tissue organs. J Bone Miner Metab *18*, 305-316.

41. Gerdes, J., Li, L., Schlueter, C., Duchrow, M., Wohlenberg, C., Gerlach, C., Stahmer, I., Kloth, S., Brandt, E., and Flad, H.D. (1991). Immunobiochemical and molecular biologic characterization of the cell proliferation-associated nuclear antigen that is defined by monoclonal antibody Ki-67. Am J Pathol *138*, 867-873.

42. Gerdes, J., Schwab, U., Lemke, H., and Stein, H. (1983). Production of a mouse monoclonal antibody reactive with a human nuclear antigen associated with cell proliferation. Int J Cancer *31*, 13-20.

43. Gerety, S.S., Wang, H.U., Chen, Z.F., and Anderson, D.J. (1999). Symmetrical mutant phenotypes of the receptor EphB4 and its specific transmembrane ligand ephrin-B2 in cardiovascular development. Mol Cell *4*, 403-414.

44. Hayashi, Y., Kato, K., and Kimura, K. (2017). The hierarchical structure of the perichromosomal layer comprises Ki67, ribosomal RNAs, and nucleolar proteins. Biochem Biophys Res Commun *493*, 1043-1049.

45. Himanen, J.P., Chumley, M.J., Lackmann, M., Li, C., Barton, W.A., Jeffrey, P.D., Vearing, C., Geleick, D., Feldheim, D.A., Boyd, A.W.*, et al.* (2004). Repelling class discrimination: ephrin-A5 binds to and activates EphB2 receptor signaling. Nat Neurosci *7*, 501-509.

46. Hirai, H., Maru, Y., Hagiwara, K., Nishida, J., and Takaku, F. (1987). A novel putative tyrosine kinase receptor encoded by the eph gene. Science *238*, 1717-1720.

47. Ito, Y., Yeo, J.Y., Chytil, A., Han, J., Bringas, P., Nakajima, A., Shuler, C., Moses, H., and Chai, Y. (2003). Conditional inactivation of Tgfbr2 in cranial neural crest causes cleft palate and calvaria defects. Paper presented at: Development.

48. Jacob, S., Wu, C., Freeman, T.A., Koyama, E., and Kirschner, R.E. (2007). Expression of Indian Hedgehog, BMP-4 and Noggin in craniosynostosis induced by fetal constraint. Ann Plast Surg *58*, 215-221.

49. Jiang, X., Iseki, S., Maxson, R.E., Sucov, H.M., and Morriss-Kay, G.M. (2002). Tissue origins and interactions in the mammalian skull vault. Dev Biol *241*, 106-116.

50. Jiang, Y., Zhang, S., Mao, C., Lai, Y., Wu, D., Zhao, H., Liao, C., and Chen, W. (2019). Defining a critical period in calvarial development for Hedgehog pathway antagonist-induced frontal bone dysplasia in mice. Int J Oral Sci *11*, 3.

51. Jing, J., Hinton, R.J., Jing, Y., Liu, Y., Zhou, X., and Feng, J.Q. (2014). Osterix couples chondrogenesis and osteogenesis in post-natal condylar growth. J Dent Res *93*, 1014-1021.

52. Kametaka, A., Takagi, M., Hayakawa, T., Haraguchi, T., Hiraoka, Y., and Yoneda, Y. (2002). Interaction of the chromatin compaction-inducing domain (LR domain) of Ki-67 antigen with HP1 proteins. Genes Cells *7*, 1231-1242.

53. Kania, A., and Klein, R. (2016). Mechanisms of ephrin-Eph signalling in development, physiology and disease. Nat Rev Mol Cell Biol *17*, 240-256.

54. Kariminejad, A., Kariminejad, R., Tzschach, A., Ullmann, R., Ahmed, A., Asghari-Roodsari, A., Salehpour, S., Afroozan, F., Ropers, H.H., and Kariminejad, M.H. (2009). Craniosynostosis in a patient with 2q37.3 deletion 5q34 duplication: association of extra copy of MSX2 with craniosynostosis. Am J Med Genet A *149a*, 1544-1549.

55. Kawabe, M., Herrem, C.J., Finke, J.H., and Storkus, W.J. (2009). EphA2: A Novel Target in Renal Cell Carcinoma. In Renal Cell Carcinoma: Molecular Targets and Clinical Applications, R.M. Bukowski, R.A. Figlin, and R.J. Motzer, eds. (Totowa, NJ: Humana Press), pp. 347-366.

56. Kill, I.R. (1996). Localisation of the Ki-67 antigen within the nucleolus. Evidence for a fibrillarin-deficient region of the dense fibrillar component. J Cell Sci *109 (Pt 6)*, 1253-1263.

57. Kim, H.J., Rice, D.P., Kettunen, P.J., and Thesleff, I. (1998). FGF-, BMP- and Shh-mediated signalling pathways in the regulation of cranial suture morphogenesis and calvarial bone development. Development *125*, 1241-1251.

58. Kullander, K., and Klein, R. (2002). Mechanisms and functions of Eph and ephrin signalling. Nat Rev Mol Cell Biol *3*, 475-486.

59. Lenton, K.A., Nacamuli, R.P., Wan, D.C., Helms, J.A., and Longaker, M.T. (2005). Cranial suture biology. Curr Top Dev Biol *66*, 287-328.

60. Li, S., Quarto, N., and Longaker, M.T. (2010). Activation of FGF signaling mediates proliferative and osteogenic differences between neural crest derived frontal and mesoderm parietal derived bone. PLoS One *5*, e14033.

61. Lim, X., Tan, S.H., Koh, W.L., Chau, R.M., Yan, K.S., Kuo, C.J., van Amerongen, R., Klein, A.M., and Nusse, R. (2013). Interfollicular epidermal stem cells self-renew via autocrine Wnt signaling. Science *342*, 1226-1230.

62. Lin, T.C., Su, C.Y., Wu, P.Y., Lai, T.C., Pan, W.A., Jan, Y.H., Chang, Y.C., Yeh, C.T., Chen, C.L., Ger, L.P.*, et al.* (2016). The nucleolar protein NIFK promotes cancer progression via CK1α/β-catenin in metastasis and Ki-67-dependent cell proliferation. Elife *5*.

63. Lu, Q., Sun, E.E., Klein, R.S., and Flanagan, J.G. (2001). Ephrin-B reverse signaling is mediated by a novel PDZ-RGS protein and selectively inhibits G protein-coupled chemoattraction. Cell *105*, 69-79.

64. Maddala, R., Nagendran, T., Lang, R.A., Morozov, A., and Rao, P.V. (2015). Rap1 GTPase is required for mouse lens epithelial maintenance and morphogenesis. Dev Biol *406*, 74-91.

65. Makarov, R., Steiner, B., Gucev, Z., Tasic, V., Wieacker, P., and Wieland, I. (2010). The impact of CFNS-causing EFNB1 mutations on ephrin-B1 function. BMC Medical Genetics *11*, 98.

66. Martin, T.J., Allan, E.H., Ho, P.W., Gooi, J.H., Quinn, J.M., Gillespie, M.T., Krasnoperov, V., and Sims, N.A. (2010). Communication between ephrin-B2 and EphB4 within the osteoblast lineage. Adv Exp Med Biol *658*, 51-60.

67. Maruyama, T., Jeong, J., Sheu, T.J., and Hsu, W. (2016). Stem cells of the suture mesenchyme in craniofacial bone development, repair and regeneration. Nat Commun *7*, 10526.

68. Maruyama, T., Jiang, M., Abbott, A., Yu, H.I., Huang, Q., Chrzanowska-Wodnicka, M., Chen, E.I., and Hsu, W. (2017). Rap1b Is an Effector of Axin2 Regulating Crosstalk of Signaling Pathways During Skeletal Development. J Bone Miner Res *32*, 1816-1828.

69. Maruyama, T., Mirando, A.J., Deng, C.-X., and Hsu, W. (2010). The Balance of WNT and FGF Signaling Influences Mesenchymal Stem Cell Fate During Skeletal Development. Science Signaling *3*, ra40-ra40.

70. Matsubara, T., Suardita, K., Ishii, M., Sugiyama, M., Igarashi, A., Oda, R., Nishimura, M., Saito, M., Nakagawa, K., Yamanaka, K.*, et al.* (2005). Alveolar bone marrow as a cell source for regenerative medicine: differences between alveolar and iliac bone marrow stromal cells. J Bone Miner Res *20*, 399-409.

71. Matsuo, K., and Otaki, N. (2012). Bone cell interactions through Eph/ephrin: bone modeling, remodeling and associated diseases. Cell Adh Migr *6*, 148-156.

72. Méndez-Ferrer, S., Michurina, T.V., Ferraro, F., Mazloom, A.R., MacArthur, B.D., Lira, S.A., Scadden, D.T., Ma'ayan, A., Enikolopov, G.N., and Frenette, P.S. (2010). Mesenchymal and haematopoietic stem cells form a unique bone marrow niche. Nature *466*, 829-834.

73. Merrill, A.E., Bochukova, E.G., Brugger, S.M., Ishii, M., Pilz, D.T., Wall, S.A., Lyons, K.M., Wilkie, A.O., and Maxson, R.E., Jr. (2006). Cell mixing at a neural crest-mesoderm boundary and deficient ephrin-Eph signaling in the pathogenesis of craniosynostosis. Hum Mol Genet *15*, 1319-1328.

74. Miao, D., He, B., Jiang, Y., Kobayashi, T., Sorocéanu, M.A., Zhao, J., Su, H., Tong, X., Amizuka, N., Gupta, A.*, et al.* (2005). Osteoblast-derived PTHrP is a potent endogenous bone anabolic agent that modifies the therapeutic efficacy of administered PTH 1-34. J Clin Invest *115*, 2402-2411.

75. Migeon, B.R. (2007). Why females are mosaics, X-chromosome inactivation, and sex differences in disease. Gend Med *4*, 97-105.

76. Mirando, A.J., Maruyama, T., Fu, J., Yu, H.M., and Hsu, W. (2010). β-catenin/cyclin D1 mediated development of suture mesenchyme in calvarial morphogenesis. BMC Dev Biol *10*, 116.

77. Mizuguchi, T., and Matsumoto, N. (2007). Recent progress in genetics of Marfan syndrome and Marfan-associated disorders. J Hum Genet *52*, 1-12.

78. Moore, J.D., Yang, J., Truant, R., and Kornbluth, S. (1999). Nuclear import of Cdk/cyclin complexes: identification of distinct mechanisms for import of Cdk2/cyclin E and Cdc2/cyclin B1. J Cell Biol *144*, 213-224.

79. Nakashima, K., Zhou, X., Kunkel, G., Zhang, Z., Deng, J.M., Behringer, R.R., and de Crombrugghe, B. (2002). The Novel Zinc Finger-Containing Transcription Factor Osterix Is Required for Osteoblast Differentiation and Bone Formation. Cell *108*, 17-29.

80. Nguyen, T.M., Arthur, A., Paton, S., Hemming, S., Panagopoulos, R., Codrington, J., Walkley, C.R., Zannettino, A.C., and Gronthos, S. (2016). Loss of ephrin-B1 in osteogenic progenitor cells impedes endochondral ossification and compromises bone strength integrity during skeletal development. Bone *93*, 12-21.

81. Niethamer, T.K., Teng, T., Franco, M., Du, Y.X., Percival, C.J., and Bush, J.O. (2020). Aberrant cell segregation in the craniofacial primordium and the emergence of facial dysmorphology in craniofrontonasal syndrome. PLoS Genet *16*, e1008300.

82. Opperman, L.A. (2000). Cranial sutures as intramembranous bone growth sites. Developmental Dynamics *219*, 472-485.

83. Opperman, L.A., Nolen, A.A., and Ogle, R.C. (1997). TGF-beta 1, TGF-beta 2, and TGF-beta 3 exhibit distinct patterns of expression during cranial suture formation and obliteration in vivo and in vitro. J Bone Miner Res *12*, 301-310.

84. Orioli, D., Henkemeyer, M., Lemke, G., Klein, R., and Pawson, T. (1996). Sek4 and Nuk receptors cooperate in guidance of commissural axons and in palate formation. EMBO J *15*, 6035-6049.

85. Ornitz, D.M. (2000). FGFs, heparan sulfate and FGFRs: complex interactions essential for development. Bioessays *22*, 108-112.

86. Ornitz, D.M., Xu, J., Colvin, J.S., McEwen, D.G., MacArthur, C.A., Coulier, F., Gao, G., and Goldfarb, M. (1996). Receptor specificity of the fibroblast growth factor family. J Biol Chem *271*, 15292-15297.

87. Ouyang, Z., Chen, Z., Ishikawa, M., Yue, X., Kawanami, A., Leahy, P., Greenfield, E.M., and Murakami, S. (2014). Prx1 and 3.2kb Col1a1 promoters target distinct bone cell populations in transgenic mice. Bone *58*, 136-145.

88. Pan, A., Chang, L., Nguyen, A., and James, A.W. (2013). A review of hedgehog signaling in cranial bone development. Front Physiol *4*, 61.

89. Park, D., Spencer, J.A., Koh, B.I., Kobayashi, T., Fujisaki, J., Clemens, T.L., Lin, C.P., Kronenberg, H.M., and Scadden, D.T. (2012). Endogenous bone marrow MSCs are dynamic, fate-restricted participants in bone maintenance and regeneration. Cell Stem Cell *10*, 259-272.

90. Park, S., Zhao, H., Urata, M., and Chai, Y. (2016). Sutures Possess Strong Regenerative Capacity for Calvarial Bone Injury. Stem Cells Dev *25*, 1801-1807.

91. Pasquale, E.B. (2010). Eph receptors and ephrins in cancer: bidirectional signalling and beyond. Nature Reviews Cancer *10*, 165-180.

92. Passos-Bueno, M.R., Sertié, A.L., Jehee, F.S., Fanganiello, R., and Yeh, E. (2008). Genetics of craniosynostosis: genes, syndromes, mutations and genotype-phenotype correlations. Front Oral Biol *12*, 107-143.

93. Pezzilli, R., Partelli, S., Cannizzaro, R., Pagano, N., Crippa, S., Pagnanelli, M., and Falconi, M. (2016). Ki-67 prognostic and therapeutic decision driven marker for pancreatic neuroendocrine neoplasms (PNENs): A systematic review. Adv Med Sci *61*, 147-153.

94. Picco, V., Hudson, C., and Yasuo, H. (2007). Ephrin-Eph signalling drives the asymmetric division of notochord/neural precursors in Ciona embryos. Development *134*, 1491-1497.

95. Poenaru, D., Lin, D., and Corlew, S. (2016). Economic Valuation of the Global Burden of Cleft Disease Averted by a Large Cleft Charity. World Journal of Surgery *40*, 1053-1059.

96. Pyo, J.S., Kang, G., and Sohn, J.H. (2016). Ki-67 labeling index can be used as a prognostic marker in gastrointestinal stromal tumor: a systematic review and meta-analysis. Int J Biol Markers *31*, e204-210.

97. Quarto, N., Wan, D.C., Kwan, M.D., Panetta, N.J., Li, S., and Longaker, M.T. (2010). Origin matters: differences in embryonic tissue origin and Wnt signaling determine the osteogenic potential and healing capacity of frontal and parietal calvarial bones. J Bone Miner Res *25*, 1680-1694.

98. Raaijmakers, J.H., and Bos, J.L. (2009). Specificity in Ras and Rap signaling. J Biol Chem *284*, 10995-10999.

99. Ransom, R.C., Hunter, D.J., Hyman, S., Singh, G., Ransom, S.C., Shen, E.Z., Perez, K.C., Gillette, M., Li, J., Liu, B.*, et al.* (2016). Axin2-expressing cells execute regeneration after skeletal injury. Sci Rep *6*, 36524.

100. Rebelo, S., Santos, M., Martins, F., da Cruz e Silva, E.F., and da Cruz e Silva, O.A. (2015). Protein phosphatase 1 is a key player in nuclear events. Cell Signal *27*, 2589-2598.

101. Rieckmann, T., Zhuang, L., Flück, C.E., and Trueb, B. (2009). Characterization of the first FGFRL1 mutation identified in a craniosynostosis patient. Biochim Biophys Acta *1792*, 112-121.

102. Rodda, S.J., and McMahon, A.P. (2006). Distinct roles for Hedgehog and canonical Wnt signaling in specification, differentiation and maintenance of osteoblast progenitors. Development *133*, 3231-3244.

103. Rollnick, B., Day, D., Tissot, R., and Kaye, C. (1981). A pedigree possible evidence for the metabolic interference hypothesis. Am J Hum Genet *33*, 823-826.

104. Roth, D.A., Longaker, M.T., McCarthy, J.G., Rosen, D.M., McMullen, H.F., Levine, J.P., Sung, J., and Gold, L.I. (1997). Studies in cranial suture biology: Part I. Increased immunoreactivity for TGF-beta isoforms (beta 1, beta 2, and beta 3) during rat cranial suture fusion. J Bone Miner Res *12*, 311-321.

105. Rundle, C.H., Xing, W., Lau, K.-H.W., and Mohan, S. (2016). Bidirectional ephrin signaling in bone. Osteoporosis and Sarcopenia *2*, 65-76.

106. Sacchetti, B., Funari, A., Michienzi, S., Di Cesare, S., Piersanti, S., Saggio, I., Tagliafico, E., Ferrari, S., Robey, P.G., Riminucci, M*., et al.* (2007). Self-renewing osteoprogenitors in bone marrow sinusoids can organize a hematopoietic microenvironment. Cell *131*, 324-336.

107. Saiwaki, T., Kotera, I., Sasaki, M., Takagi, M., and Yoneda, Y. (2005). In vivo dynamics and kinetics of pKi-67: transition from a mobile to an immobile form at the onset of anaphase. Exp Cell Res *308*, 123-134.

108. Sancho, E., Batlle, E., and Clevers, H. (2003). Live and let die in the intestinal epithelium. Curr Opin Cell Biol *15*, 763-770.

109. Schindeler, A., McDonald, M.M., Bokko, P., and Little, D.G. (2008). Bone remodeling during fracture repair: The cellular picture. Semin Cell Dev Biol *19*, 459-466.

110. Schlüter, C., Duchrow, M., Wohlenberg, C., Becker, M.H., Key, G., Flad, H.D., and Gerdes, J. (1993). The cell proliferation-associated antigen of antibody Ki-67: a very large, ubiquitous nuclear protein with numerous repeated elements, representing a new kind of cell cycle-maintaining proteins. J Cell Biol *123*, 513-522.

111. Schmidt, M.H., Broll, R., Bruch, H.P., Finniss, S., Bögler, O., and Duchrow, M. (2004). Proliferation marker pKi-67 occurs in different isoforms with various cellular effects. J Cell Biochem *91*, 1280-1292.

112. Scholzen, T., Endl, E., Wohlenberg, C., van der Sar, S., Cowell, I.G., Gerdes, J., and Singh, P.B. (2002). The Ki-67 protein interacts with members of the heterochromatin protein 1 (HP1) family: a potential role in the regulation of higher-order chromatin structure. J Pathol *196*, 135-144.

113. Sharfe, N., Freywald, A., Toro, A., Dadi, H., and Roifman, C. (2002). Ephrin stimulation modulates T cell chemotaxis. European Journal of Immunology *32*, 3745-3755.

114. Shi, Y., He, G., Lee, W.-C., McKenzie, J.A., Silva, M.J., and Long, F. (2017). Gli1 identifies osteogenic progenitors for bone formation and fracture repair. Nature Communications *8*, 2043.

115. Slater, B.J., Lenton, K.A., Kwan, M.D., Gupta, D.M., Wan, D.C., and Longaker, M.T. (2008). Cranial sutures: a brief review. Plast Reconstr Surg *121*, 170e-178e.

116. Smith, J.K. (2020). Osteoclasts and Microgravity. Life *10*, 207.

117. Sobecki, M., Mrouj, K., Colinge, J., Gerbe, F., Jay, P., Krasinska, L., Dulic, V., and Fisher, D. (2017). Cell-Cycle Regulation Accounts for Variability in Ki-67 Expression Levels. Cancer Res *77*, 2722-2734.

118. St-Jacques, B., Hammerschmidt, M., and McMahon, A.P. (1999). Indian hedgehog signaling regulates proliferation and differentiation of chondrocytes and is essential for bone formation. Genes Dev *13*, 2072-2086.

119. Suda, T., Takahashi, N., Udagawa, N., Jimi, E., Gillespie, M.T., and Martin, T.J. (1999). Modulation of Osteoclast Differentiation and Function by the New Members of the Tumor Necrosis Factor Receptor and Ligand Families. Endocrine Reviews *20*, 345-357.

120. Sun, X., and Kaufman, P.D. (2018). Ki-67: more than a proliferation marker. Chromosoma *127*, 175-186.

121. Takagi, M., Natsume, T., Kanemaki, M.T., and Imamoto, N. (2016). Perichromosomal protein Ki67 supports mitotic chromosome architecture. Genes Cells *21*, 1113-1124.

122. Takagi, M., Nishiyama, Y., Taguchi, A., and Imamoto, N. (2014). Ki67 antigen contributes to the timely accumulation of protein phosphatase 1γ on anaphase chromosomes. J Biol Chem *289*, 22877-22887.

123. Takagi, M., Ono, T., Natsume, T., Sakamoto, C., Nakao, M., Saitoh, N., Kanemaki, M.T., Hirano, T., and Imamoto, N. (2018). Ki-67 and condensins support the integrity of mitotic chromosomes through distinct mechanisms. J Cell Sci *131*.

124. Takyar, F.M., Tonna, S., Ho, P.W., Crimeen-Irwin, B., Baker, E.K., Martin, T.J., and Sims, N.A. (2013). Ephrin-B2/EphB4 inhibition in the osteoblast lineage modifies the anabolic response to parathyroid hormone. J Bone Miner Res *28*, 912-925.

125. Tan, S.H., Senarath-Yapa, K., Chung, M.T., Longaker, M.T., Wu, J.Y., and Nusse, R. (2014). Wnts produced by Osterix-expressing osteolineage cells regulate their proliferation and differentiation. Proc Natl Acad Sci U S A *111*, E5262-5271.

126. Teitelbaum, S.L., and Ross, F.P. (2003). Genetic regulation of osteoclast development and function. Nature Reviews Genetics *4*, 638-649.

127. Tonna, S., and Sims, N.A. (2014). Talking among ourselves: paracrine control of bone formation within the osteoblast lineage. Calcif Tissue Int *94*, 35-45.

128. Tonna, S., Takyar, F.M., Vrahnas, C., Crimeen-Irwin, B., Ho, P.W., Poulton, I.J., Brennan, H.J., McGregor, N.E., Allan, E.H., Nguyen, H.*, et al.* (2014). Ephrin-B2 signaling in osteoblasts promotes bone mineralization by preventing apoptosis. Faseb j *28*, 4482-4496.

129. Twigg, S.R., Babbs, C., van den Elzen, M.E., Goriely, A., Taylor, S., McGowan, S.J., Giannoulatou, E., Lonie, L., Ragoussis, J., Sadighi Akha, E.*, et al.* (2013). Cellular interference in craniofrontonasal syndrome: males mosaic for mutations in the X-linked EFNB1 gene are more severely affected than true hemizygotes. Hum Mol Genet *22*, 1654-1662.

130. Twigg, S.R., Kan, R., Babbs, C., Bochukova, E.G., Robertson, S.P., Wall, S.A., Morriss-Kay, G.M., and Wilkie, A.O. (2004). Mutations of ephrin-B1 (EFNB1), a marker of tissue boundary formation, cause craniofrontonasal syndrome. Proc Natl Acad Sci U S A *101*, 8652-8657.

131. van den Elzen, M.E., Twigg, S.R., Goos, J.A., Hoogeboom, A.J., van den Ouweland, A.M., Wilkie, A.O., and Mathijssen, I.M. (2014). Phenotypes of craniofrontonasal syndrome in patients with a pathogenic mutation in EFNB1. Eur J Hum Genet *22*, 995-1001.

132. Van Hooser, A.A., Yuh, P., and Heald, R. (2005). The perichromosomal layer. Chromosoma *114*, 377-388.

133. Vanneste, D., Takagi, M., Imamoto, N., and Vernos, I. (2009). The role of Hklp2 in the stabilization and maintenance of spindle bipolarity. Curr Biol *19*, 1712-1717.

134. Wan, D.C., Kwan, M.D., Lorenz, H.P., and Longaker, M.T. (2008). Current treatment of craniosynostosis and future therapeutic directions. Front Oral Biol *12*, 209-230.

135. Wang, F., Flanagan, J., Su, N., Wang, L.C., Bui, S., Nielson, A., Wu, X., Vo, H.T., Ma, X.J., and Luo, Y. (2012). RNAscope: a novel in situ RNA analysis platform for formalin-fixed, paraffin-embedded tissues. J Mol Diagn *14*, 22-29.

136. Wang, H.U., Chen, Z.-F., and Anderson, D.J. (1998). Molecular Distinction and Angiogenic Interaction between Embryonic Arteries and Veins Revealed by ephrin-B2 and Its Receptor Eph-B4. Cell *93*, 741-753.

137. Wang, Z., Cohen, K., Shao, Y., Mole, P., Dombkowski, D., and Scadden, D.T. (2004). Ephrin receptor, EphB4, regulates ES cell differentiation of primitive mammalian hemangioblasts, blood, cardiomyocytes, and blood vessels. Blood *103*, 100-109.

138. Wieland, I. (2011). Craniofrontonasal Syndrome: Molecular Genetics, EFNB1 Mutations and the Concept of Cellular Interference.

139. Wieland, I., Jakubiczka, S., Muschke, P., Cohen, M., Thiele, H., Gerlach, K.L., Adams, R.H., and Wieacker, P. (2004). Mutations of the ephrin-B1 gene cause craniofrontonasal syndrome. American journal of human genetics *74*, 1209-1215.

140. Wieland, I., Makarov, R., Reardon, W., Tinschert, S., Goldenberg, A., Thierry, P., and Wieacker, P. (2008). Dissecting the molecular mechanisms in craniofrontonasal syndrome: differential mRNA expression of mutant EFNB1 and the cellular mosaic. European Journal of Human Genetics *16*, 184-191.

141. Wilk, K., Yeh, S.A., Mortensen, L.J., Ghaffarigarakani, S., Lombardo, C.M., Bassir, S.H., Aldawood, Z.A., Lin, C.P., and Intini, G. (2017). Postnatal Calvarial Skeletal Stem Cells Expressing PRX1 Reside Exclusively in the Calvarial Sutures and Are Required for Bone Regeneration. Stem Cell Reports *8*, 933-946.

142. Wilkie, A.O. (2005). Bad bones, absent smell, selfish testes: the pleiotropic consequences of human FGF receptor mutations. Cytokine Growth Factor Rev *16*, 187-203.

143. Williams, S.A., Chastek, B., Sundquist, K., Barrera-Sierra, S., Leader, D., Jr., Weiss, R.J., Wang, Y., and Curtis, J.R. (2020). Economic burden of osteoporotic fractures in US managed care enrollees. Am J Manag Care *26*, e142-e149.

144. Worthley, D.L., Churchill, M., Compton, J.T., Tailor, Y., Rao, M., Si, Y., Levin, D., Schwartz, M.G., Uygur, A., Hayakawa, Y.*, et al.* (2015). Gremlin 1 identifies a skeletal stem cell with bone, cartilage, and reticular stromal potential. Cell *160*, 269-284.

145. Wu, N., Yuan-chi, L., Segina, D., Murray, H., Wilcox, T., and Boulanger, L. (2013). Economic burden of illness among US patients experiencing fracture nonunion. Orthopedic Research and Reviews *5*, 21-33.

146. Xiao, G., Wang, D., Benson, M.D., Karsenty, G., and Franceschi, R.T. (1998). Role of the alpha2-integrin in osteoblast-specific gene expression and activation of the Osf2 transcription factor. J Biol Chem *273*, 32988-32994.

147. Xing, W., Kim, J., Wergedal, J., Chen, S.T., and Mohan, S. (2010). Ephrin B1 regulates bone marrow stromal cell differentiation and bone formation by influencing TAZ transactivation via complex formation with NHERF1. Mol Cell Biol *30*, 711-721.

148. Xu, Y., Malladi, P., Chiou, M., and Longaker, M.T. (2007). Isolation and characterization of posterofrontal/sagittal suture mesenchymal cells in vitro. Plast Reconstr Surg *119*, 819-829.

149. Yen, H.Y., Ting, M.C., and Maxson, R.E. (2010). Jagged1 functions downstream of Twist1 in the specification of the coronal suture and the formation of a boundary between osteogenic and non-osteogenic cells. Dev Biol *347*, 258-270.

150. Yilmaz, E., Mihci, E., Guzel Nur, B., and Alper, O.M. (2018). A novel AXIN2 gene mutation in sagittal synostosis. Am J Med Genet A *176*, 1976-1980.

151. Yoshida, T., Vivatbutsiri, P., Morriss-Kay, G., Saga, Y., and Iseki, S. (2008). Cell lineage in mammalian craniofacial mesenchyme. Mech Dev *125*, 797-808.

152. Yu, G., Luo, H., Wu, Y., and Wu, J. (2003). Ephrin B2 induces T cell costimulation. J Immunol *171*, 106-114.

153. Yu, H.M., Jerchow, B., Sheu, T.J., Liu, B., Costantini, F., Puzas, J.E., Birchmeier, W., and Hsu, W. (2005). The role of Axin2 in calvarial morphogenesis and craniosynostosis. Development *132*, 1995-2005.

154. Zhang, X., Ibrahimi, O.A., Olsen, S.K., Umemori, H., Mohammadi, M., and Ornitz, D.M. (2006). Receptor specificity of the fibroblast growth factor family. The complete mammalian FGF family. J Biol Chem *281*, 15694-15700.

155. Zhao, C., Irie, N., Takada, Y., Shimoda, K., Miyamoto, T., Nishiwaki, T., Suda, T., and Matsuo, K. (2006). Bidirectional ephrin-B2-EphB4 signaling controls bone homeostasis. Cell Metab *4*, 111-121.

156. Zhao, H., Feng, J., Ho, T.V., Grimes, W., Urata, M., and Chai, Y. (2015). The suture provides a niche for mesenchymal stem cells of craniofacial bones. Nat Cell Biol *17*, 386-396.

157. Zhou, R. (1998). The Eph family receptors and ligands. Pharmacol Ther *77*, 151-181.

CHAPTER II

MATERIAL AND METHODS

2.1 Generation of ephrin-B2/GFP$^{+/-}$; cre$^{+/-}$; Rosa26tdTomato+ mice

The *ephrin-B2/GFP* allele was used to identify ephrin-B2 expression (Davy and Soriano, 2007). This allele contains an acetylated histone H2B promoter fused to the GFP-coding sequence that is knocked into the ephrin-B2 locus by homologous recombination. The result is constitutive GFP fluorescence in the nuclei of all ephrin-B2-expressing cells. The GFP knock-in allele is maintained as a heterozygote where the knock-in replaces a functional ephrin-B2 protein, as homozygous loss of ephrin-B2 is lethal beyond e9.5 (Gerety and Anderson, 2002). Axin2 expression is marked with *Axin2-cre^{ERT2}* (van Amerongen et al., 2012) in which an estrogen-responsive cre is knocked into the Axin2 locus such that administration of tamoxifen (an estrogen analog) causes the cre protein, expressed in the same pattern as native Axin2, to be active. When paired with the *Rosa26-STOP-loxP-tdTomato* allele, the active cre excises the STOP sequence upstream of the tomato allele producing a strong red fluorescence (Madisen et al., 2010). The tomato allele is typically maintained in the homozygous state, while the cre and GFP alleles are kept heterozygous. For Gli1 lineage tracing, we used the same strategy, but with the *Gli1-cre^{ERT2}* allele (Ahn and Joyner, 2004). Thus, in both lineage tracing experiments, Axin2 or Gli1+ cells fluoresce red, while ephrin-B2-expressing cells glow green.

2.2 Generation of ephrin-B1rTtA/TetOptdTomato$^{+/-}$; cre$^{+/-}$; Rosa26Ai47+ mice

Similarly, the *ephrin-B1rtta/TetOptdTomato* marker allele was used to identify ephrin-B1-expressing cells in the cranial sutures and periosteum. The ephrin-B1 gene-controlled reverse tetracycline trans-activator (rtta) binds to the Tet Operator sequence (TRE) to drive the expression of tomato in the presence of doxycycline (Tet-On system), causing ephrin-B1-expressing cells to fluoresce red. Axin2 expression is marked with *Axin-2cre^{ERT2}* in which an estrogen-responsive cre is knocked into the Axin2 locus such that administration of tamoxifen (an estrogen analog) causes the cre protein, expressed in the same pattern as native Axin2, to be active. When paired with the *Rosa26-STOP-loxP-eGFP* allele, the active cre excises the STOP sequence upstream of the eGFP allele producing a strong green fluorescence. For Gli1 lineage tracing, we used the same strategy, but with the *Gli-1cre^{ERT2}* allele. These allele pairs are typically maintained in a heterozygous state. Thus, in both lineage tracing experiments, Axin2 or Gli1+ cells fluoresce green, while ephrin-B1-expressing cells glow red.

Formation and ossification of the cranial vault begins at around e13.5 in the mouse; therefore, we injected tamoxifen into timed pregnant *ephrin-B2/GFP$^{+/-}$; cre$^{+/-}$; tdtomato*+ females at e13.5, 14.5, and 15.5. At late-stage embryogenesis (e19.5), the embryos were harvested by cesarean section. In *ephrin-B1rtta/TetOptdTomato$^{+/-}$; cre$^{+/-}$; eGFP*+ females, we followed the same tamoxifen injection protocol followed by oral doxycycline 48-72h before late-stage (e19.5) embryo harvest via cesarean section. After light fixation in 4% PFA, the calvaria was whole-mount fluorescence imaged in TEXAS RED and GFP channels to visualize the distribution of tomato+ and GFP+ cells within

the sutures and periosteum, independently, and in merge, keeping the exposure settings for each fluorophore constant within each group (n=3). After demineralization (by immersion in 0.5M EDTA and gentle agitation at 4deg C/1-2d), the skulls were cryoprotected for 1-2d in 30% sucrose [prepared by dissolving 75g sucrose in 250ml 1X Phosphate-Buffered Saline (PBS) at room temperature], before immersion in Optical Cutting Medium (OCT) and immediate freezing in liquid nitrogen. The skulls were then cryosectioned in series at 12µm on to TOMO IHC adhesive (Sta-on coated) glass slides in either sagittal or coronal orientation to bisect the coronal, lambdoid and sagittal sutures**.** Tricolor confocal microscopy was carried out on these sections to count the number of tomato+ cells as a percentage of GFP+ cells and the vice versa (visualized by nuclear Hoechst stain) and double positive (Axin2+/EB1+ or Axin2+/EB2+) cells as a percentage of total cells for each ephrin-B; 10 sections from each suture in 3 different skulls were included using Fiji (Image J).

2.3 Generation of Ephrin-B1loxP$^{-/-}$ or $^{-/y}$; Ephrin-B2loxP$^{-/-}$; cre $^{+/-}$; Rosa26tdTomato+ mice

We generated mice homozygous for the ephrin-B1loxP (EB1loxP) and ephrin-B2loxP (EB2loxP) alleles ((Davy et al., 2004; Gerety and Anderson, 2002) with tdTomato also in homozygous state, but heterozygous for either Axin2cre or Gli1cre. Conditional knockout embryos and wild type littermates were simultaneously generated by mating one cre-heterozygous parent to another cre-negative parent. Under these conditions, cre+ pups (conditional knockouts, cko) will have tomato-labeled cells to track their number

and location, but cre- (controls) will not. To compare these parameters in cko mice to wild type, we will use cre+ mice under Aim1 that do not have the ephrin-B-loxP alleles, as controls, rather than knockout littermates. Various combinations of cko mice relative to stem cell population were generated. As described earlier, formation and ossification of the cranial vault begins at around e13.5 in the mouse; therefore, we injected tamoxifen into timed pregnant *EB1loxP*$^{-/-}$*; EB2loxP*$^{-/-}$*; cre*$^{+/-}$*; tdtomato*+ females at e13.5, 14.5, and 15.5. At late-stage embryogenesis (e19.5), the embryos were harvested by cesarean section.

After light fixation in 4% PFA, the pups were x-ray imaged to detect gross changes in skeletal phenotype, with exposure settings (26Kv/6secs) kept constant for each group. Bright field imaging of the entire embryo (upper and lower half each side) and of the skull separately was done, keeping exposure settings constant within each group. The calvaria was then whole-mount fluorescence imaged in the TEXAS RED Channel to visualize the distribution of tomato+ cells within the sutures and periosteum, keeping the exposure settings constant within each group (n=3). After demineralization (by immersion in 0.5M EDTA and gentle agitation at 4deg C/1-2d), the skulls were cryoprotected in 30% sucrose [prepared by dissolving 75g sucrose in 250ml 1X Phosphate-Buffered Saline (PBS) at room temperature] for 1-2d, before immersion in Optical Cutting Medium (OCT) and immediate freezing in liquid nitrogen. The skulls were then cryosectioned in series at 12µm on to TOMO IHC adhesive (Sta-on coated) glass slides in either sagittal or coronal orientation to bisect the coronal, lambdoid and sagittal sutures, and the sections were stained with Hematoxylin and Eosin to detect

changes in bone thickness, trabecular architecture, and osteoid thickness. Additionally, cell proliferation is a critical influence or parameter in the developing calvarial bone primordia (Jiang et al., 2019; Li et al., 2013; Sun and Kaufman, 2018), and specific markers such as Ki67 has been identified to quantify this parameter. We carried out immunofluorescence (IF) experiments on skull cryosections using a monoclonal antibody against Ki67 to identify changes in the levels of proliferation in ephrin-B1/B2-deficient tomato-labeled Axin2+ cells and compared the signal intensity overlap with that of the control to examine the effect of ephrin-B1/B2 knockout on proliferation.

2.3.1 Immunofluorescence protocol for Ki67

The slides were fixed in 4% PFA for 10mins, then washed in 1X PBS for 5mins (gentle rotation). The slides were then rinsed in PBS-T/Tween20 – 3 times (gentle rotation for 10mins, with 0.3% PBS-T/0.1% Tween20 changed each time) and washed in 1X PBS – 3 times (gentle rotation for 5mins, with 1X PBS changed each time). The slides were then drip-dried around the edges and sections. Once isolated with a PAP pen, the sections were covered with 5% donkey serum as blocking solution (BS) [prepared by adding 50µl DS to 950µl 1X PBS] and incubated for 1hour at RT. The BS was then replaced with the Ki67 primary antibody (1:100 dilution in the same BS) and the sections were incubated at 4deg. C, overnight. Following aspiration of the primary antibody, the slides were then rinsed in 1X PBS – 3 times (gentle rotation for 5mins, with 1X PBS changed each time). The sections were then covered with a fluorophore-conjugated secondary antibody (1:500 dilution) with the slides incubated for 1hour in a

humidified chamber kept in the dark. Following aspiration of the secondary antibody, the slides were then rinsed in 1X PBS 4 times (gentle rotation for 5mins, with 1X PBS changed each time). The slides were then drip-dried and cover-slipped with aqueous mounting medium until dry, after which a sealant was applied along the edges of the coverslip, and stored at 4deg C.

2.4 REFERENCES

1. Ahn, S., and Joyner, A.L. (2004). Dynamic changes in the response of cells to positive hedgehog signaling during mouse limb patterning. Cell *118*, 505-516.
2. Davy, A., Aubin, J., and Soriano, P. (2004). Ephrin-B1 forward and reverse signaling are required during mouse development. Genes Dev *18*, 572-583.
3. Davy, A., and Soriano, P. (2007). Ephrin-B2 forward signaling regulates somite patterning and neural crest cell development. Dev Biol *304*, 182-193.
4. Gerety, S.S., and Anderson, D.J. (2002). Cardiovascular ephrin-B2 function is essential for embryonic angiogenesis. Development *129*, 1397-1410.
5. Jiang, Y., Zhang, S., Mao, C., Lai, Y., Wu, D., Zhao, H., Liao, C., and Chen, W. (2019). Defining a critical period in calvarial development for Hedgehog pathway antagonist-induced frontal bone dysplasia in mice. Int J Oral Sci *11*, 3.
6. Li, S., Meyer, N.P., Quarto, N., and Longaker, M.T. (2013). Integration of multiple signaling regulates through apoptosis the differential osteogenic potential of neural crest-derived and mesoderm-derived Osteoblasts. PLoS One *8*, e58610.

7. Madisen, L., Zwingman, T.A., Sunkin, S.M., Oh, S.W., Zariwala, H.A., Gu, H., Ng, L.L., Palmiter, R.D., Hawrylycz, M.J., Jones, A.R.*, et al.* (2010). A robust and high-throughput Cre reporting and characterization system for the whole mouse brain. Nat Neurosci *13*, 133-140.

8. Sun, X., and Kaufman, P.D. (2018). Ki-67: more than a proliferation marker. Chromosoma *127*, 175-186.

9. van Amerongen, R., Bowman, A.N., and Nusse, R. (2012). Developmental stage and time dictate the fate of Wnt/beta-catenin-responsive stem cells in the mammary gland. Cell Stem Cell *11*, 387-400.

CHAPTER III

RESULTS

3.1. Colocalization of Ephrin-B2 with Axin2+ stem cells in the embryonic calvarial sutures and periosteum

Using the lacZ indicator allele, a robust expression of ephrin-B2-expressing cells was seen in the embryonic calvarial sutures and periosteum at e15.5, with a gradual down regulation of the protein in the suture mesenchyme, periosteum and osteogenic fronts of the calvarial bones at birth (p0). However, in the adult cranium ephrin-B2 expression was mainly restricted to the advancing cranial bone fronts and periosteum with occasional expression in the osteocytes (Fig. 3D). Additionally, treatment of *ex vivo* cultured embryonic calvaria (e17.5) with soluble clustered recombinant ephrin-B2-Fc resulted in a significant increase in bone mass ($p<0.05$) compared to those treated with Ig-Fc control protein (Fig. 3A-C). Furthermore, using the same lacZ indicator in the injured adult calvaria, ephrin-B2 mirrored its expression pattern in the intact calvaria with strong upregulation at the site of injury in the parietal bone adjacent to the sagittal suture (Fig. 4A&B). These observational findings suggest ephrin-B2 as a potential mediator of bone growth.

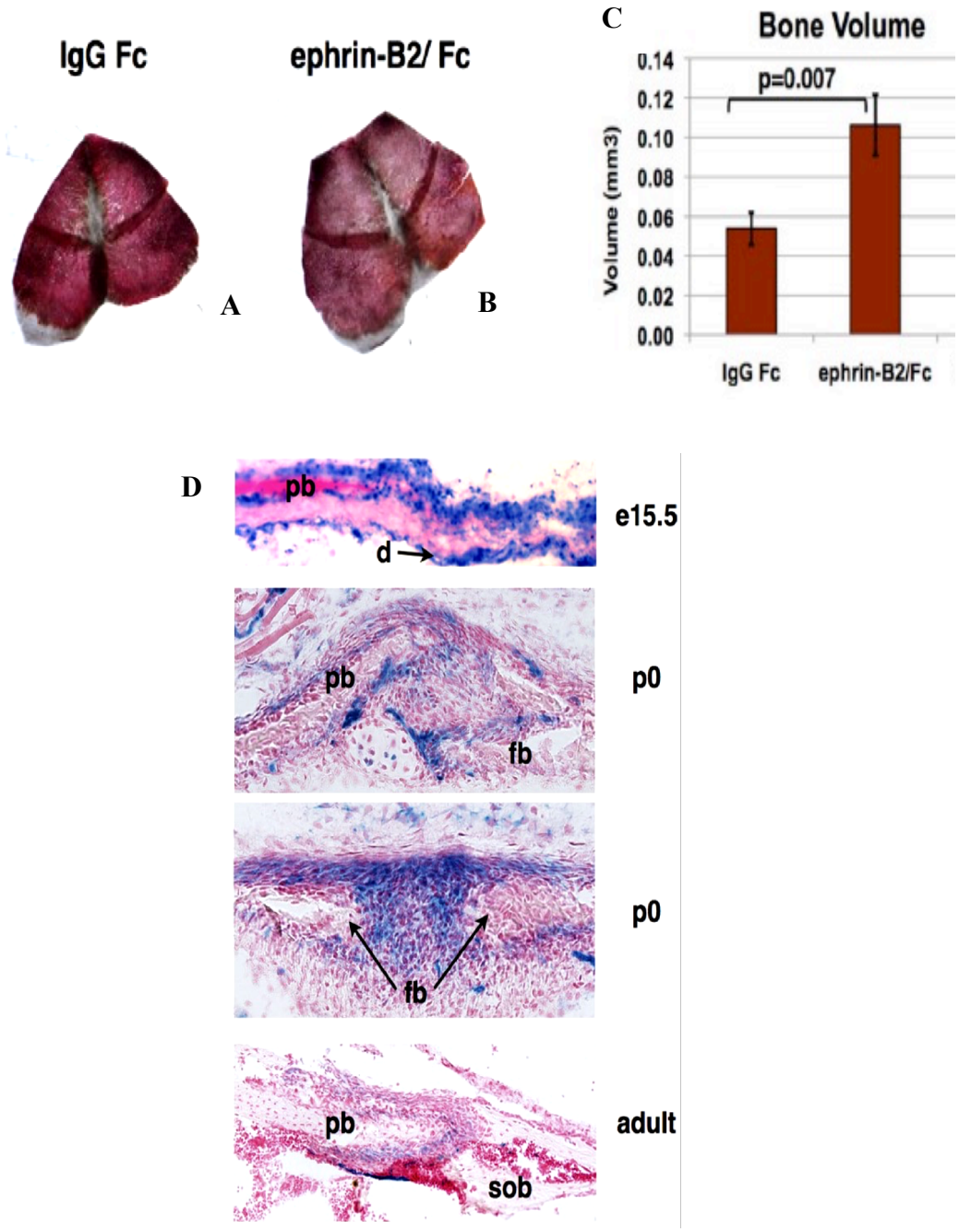

Figure 3 – Treatment of ex vivo embryonic calvaria with soluble, clustered recombinant ephrin-B2 and Ig-Fc control protein (A, B). Graph depicting significant increase in bone mass in embryonic calvaria treated with ephrin-B2-Fc compared to the Ig-Fc treated control (C). Expression of ephrin-B2 is robust in the calvarial sutures at e15.5 embryonic, is still visible in the sutures at p0, but is restricted to the suture in the adult (D).

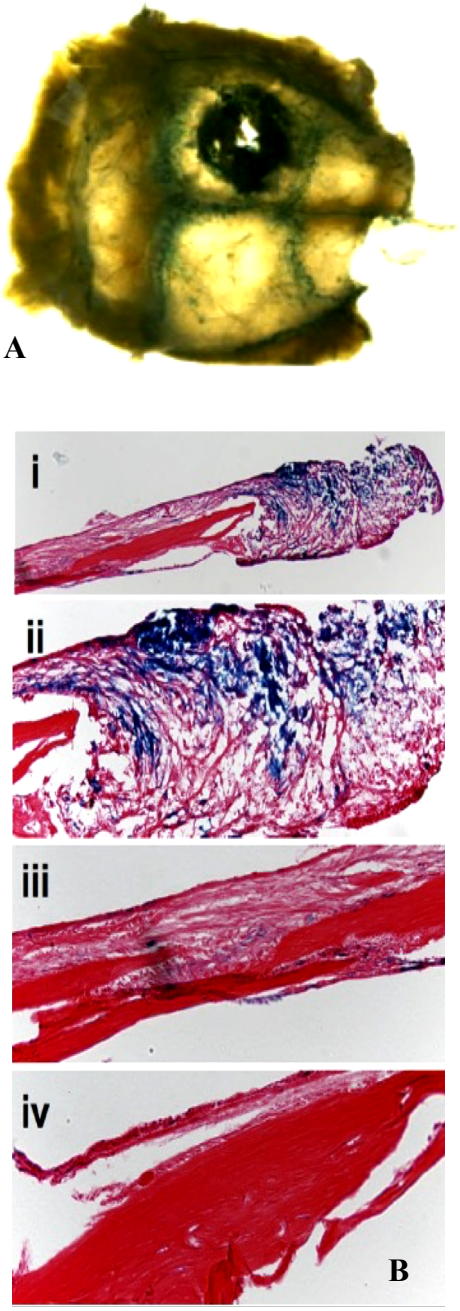

Figure 4 – Wholemount dark-field image of ephrin-B2 expression in the adult calvaria, as indicated by LacZ (A). The sutures and injury defect strongly stain with LacZ. An NFR-stained sagittal section indicating upregulation of ephrin-B2 at the margins of the defect, as indicated by the LacZ indicator (B).

To identify these ephrin-B2-expressing cells in the cranial sutures and periosteum, we hypothesized whether these cells also express Axin2, stem cell marker. Axin2+ stem cells reside in the calvarial suture mesenchyme and are injury responsive. They contribute to calvarial bone injury repair in a cell-autonomous fashion through their long-term clonal expanding, self-renewing and differentiating abilities. Axin2 is critical in calvarial growth and morphogenesis through the regulation of suture patency, as Axin2 null mutants exhibit synostosis of the metopic suture resulting in foreshortening of the anterior cranium including nasal bones, caused by accelerated mineralization and ossification of the sutures through enhanced osteogenic marker expression and increased osteoprogenitor commitment. This suggests that Axin2 is required for 'stemness' or the maintenance of stem cells in their undifferentiated state.

To test the hypothesis, we used a constitutively expressed GFP indicator allele to mark the ephrin-B2-expressing cell and a tomato indicator allele to label Axin2-expressing cells. On wholemount fluorescence imaging of the late-stage embryonic skull, coexpression of Axin2 (in red) and ephrin-B2 (in green) was visible in the calvarial sutures, particularly the coronal and lambdoid sutures. However, in the midline sutures – metopic and sagittal, co-expression of ephrion-B2 and Axin2 was largely confined to the bone fronts flanking the mesenchyme of these sutures. Using confocal microscopy, we found a number of ephrin-B2-expressing cells (green) also expressing Axin2 (red cells) in the e19.5 cranial sutures – mainly in coronal (Fig. 5A-E) and lambdoid sutures (Fig. 7A-E) and periosteum. There was greater variability in the extent of colocalization of ephrin-B2 with Axin2 than in the ratio of double positive cells to

total cells in the coronal (Fig. 6A&B) and lambdoid sutures and periosteum (Fig. 8A&B). However, in the metopic and sagittal sutures, ephrin-B2+ cells colocalized with Axin2+ cells only in the parietal bone fronts (Fig. 9A-E), with absence of this colocalization pattern in the suture mesenchyme (Fig. 10A&B). A total of 12 sutures each for coronal and lambdoid (12 sections/skull – 24 sutures) and 16 for the metopic/sagittal suture (16 sections/skull) were included in the colocalization analysis (n=3). Robust expression of ephrin-B2 (green cells) was also seen in the underlying brain, with Axin2 seen to colocalize with the green cells, though sparse. Some of the chondrocytes in the occipital bone were seen to express both ephrin-B2 and Axin2 suggesting that chondrocytic ephrin-B2 may be required for endochondral bone formation during post-natal growth of the basal cranium. This colocalization pattern therefore suggests that a subset of Axin2+ stem cells is subject to ephrin-B signaling, implying a role for ephrin-B2 signaling in the Axin2+ osteogenic suture mesenchyme. This defines ephrin-B2 as a feature of the Axin2 stem cell niche in the sutures and periosteum of the developing cranium.

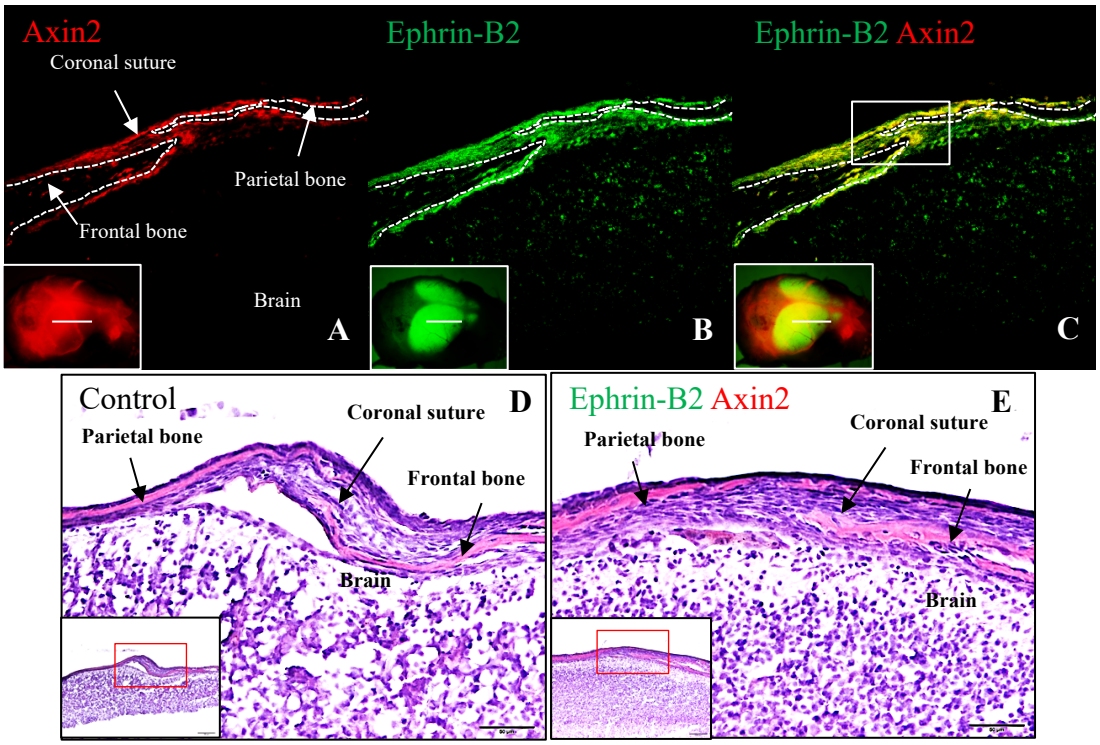

Figure 5 –Green ephrin-B2+ cells (B) colocalize with red Axin2+ stem cells (A) in the Coronal suture and periosteum (C). Inset: corresponding wholemount fluorescent images of an e19.5 calvaria in red, green and merge. H/E-stained images of an adjacent sagittal section (D, E)– Coronal suture – in a GFP+/Tomato+ skull, and a control skull

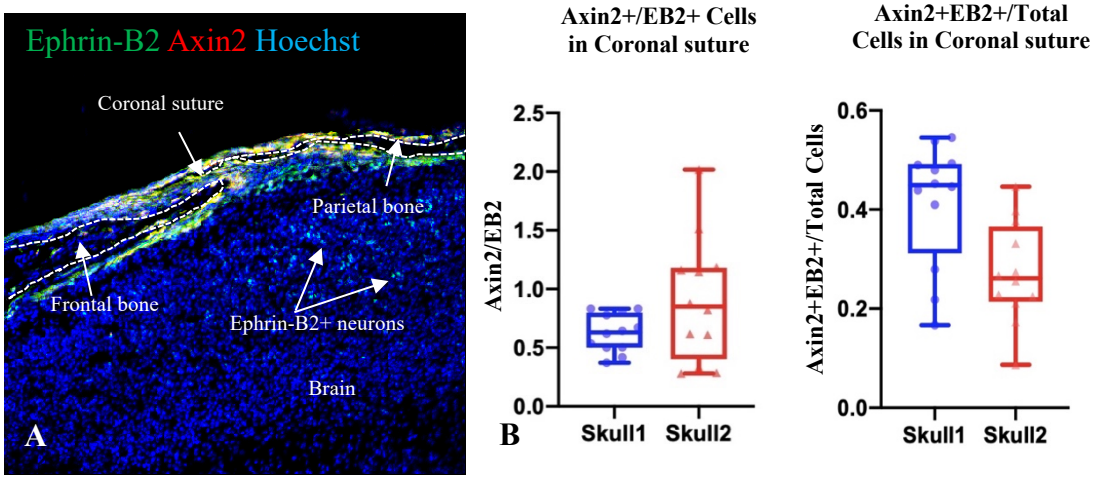

Figure 6 – Hoechst-stained image of the Coronal suture of a GFP+/Tomato+ e19.5 skull (A) to quantify the number of EB2+ cells that also express Axin2, and ratio of Axin2+/EB2+ cells to total cells (B). Hoechst stain was used at 1:1000 dilution.

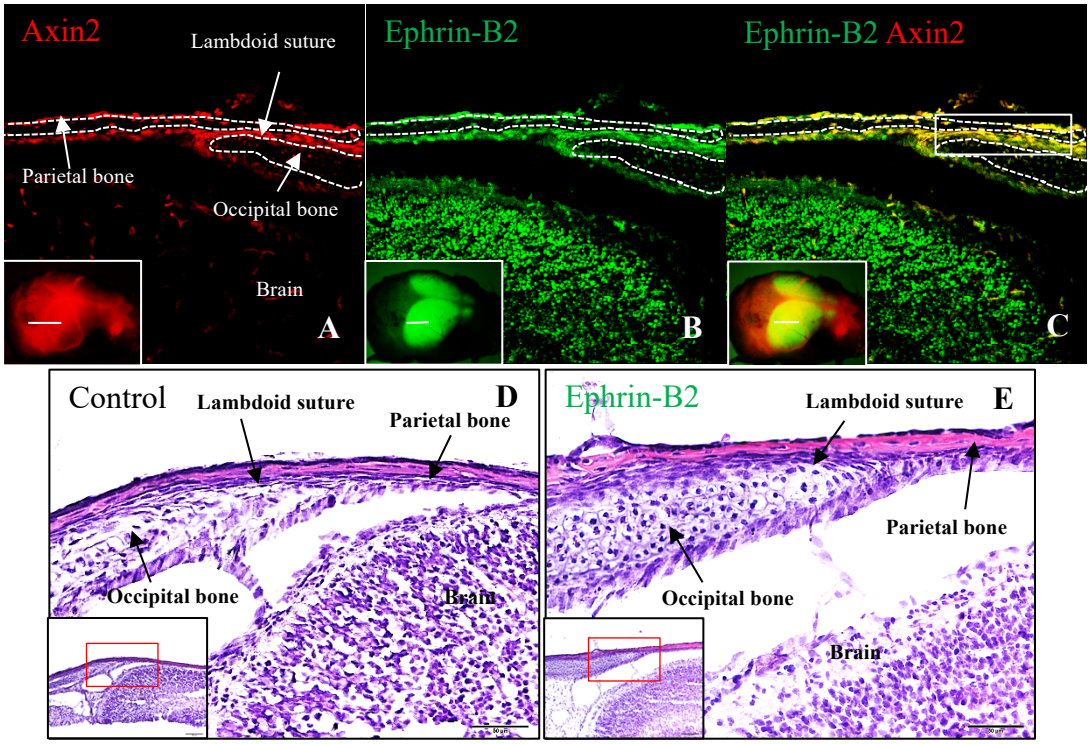

Figure 7 – Green ephrin-B2+ cells (B) colocalize with red Axin2+ stem cells (A) in the Lambdoid suture and periosteum (C). Inset: corresponding wholemount fluorescent images of an e19.5 calvaria in red, green and merge. H/E-stained images of an adjacent sagittal section (D, E) – Lambdoid suture – in a GFP+/Tomato+ skull, and a control skull.

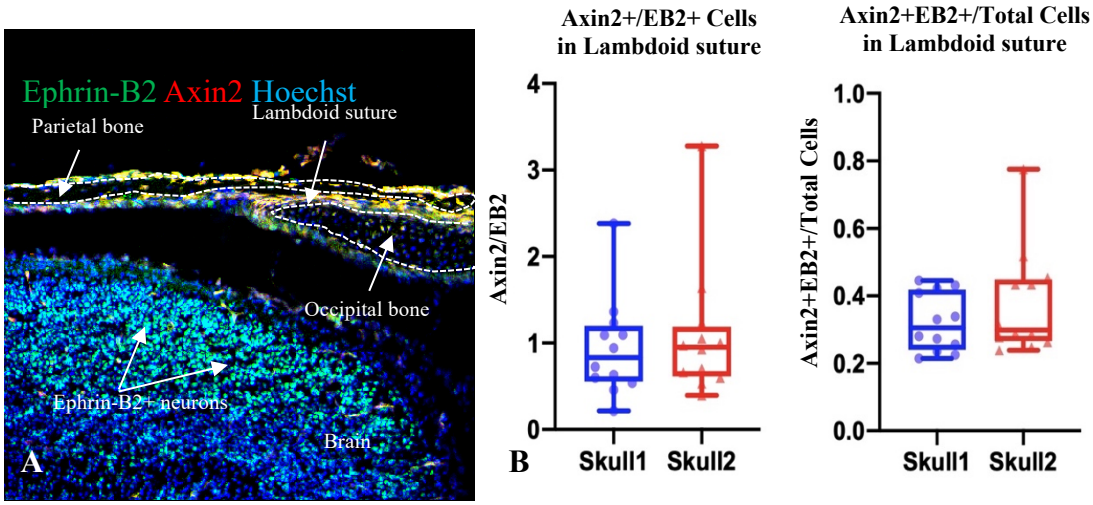

Figure 8 – Hoechst-stained image of the Coronal suture of a GFP+/Tomato+ e19.5 skull (A) to quantify the number of EB2+ cells that also express Axin2, and ratio of Axin2+/EB2+ cells to total cells (B). Hoechst stain was used at a 1:1000 dilution.

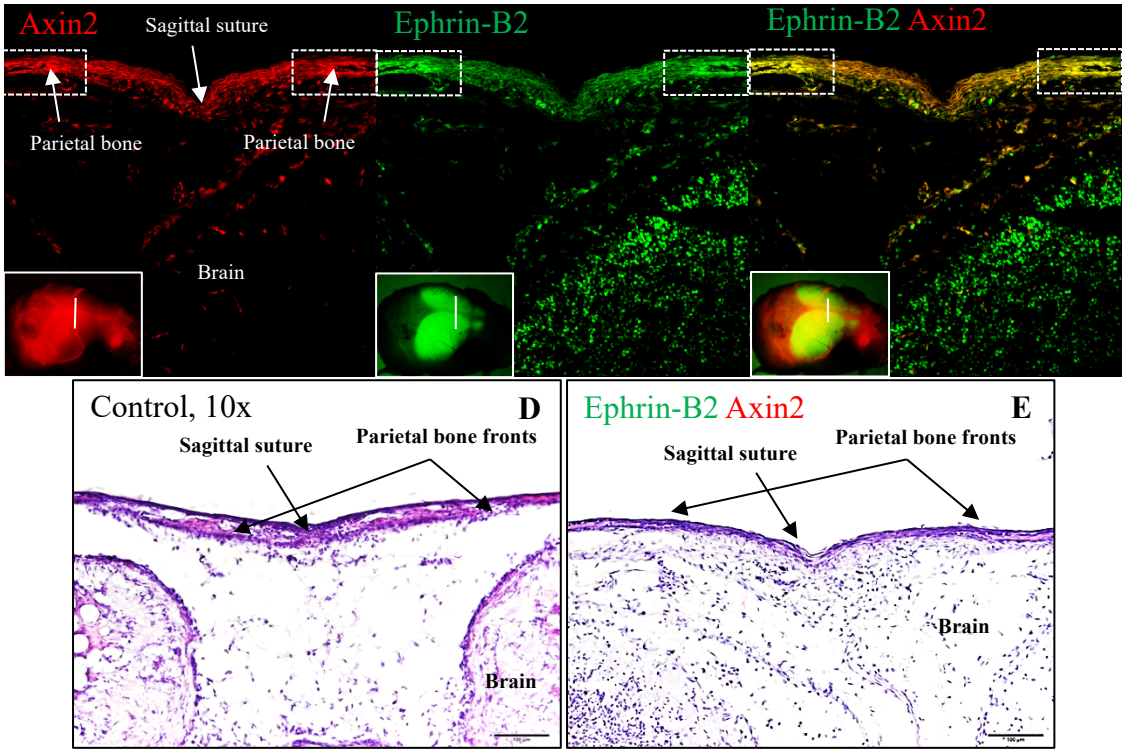

Figure 9 – Green ephrin-B2+ cells (B) colocalize with red Axin2+ stem cells (A) in the periosteum of the parietal bone fronts flanking the Sagittal suture mesenchyme (C). Inset: corresponding wholemount fluorescent images of an e19.5 calvaria in red, green and merge. H/E-stained images of an adjacent coronal section (D, E) – Sagittal suture – in a GFP+/Tomato+ skull, and a control skull.

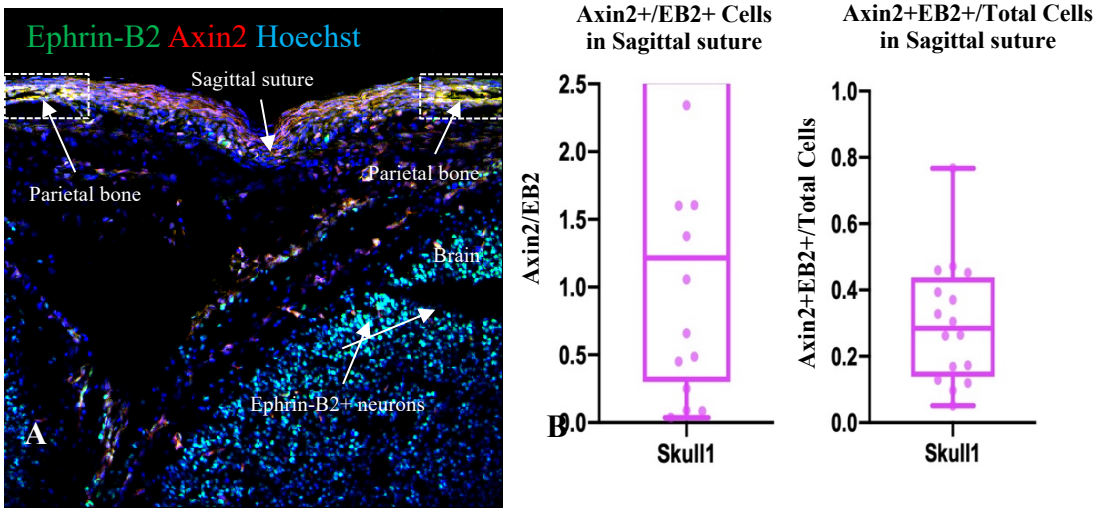

Figure 10 – Hoechst-stained image of the Sagittal suture of a GFP+/Tomato+ e19.5 skull (A) to quantify the number of EB2+ cells that also express Axin2, and ratio of Axin2+/EB2+ cells to total cells (B). Hoechst stain was used at a 1:1000 dilution.

3.2. Colocalization of Ephrin-B1 with Axin2+ stem cells in the embryonic calvarial sutures and periosteum

We generated the EB1rtta+/TetOptdTomato+; Axin2Cre+/Rosa26GteGFP+ line to determine whether ephrin-B1-expressing cells also express Axin2 in late-stage (e19.5) embryonic calvaria. The tomato allele marks ephrin-B1, and eGFP marks the Axin2+ suture stem cells and periosteum. Typically, one of the breeders was heterozygous for Axin2cre-recombinase, with the other three alleles – EB1rtta, TetOp-tdTomato and eGFP – constant in both breeders used for the timed/plug breeding. After 5 attempts, we obtained the desired proportion of embryos in which the expression patterns of ephrin-B1 and Axin2 in the cranial sutures and periosteum were found to be consistent on wholemount fluorescence microscopy. Using confocal microscopy, we found ephrin-B1-expressing cells (red) colocalizing with Axin2-expressing cells (green) in the e19.5 cranial sutures – mainly in coronal (Fig. 11A-E) and lambdoid sutures (Fig. 13A-E) and periosteum, with variability in the extent of colocalization of ephrin-B1 with Axin2 and variability in the ratio of double positive cells to total cells in the coronal (Fig. 12A&B) and lambdoid sutures and periosteum (Fig. 14A&B). A total of 13 sutures each for coronal and lambdoid (13 sections/skull – 26 sutures), and 16 for the sagittal suture (16 sections/skull) were included for colocalization analysis (n=3). However, in the metopic or sagittal sutures (Fig. 15A-E) only the parietal bone fronts flanking the mesenchyme of these sutures were positive for Axin2 (green cells) but not ephrin-B1(red cells); the mesenchyme exhibited no overlap of red with green, as indicated by the quantification results (Fig. 16A&B). Ephrin-B1 expression was robust in the underlying brain, with

Axin2 sparsely colocalizing with ephrin-B1+ neurons. This colocalization pattern suggests that a subset of Axin2+ stem cells is subject to ephrin-B signaling, implying a role for ephrin-B1 signaling in the Axin2+ osteogenic suture mesenchyme. This defines ephrin-B1 a feature of the Axin2 stem cell niche in the sutures and periosteum of the developing calvaria.

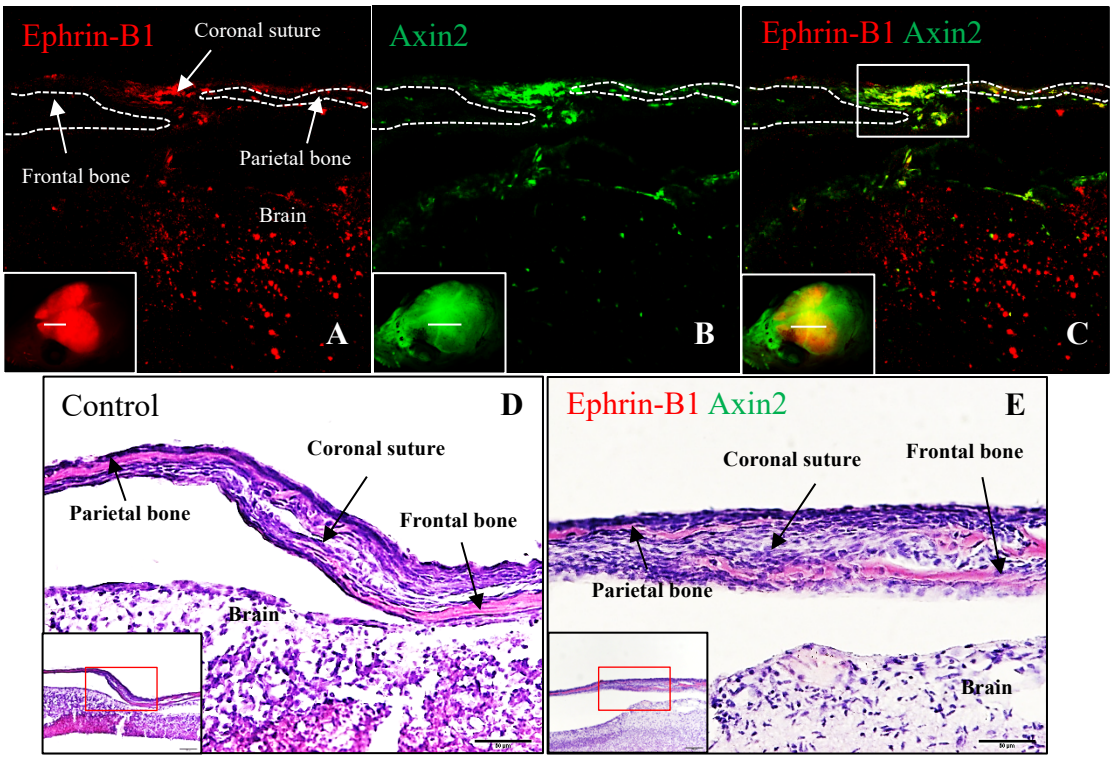

Figure 11 – Red ephrin-B1+ cells colocalize (A) with green Axin2+ stem cells (B) in the Coronal suture and periosteum (C). Inset: corresponding wholemount fluorescence images of an e19.5 calvaria in red, green and merge. H/E-stained images of an adjacent sagittal section (D, E) – Coronal suture – in a Tomato+/eGFP+ skull, and a control skull.

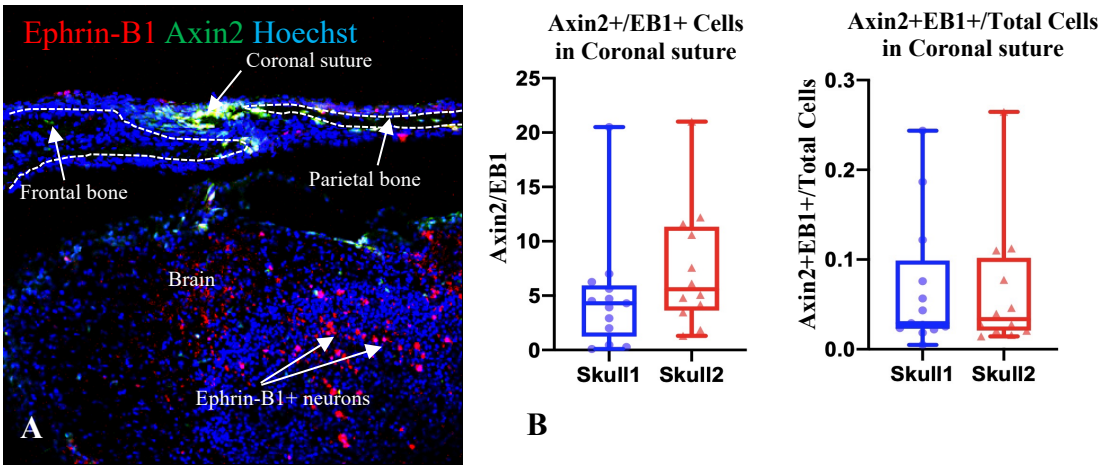

Figure 12 – Hoechst-stained image of the Coronal suture of a Tomato+/eGFP+ e19.5 skull (A) to quantify the number of EB1+ cells that also express Axin2, and ratio of Axin2+/EB1+ cells to total cells (B). Hoechst stain was used at a 1:1000 dilution.

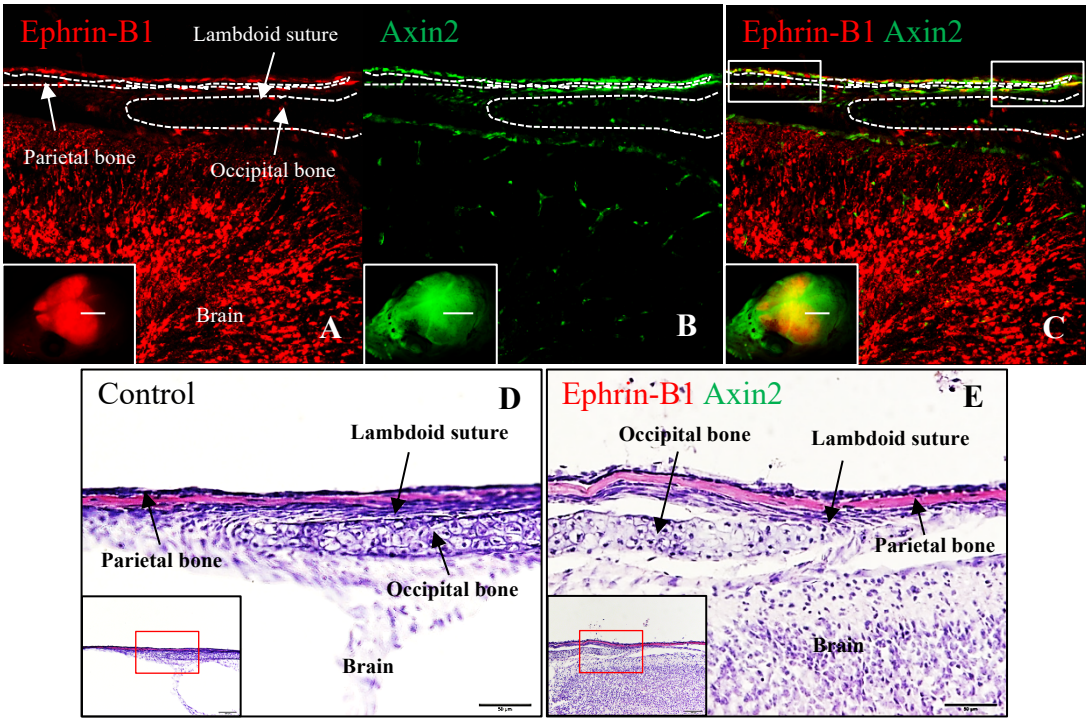

Figure 13 – Red ephrin-B1+ cells (A) colocalize with green Axin2+ stem cells (B) in the Lambdoid suture and periosteum (C). Inset: corresponding wholemount fluorescence images of an e19.5 calvaria in red, green and in merge. H/E-stained images of an adjacent sagittal section (D, E) – Lambdoid suture – in a Tomato+/eGFP+ skull, and a control skull.

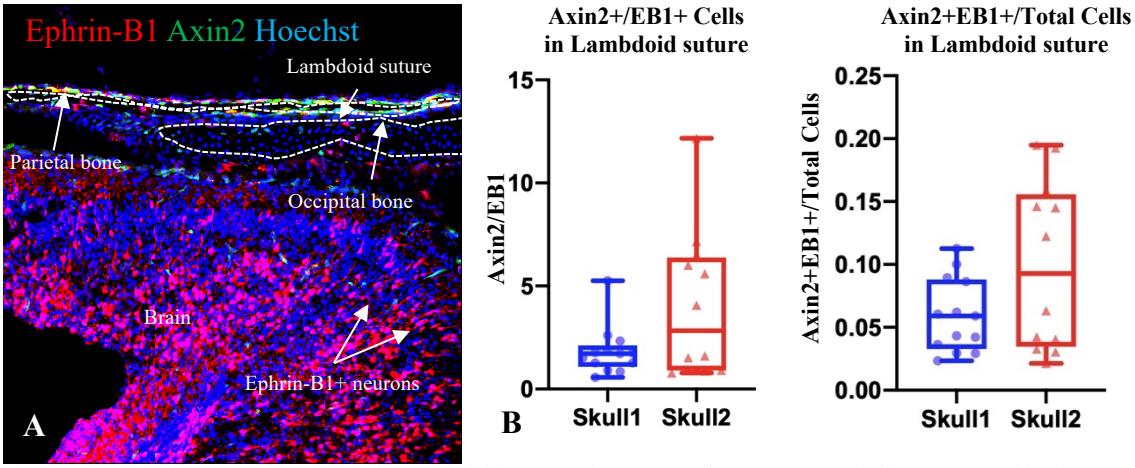

Figure 14 – Hoechst-stained image of the Lambdoid suture of a Tomato+/eGFP+ e19.5 skull (A) to quantify the number of EB1+ cells that also express Axin2, and ratio of Axin2+/EB1+ cells to total cells (B). Hoechst stain was used at a 1:1000 dilution.

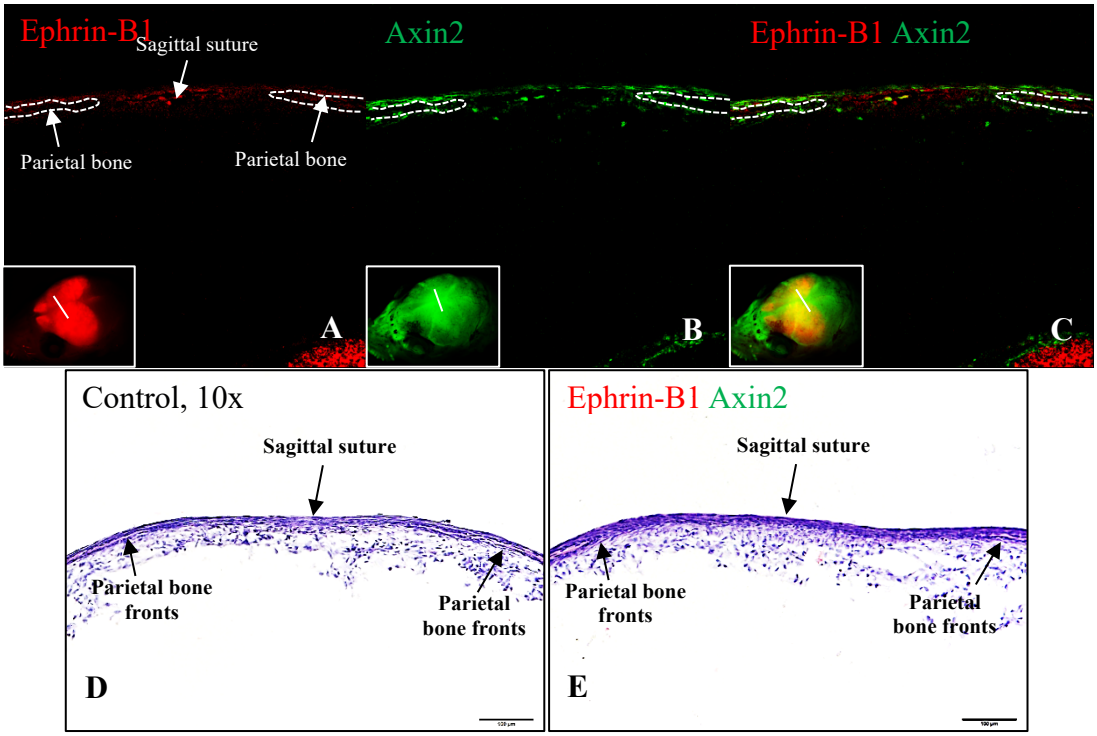

Figure 15A –Absence of colocalization of red ephrin-B1+ cells (A) with the green Axin2+ stem cells (B) in the periosteum of the parietal bone fronts and mesenchyme of the Sagittal suture (C). Inset: corresponding wholemount fluorescence images of an e19.5 calvaria in red, green and merge. H/E-stained images of an adjacent coronal section (D, E) – Sagittal suture – in a Tomato+/eGFP+ skull and a control skull.

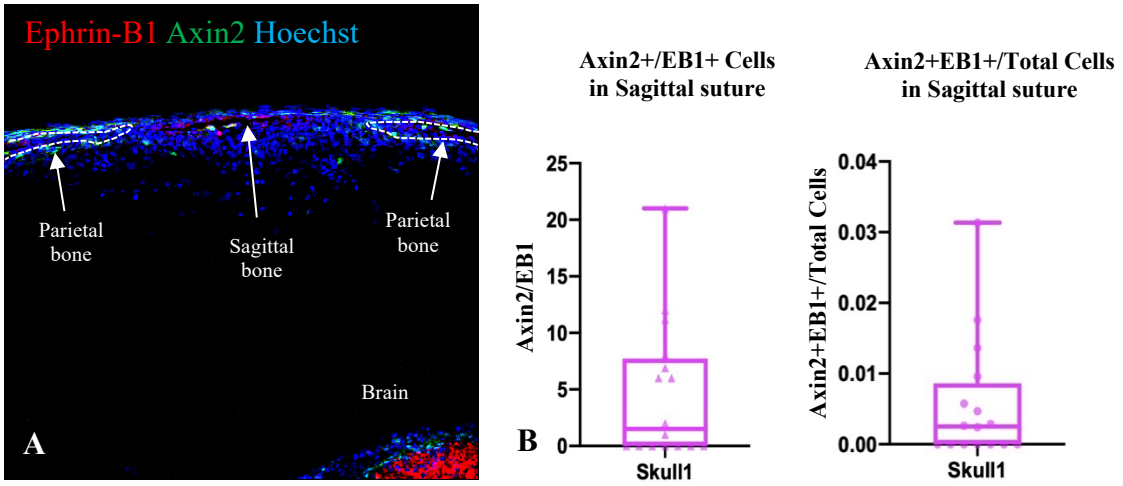

Figure 16 – Hoechst-stained image of the Sagittal suture of a Tomato+/eGFP+ e19.5 skull (A) to quantify the number of EB1+ cells that also express Axin2, and ratio of Axin2+/EB1+ cells to total cells (B). Hoechst stain was used at a 1:1000 dilution.

3.3 Colocalization of ephrin-B2 with Gli1+ stem cells in the calvarial sutures and periosteum

In the adult calvaria, ephrin-B2 colocalized with the Gli1+ stem cells and periosteum of the coronal (Fig. 18A, D, G), lambdoid (Fig. 18B, E, H), and sagittal sutures (Fig. 18C, F, I). Several ephrin-B2-expressing cells were seen to colocalize with Gli1+ cells in the sagittal suture when compared to the coronal and lambdoid sutures. Furthermore, ablation of ephrin-B1/B2 in the Gli1+ sutures and periosteum of the injured adult calvaria (4-6w old mice) did not significantly alter bone healing (Fig. 17C) in both the knockout and control calvaria, as visualized on x-ray (Fig. 17A&B). Moreover, knocking out both these B-ephrins (Fig. 19A-D, E) or ephrin-B2 alone (Fig. 20A-D, E) from e13.5 – e15.5 in the Gli1+ sutures and periosteum of the developing calvaria did not impair cranial or skeletal growth, when analyzed at late gestation (e19.5) using x-ray, bright field imaging, and wholemount fluorescence microscopy (not shown). A total

of 43 late-stage embryos were generated for the combined ephrin-B ablation, and 101 embryos for ablation of ephrin-B2 alone. Because the combined ablation of ephrin-B1/B2 did not perturb cranial growth in the developing Gli1+ embryo, we did not generate Gli1cre/ephrin-B1floxed allele embryos. Thus, further Gli1 conditional knockout studies were discontinued. Hence, colocalization analysis of ephrin-B2 with Gli1+ suture stem cells and periosteum in late-stage embryonic calvaria was not carried out. For similar reasons, colocalization of ephrin-B1 with Gli1 (using the monoclonal ephrin-B1 antibody on cryosections of late-stage ephrin-B2/GFP-; Gli1+/Tomato+ skulls) was not performed.

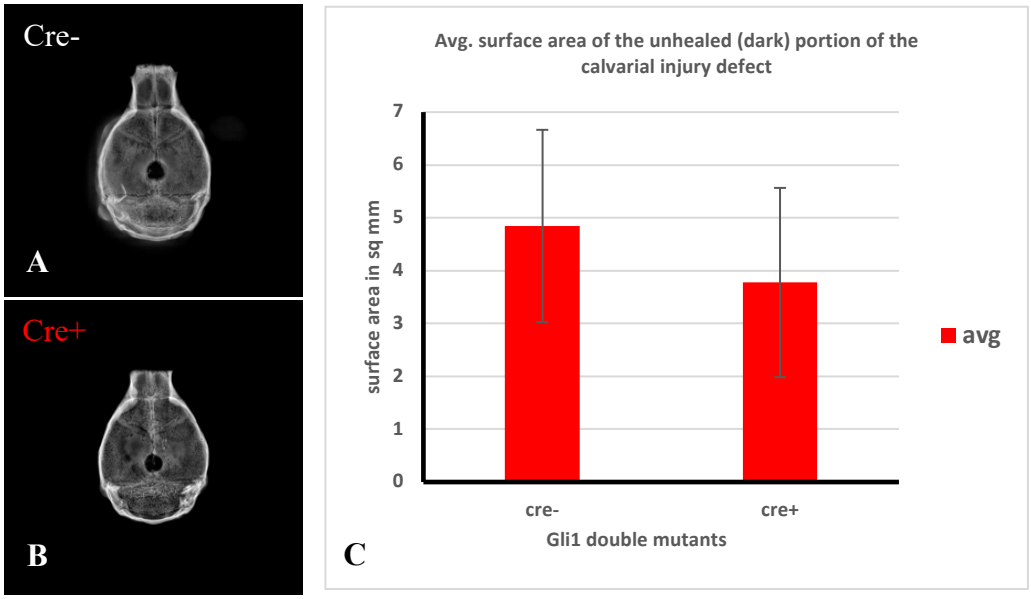

Figure 17 – X-ray images of an injured adult calvaria – Gli1 double knockout (B) and littermate control (A). Comparison of healing rates between the mutant and control calvaria showed no significant differences between them (C); $p>0.05$ ($p=0.22$), using student 't' test, with $n=3$.

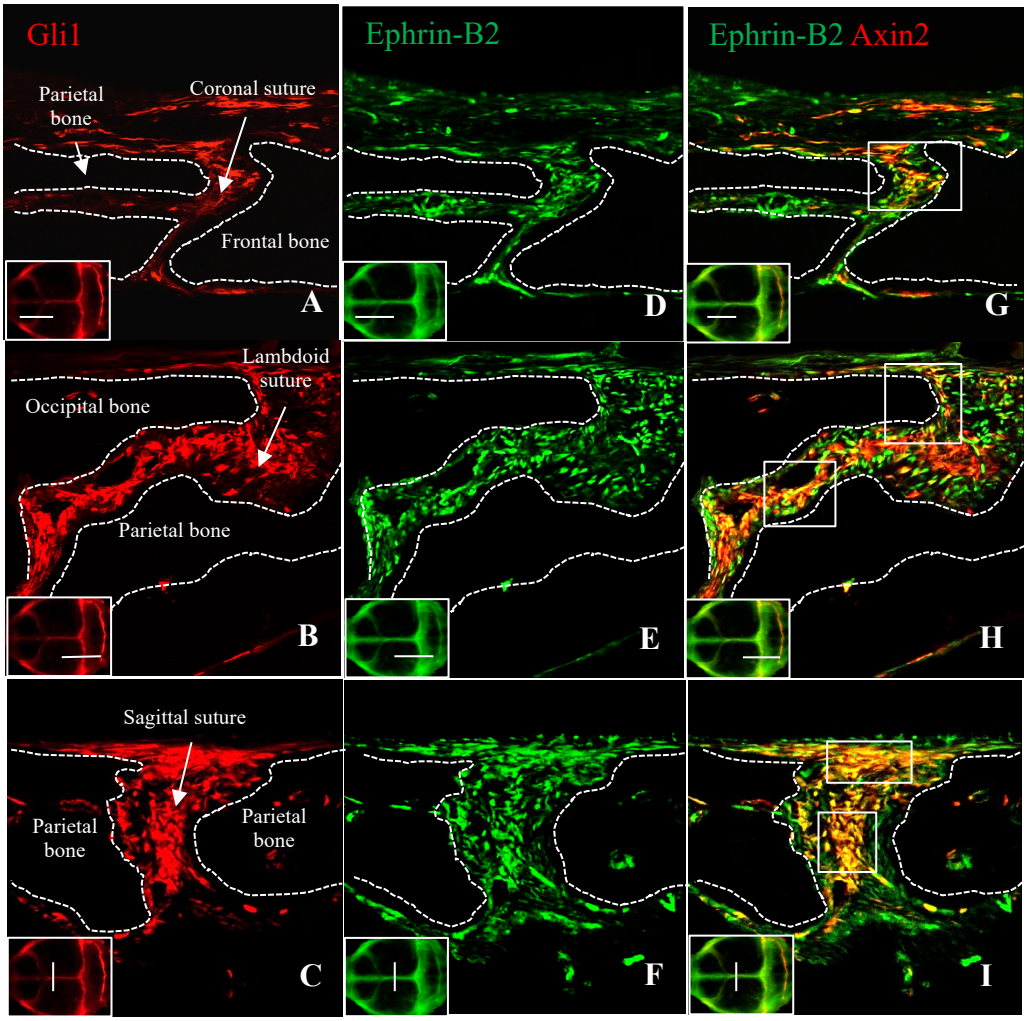

Figure 18 – Robust expression of Axin2+ stem cells in the sutures and periosteum of the adult calvaria (A-C, red panel). Ephrin-B2+ cells seen in the same sutures and periosteum of the calvaria (D-F, green panel). Green ephrin-B2+ cells colocalize with red Axin2+ stem cells in all the cranial sutures and periosteum (C-I). Inset: corresponding wholemount fluorescence images of the adult calvaria in red, green and merge.

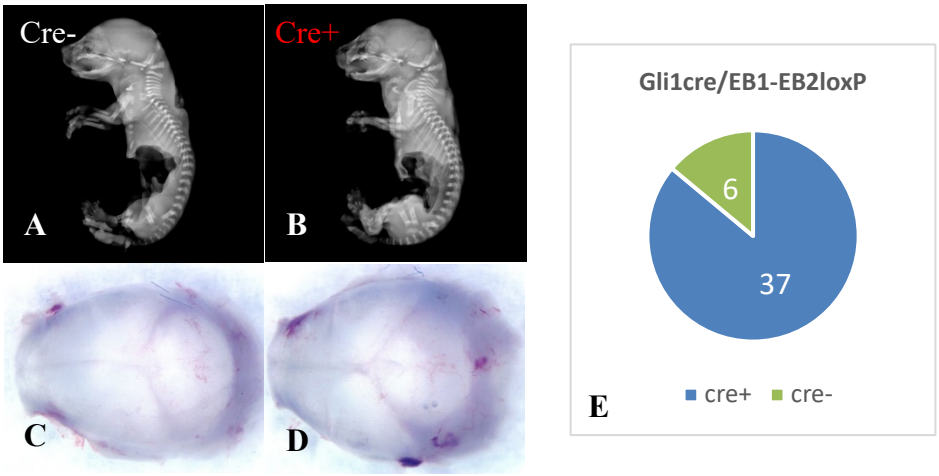

Figure 19 – X-ray and bright field images of late-stage Gli1 double knockout (B) and control embryos (A) and calvaria (D, C) respectively. A total of 43 pups were included in the analysis (n=3). Pie chart depicting proportions of cre- and cre+ late-stage embryos in a 1:6 ratio (E).

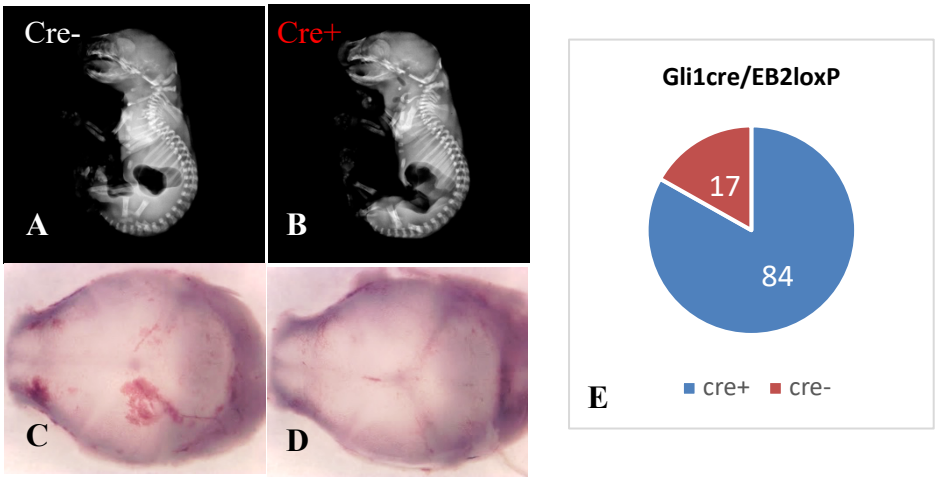

Figure 20 – X-ray and bright field images of late-stage Gli1(ephrin-B2) knockout (B)and control embryos (A) and calvaria (D, C) respectively. A total of 101 pups were included in the analysis (n=3). Pie chart depicting proportions of cre- and cre+ late-stage embryos in a 1:5 ratio (E).

3.4 Role of ephrin-B2 in Axin2+ osteogenic stem cell niche of the developing calvaria

Knocking out ephrin-B2 alone in the Axin2+ suture mesenchyme and periosteum did not impair cranial growth when analyzed at late gestation (e19.5) using x-ray, bright field imaging, and wholemount fluorescence microscopy (not shown) (Fig. 21A-D, E). Fifty-four late-stage embryos were generated of which 31 were cre+ (57%), and the ratio of cre- to cre+ embryos was 2:3. The induction time-points in the pregnant dams were consistently maintained (e13.5-e15.5) and the pups were surgically harvested at e19.5. Ephrin-B2 was maintained in the homozygous state, with ephrin-B1 maintained in the wild-type state, and the tomato-indicator allele identified those embryos with site-specific recombination in the Axin2+ calvarial suture mesenchyme and periosteum. The height and weight of the harvested embryos were not recorded; also, gender assay was done because ephrin-B2 mutations are not sex-linked, but the absence of a cranial phenotype suggests possible functional redundancy between ephrin-B2 and ephrin-B1.

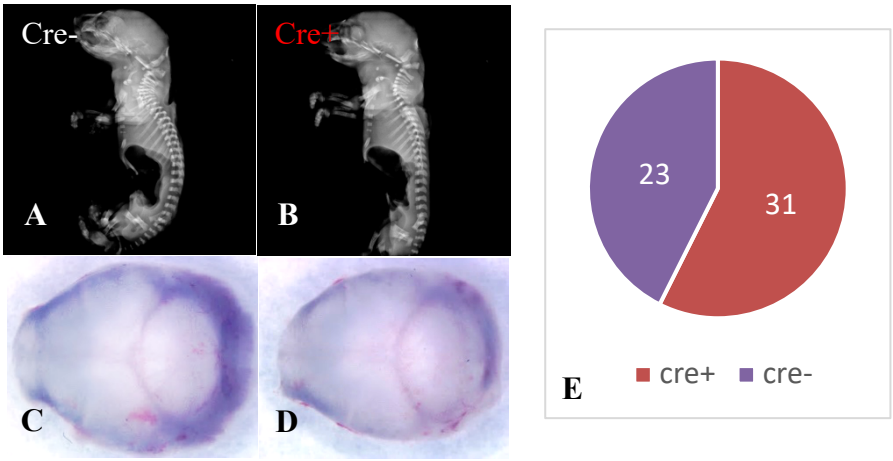

Figure 21 – X-ray and bright field images of late-stage Axin2 (ephrin-B2) knockout (B) and control embryos (A) and calvaria (D, C) respectively. A total of 54 pups were included in the analysis (n=3). Pie chart depicting proportions of cre- and cre+ late-stage embryos in a 2:3 ratio (E).

3.5. Role of ephrin-B1/B2 in Axin2+ osteogenic stem cell niche of the developing calvaria

In applying the same experimental conditions, we analyzed the effect of combined ablation of ephrin-B1/B2 in Axin2+ developing suture niche. The ablation of both these ephrins in the Axin2+ osteogenic niche and periosteum of the developing calvaria resulted in significant perturbation of calvarial bone growth. The bones of both the neural crest and paraxial mesoderm failed to form resulting in exposure of the underlying brain, a condition termed exencephaly. Calvarial agenesis was accompanied by varying degrees of facial dysmorphogenesis with foreshortening of the cranial base and cervical spine disruption, while the remainder of skeleton appeared normal on x-ray. A range of craniofacial phenotypes including exencephaly were appreciable on bright field imaging (Fig. 22A-F). A total of 181 pups were generated of which 74 were cre+ (Fig. 22G&H); of these, 15 embryos exhibited exencephaly at a 20% penetrance that was consistently maintained during individual timed breedings, with females exhibiting the phenotype more frequently than males in the ratio of ~3:1. The height and weight of the embryos harvested from rounds 3, 4 and 5 were recorded, but gender determination (Y allele, 185bp) was done for all the embryos, as mutation in ephrin-B1 is sex-linked. Though there was a significant difference in weight ($p<0.05$), though not in height between the knockout and control embryos. Though height was not greatly affected, the embryos with exencephaly had significantly lower body weight, when compared to the non-knockout littermates (Fig. 23A&B). This could be due to an actual decrease in body weight without any effect on body length (height) in each of the affected pups.

Interestingly, 59 of the 74 pups were also cre+ but did not exhibit exencephaly, suggesting possible presence of a threshold for site-specific recombination in the cranial sutures and periosteum in this proportion of knockouts, while in those that exhibited exencephaly the threshold was achieved. Further, knocking out both ephrin-B1/B2 adversely impaired Axin2+ stem cell function in the osteogenic suture niche, suggesting that these ephrins work in tandem in regulating the suture niche.

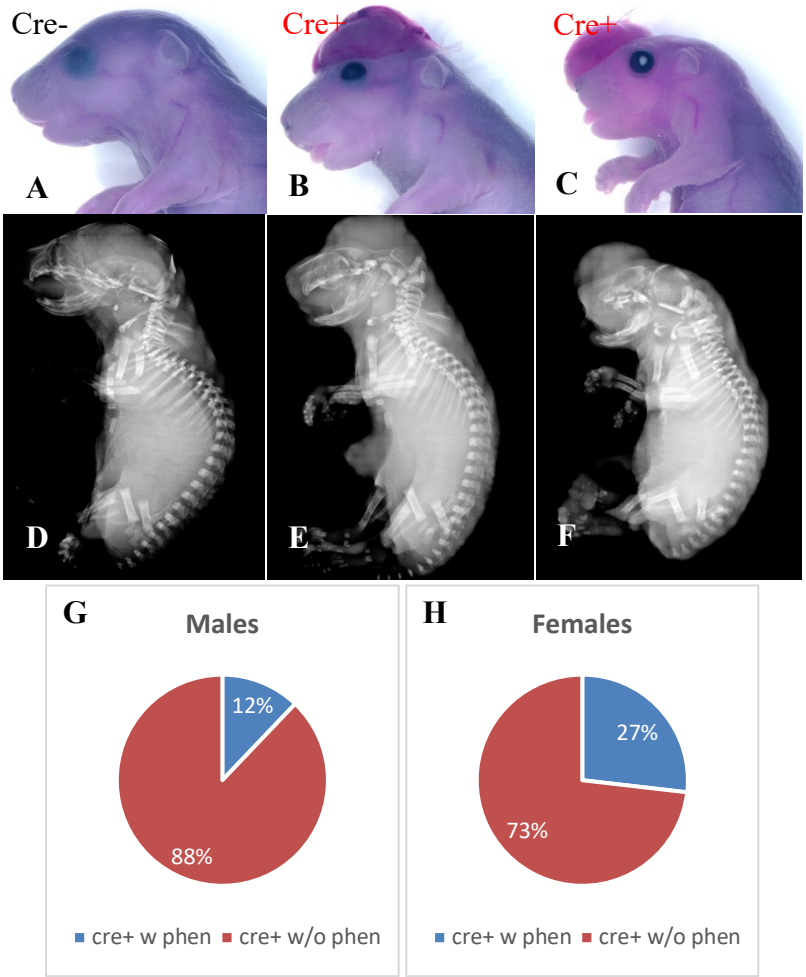

Figure 22 – Bright field and x-ray images of late-stage Axin2 double knockout (B, E/ C, F) and control embryos (A, D). Pie chart depicting proportions of late-stage male and female embryos with or without exencephaly. The ratio of male to female embryos with exencephaly was 1:3, with a phenotypic penetrance of 20% (G, H).

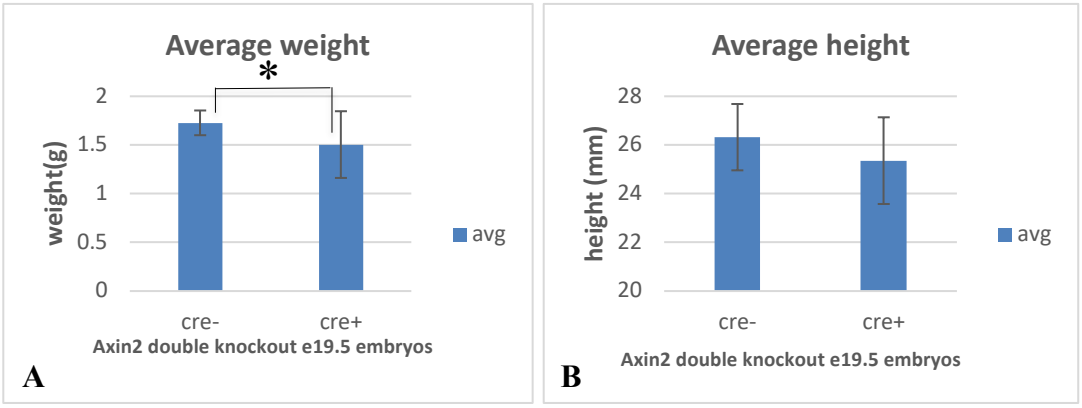

Figure 23 – Graphs representing average weight (A) and height (B)between Axin2 double mutants and littermate controls. $p<0.05$ was considered significant, using student 't' test. At $p<0.05$, there was significant difference in weight ($p=0.003$) but not height ($p=0.058$) between the two groups.

It may also be hypothesized that calvarial agenesis may be the direct result of failure of stem cell migration from the cranial neural crest i.e., from the supraorbital ridge where they initially condense before migrating to the apex of the calvaria – in a caudal-to-rostral direction, beginning at e11.5, followed by apical migration at e13.5, to form the frontal bone primordia – including those precursors from the paraxial mesoderm. This failure of migration may occur in conjunction with other effects such as decreased stem cell proliferation or increased apoptosis of the neural crest and mesoderm mesenchymal precursors. Further experiments are warranted to test these hypotheses. On histology, the mutant skull was devoid of the cranial bones with an apparent overall decrease in length of the cranial base synchondrosis with varying degrees of facial bone dysmorphogenesis. The tooth germs also appeared smaller in the mutant compared to the littermate control. Tooth growth arrest in the mutant resulted in tooth buds acquiring a cap-stage phenotype in comparison to those of the control littermate that exhibited the relatively normal bell-stage phenotype. (Fig. 24A-E).

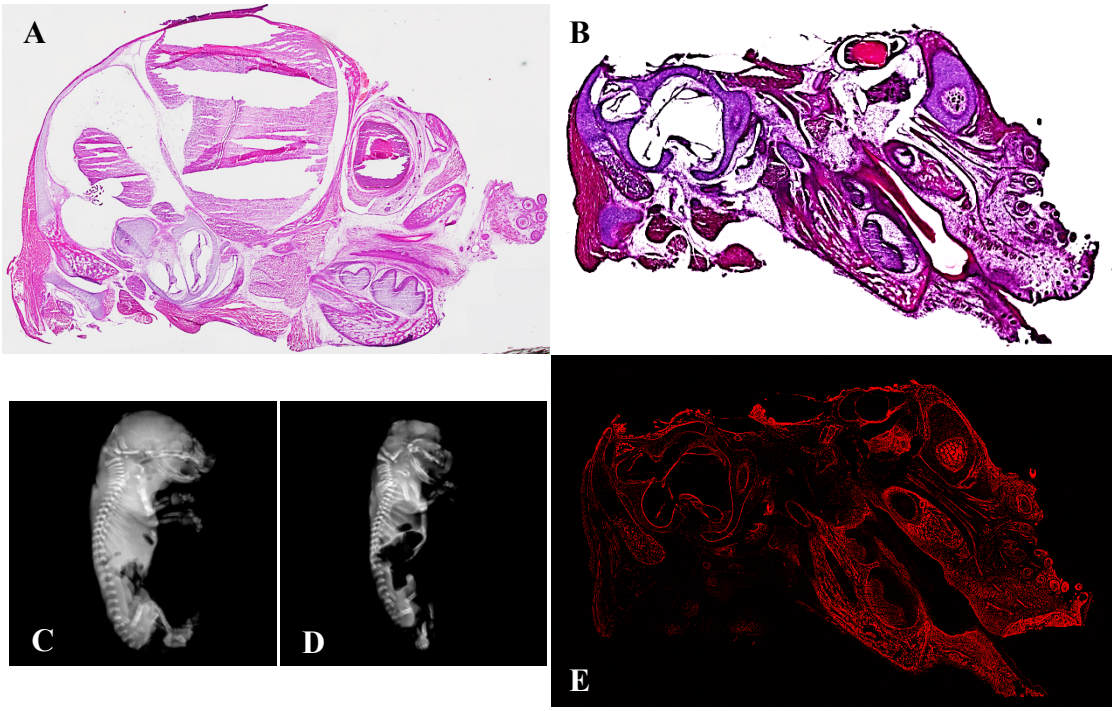

Figure 24 – H/E-stained sagittal sections of the control and exencephalic mutant skull. The calvarial sutures noted in the control skull (A) are not seen in the mutant (B), owing to agenesis of the calvarial bones. Skull growth arrest caused by foreshortening of the cranial base synchondrosis, as visualized on x-ray (C, D). An adjacent sagittal section of the exencephalic mutant showing tomato-labeled ephrin-B1/B2-deficient Axin2-expressing cells throughout the skull (E).

The failure of the calvarial bones to form following ablation of ephrin-B1/B2 in the Axin2 suture stem cell population may be more attributable to a failure in stem cell migration than a decrease in cell proliferation, as Ki67+/Axin2+ cells were seen to aggregate at the edge of the posterior calvarial defect (Fig. 25A&B, C-F) However, the effect of this combined ephrin-B ablation on Axin2 stem cell apoptosis or differentiation to form the frontal and parietal bone primordia cannot be ruled out. Moreover, earlier serial induction-harvest timepoints would provide a more informative picture of the effect of combined ephrin-B ablation in the Axin2 stem cell migration, proliferation, apoptosis and differentiation. Hence, more experiments are warranted to confirm these.

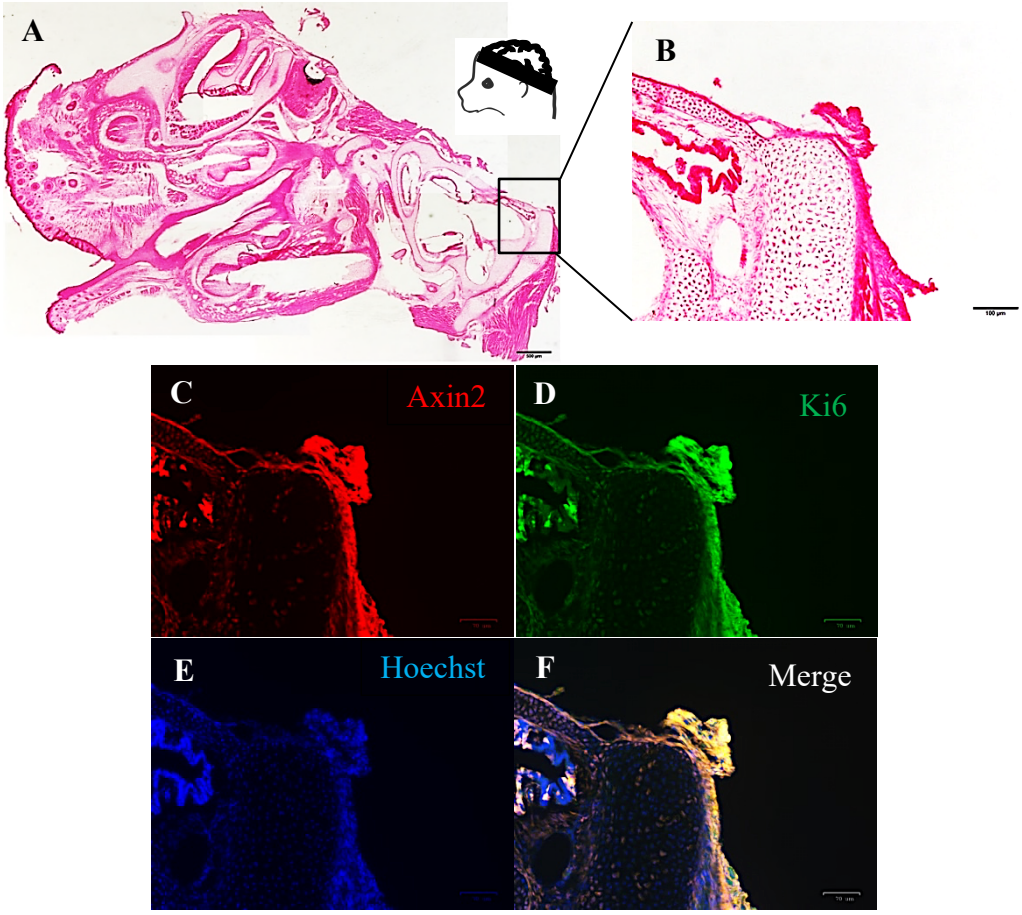

Figure 25 – NFR-stained sagittal section of an exencephalic mutant skull (A, B). Inset depicting a schematic representation of the exencephalic skull. Adjacent section in B exhibiting an aggregation of Ki67+/Axin2+ cells at the edge of the posterior calvarial defect, suggesting that actively proliferating Axin2-expressing cells fail to migrate in a caudal-to-rostral direction following ablation of ephrin-B1/B2 in these cells (C-F).

Further, we wanted to analyze the effect of combined ablation of these ephrins on postnatal calvarial and/or skeletal bone growth, using the same prenatal induction protocol (e13.5 -e15.5). Initially, we allowed the induced pregnant dams to deliver their babies at full term, but on both the occasions we lost two dams to respiratory distress following extreme labor. To overcome this, we surgically harvested the pups at e20.5 and surrogate them to another nursing/ lactating dam belonging to the same line.

Unfortunately, the surrogated pups did not survive for more than a day because the induced pups were not functionally viable and so the nursing dam rejected them. This procedure was repeated at least 8 times and on all the occasions we failed to obtain progeny that would permit analysis of a post-natal skeletal phenotype.

Stochastic events, possibly arising from epigenetic factors, gene pleiotropism or teratogenesis occurred in three late-stage embryos – two that exhibited exencephaly following combined ablation of ephrin-B1/B2 in the Axin2+ suture stem cell population, and one embryo that exhibited anencephaly following ablation of only ephrin-B1 from this stem cell population. To that end, it is possible that one of the double knockout embryos exhibited exencephaly through Axin2cre-mediated excision of the cre-coding domain of the genomic DNA (called gene auto-excision or self-excision), as the embryo typed negative for the Axin2cre allele (as indicated by a 500bp band) on GE; in the other embryo, the phenotype was clearly a consequence of Axin2cre homozygosity, as the embryo typed positive for an extra copy of the Axin2cre knock-in allele (as indicated by a 300bp band) on GE. The anencephalic phenotype in the ephrin-B1 single knockout embryo may be the result of gene auto-excision, because it typed negative for both Axin2cre allele (as indicated by a 500bp band) and Ephrin-B1 'del' allele (as indicated by a 700bp band) on GE, or it could be a consequence of drug-induced teratogenesis. Therefore, these embryos were not included in the analysis. Further, in generating late-stage embryos for ephrin-B1/Axin2 colocalization analysis, we did obtain two embryos that exhibited exencephaly following tamoxifen induction (at e13.5-e15.5) together with oral doxycycline but both the embryos typed positive for EB1rtta (as indicated by a

400bp band) and cre (as indicated by a 534bp band) on GE, implying that this phenotypic consequence may be the result of drug-induced teratogenesis only.

3.6. Role of ephrin-B1 in Axin2+ osteogenic stem cell niche of the developing calvaria

Because ephrin-B2 failed to perturb cranial bone growth following its ablation in the Axin2+ suture stem cells and periosteum, Axin2cre/EB1loxP embryos were generated to define the functional contribution of ephrin-B1 in niche establishment and maintenance during calvarial growth and morphogenesis. This ephrin is important in calvarial bone growth, because mutations in ephrin-B1 result in human cranio-frontonasal syndrome in which synostosis of the coronal suture is a typical manifestation. Eighty-one late-stage embryos were harvested following ablation of ephrin-B1 (e13.5-e15.5); of these, 28 pups were cre+ i.e., 10 males and 18 females. Only 1 male embryo exhibited considerable facial dysmorphogenesis sparing the frontal bones and the rest of the cranial vault when examined on bright field imaging and wholemount fluorescence microscopy (not shown), with the remainder of the skeleton appearing unaffected on x-ray (Fig. 26A-D, E). The height and weight including gender determination of all the pups were recorded. The differences in height and weight between the ephrin-B1 knockout and control embryos was significant ($p<0.05$), possibly due to deficient functional ephrin-B1 protein in the mutant skeleton (Fig. 27A&B) and again in those embryos where ephrin-B1 was knocked out, there was no observable phenotype in the cranial vault, suggesting possible

functional redundancy between ephrin-B1 and ephrin-B2. Interestingly, none of the female embryos exhibited the phenotype of exencephaly.

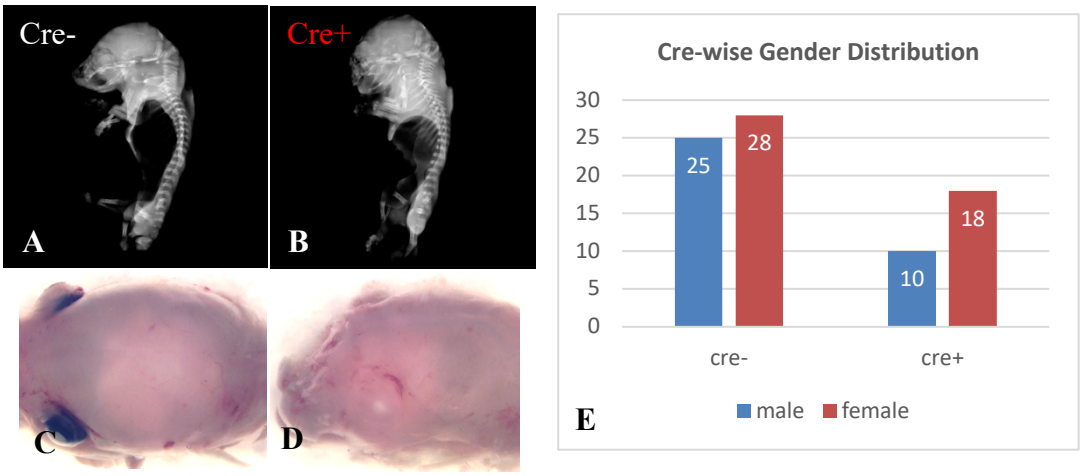

Figure 26 – X-ray and bright field images of late-stage Axin2 (ephrin-B1) knockout (B) and control (A) embryos and skulls (D, C), respectively. Graph depicting twice as many females compared to males that did not exhibit the calvarial phenotype, though only one male exhibited facial dysmorphogenesis sparing the frontal calvaria (E).

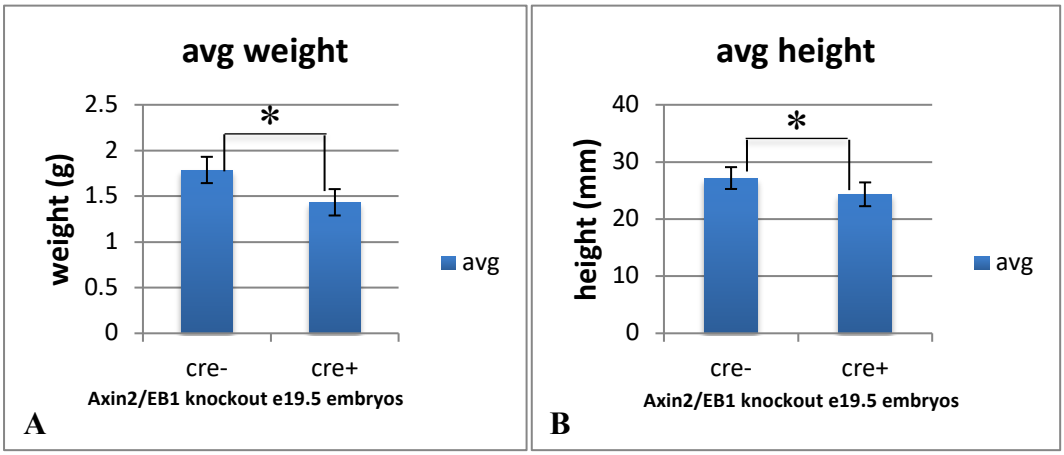

Figure 27 – Graphs representing average weight (A) and height (B) between Axin2 ephrin-B1 mutants and littermate controls. $p<0.05$ was considered significant, using student t test. At $p<0.05$, there was significant difference in weight ($p=0.001$) and height ($p=0.03$) between the two groups.

CHAPTER IV

DISCUSSION

Skeletal growth deficiencies arising from birth defects, injury or disease exist despite advances in therapy, and this reflects the need for a deeper understanding of its causes before more effective therapies can be designed and applied in the setting of defective bone growth. The morbidity associated with defective or deficient bone growth is considerable and affects the majority of the American population, with high management costs that inevitably burden the economy (Williams et al., 2020). Though autogenous bone grafts remain the cornerstone of treatment for bone growth deficiencies, cell-based therapies offer viable treatment alternatives in this setting.

The molecular underpinnings controlling bone growth are complex, however, the exact mechanism remains unclear. It is well known that the craniofacial skeleton forms from the neural crest mesenchyme, with the parietal bones forming from paraxial mesoderm. Calvarial bone growth is regulated by interactions between the cranial sutures and periosteum and involves a complex network of signaling pathways and growth factors that ultimately specify mesenchymal lineage fate, the mutations of which frequently result in craniosynostosis (Benson and Opperman, 2011). Ephrins and Eph-kinases constitute a unique signaling system in calvarial bone growth, and mutations in genes encoding these proteins result in synostosis of the cranial sutures. Discovered in 1987, Eph kinases constitute the largest subfamily of Receptor Tyrosine Kinases, totaling 14 and are classified into EphA and EphB kinases, based on sequence of

homology and ligand binding affinity. The ligands or 'ephrins' total 8 and are classified in a similar manner into A-ephrins and B-ephrins (Hirai et al., 1987; Rundle et al., 2016). The membrane-bound ephrin-B ligands are of importance because important roles for them have been described in developmental and reparative osteogenesis including bone homeostasis through bidirectional signaling events (Xing et al., 2010; Zhao et al., 2006).

Using the lacZ indicator allele, we found a robust expression of ephrin-B2-expressing cells in the embryonic calvarial sutures and periosteum at e15.5, with a gradual down regulation of the B-ephrin in the suture mesenchyme and periosteum, and osteogenic fronts of the calvarial bones at birth (p0). However, in the adult cranium ephrin-B2 expression was mainly restricted to the suture mesenchyme and periosteum with occasional expression in the osteocytes. Furthermore, using the same lacZ indicator in the injured adult calvaria, ephrin-B2 mirrored the expression pattern in the sutures of the (intact) calvaria with strong upregulation at the site of injury in the parietal bone adjacent to the sagittal suture. This suggests that ephrin-B2 controls the migration of stem cells from the suture mesenchyme to the site of injury. Additionally, treatment of *ex vivo* embryonic calvaria with soluble, clustered recombinant ephrin-B2 resulted in a dramatic increase in calvarial bone mass compared to those treated with Ig-Fc control protein (Benson et al., 2012). These findings therefore hypothesized ephrin-B2 as a potential mediator of bone growth. To identify these ephrin-B2-expressing cells in the cranial sutures and periosteum, we hypothesized whether these cells also express Axin2, stem cell marker. Axin2+ is one of two major stem cell populations central to calvarial

growth and maintenance, the other being Gli1(Zhao et al., 2015). Axin2+ stem cells reside in the central portion of the calvarial sutures; being injury responsive, they contribute to calvarial bone injury repair in a cell-autonomous fashion through clonal expansion, self-renewal and *in vivo* multipotency (Maruyama et al., 2016). Axin2 is critical for suture patency during calvarial growth and morphogenesis, as Axin2 null mutants exhibit foreshortening of the frontonasal region resulting from synostosis of the metopic suture, caused by accelerated mineralization and ossification of the sutures through increased osteoprogenitor commitment. This suggests that Axin2 is required for the 'stemness' of suture stem cells (Yu et al., 2005).

Ephrin-B1 is the other B-ephrin of concern. To our knowledge, ephrin-B1 expression in the sutures and periosteum has never been characterized, though mutations in ephrin-B1 cause skeletal defects consistent with human craniofrontonasal syndrome. Proposed mechanisms underlying this syndrome include aberrant functional disomy of chromosome X, disruptive interaction between the functional and mutant ephrin-B1 protein (termed "metabolic interference") and compensation by Y-linked homologue (Twigg et al., 2004). However, cellular interference is a more recent concept that proposes divergent cellular behavior as a consequence of random inactivation of wild type and mutant *EFNB1*-carrying X chromosomes in heterozygous females with CFNS (Niethamer et al., 2020). That coronal suture synostosis is a typical manifestation of this syndrome implies the requirement of functional ephrin-B1 in coronal suture patency and maintenance during anterior cranial patterning and growth. Moreover, exencephaly in the late-stage embryo is a phenotypic consequence of the combined ablation of ephrin-

B1 and ephrin-B2 in the Axin2+ stem cells, suggesting that ephrin-B1 may possibly label the Axin2+ calvarial suture mesenchyme and periosteum. To identify these ephrin-B1-expressing cells in the cranial sutures and periosteum, we hypothesized whether these cells also express Axin2, a stem cell marker.

Using confocal microscopy, a significant number of green ephrin-B2-expressing cells colocalized with red Axin2+ cells in the e19.5 cranial sutures, mainly in coronal and lambdoid sutures and periosteum; however, in the metopic/sagittal sutures, ephrin-B2-expressing cells colocalized with Axin2 in the parietal bone fronts but not in the mesenchyme of these sutures. Interestingly, Axin2-expressing cells were faintly visible in the mesenchyme of these sutures. This expression patten may be attributable to the dual origin of the midline sutures as well as differences in the rates of stem cell division in these sutures i.e., the presence of slow cycling cells in the middle of the suture mesenchyme and fast cycling cells in the bone fronts contiguous with the lateral mesenchyme. Temporal and spatial patterns of expression may also influence the extent of colocalization of ephrin-B2 with Axin2. However, expression of ephrin-B2 (green cells) in the underlying brain was robust, with Axin2 sparsely colocalizing with ephrin-B2+ neurons. Some of the ephrin-B2+ chondrocytes in the occipital bone also coexpressed Axin2, suggesting that chondrocytic ephrin-B2 may have a role in postnatal endochondral bone growth of the basal cranium. Similarly, ephrin-B1-expressing cells almost mirrored the expression pattern of ephrin-B2 with respect to Axin2 in the cranial sutures and periosteum; however, in the metopic/sagittal suture, ephrin-B1 did not colocalize with the Axin2-expressing cells seen in the parietal bone fronts as well as

mesenchyme of these midline sutures. Again, the expression patten may be attributable to the dual origin of the midline sutures as well as differences in the rate of division of stem cells in these sutures. While the stem cells are fast cycling in the lateral portions of the suture mesenchyme where the bone fronts contiguously meet the mesenchyme, those in the central portion of the sutures are not. Temporal and spatial patterns of expression may also influence the extent of colocalization of ephrin-B1 with Axin2. Taken together, the overlap of ephrin-B1/B2 with Axin2 suggests that a subset of this stem cell population is subject to ephrin-B signaling in the osteogenic suture niche. This define ephrin-B1 and eprhin-B2 as features of the Axin2+ calvarial suture mesenchyme and periosteum in the developing embryo.

Another important stem-cell marker is Gli1 that identifies the major stem cell population and gives rise to all the bones and sutures of the craniofacial region including the duramater. They are highly injury responsive and contribute to bone regeneration in the calvaria and long bone (Shi et al., 2017; Zhao et al., 2015). In the adult calvaria, ephrin-B2 colocalized with the Gli1+ stem cells in the coronal, lambdoid and sagittal sutures including periosteum, with a significant number of ephrin-B2-expressing cells colocalizing with Gli1+ cells in the sagittal suture compared to the other two sutures. Furthermore, ablation of ephrin-B1/B2 in the Gli1+ sutures of the injured adult calvaria (4-6w old mice) did not significantly alter bone healing in both the knockout and control calvaria. This outcome may be attributed to the downregulation of ephrin-B2 in the adult calvarial sutures and periosteum; the same may be regarded for ephrin-B1 in the adult though expression studies by way of wholemount fluorescence imaging, histology and

confocal microscopy are warranted. Moreover, knocking out both these B-ephrins or ephrin-B2 alone (from e13.5 – e15.5) in the Gli1+ suture mesenchyme and periosteum of the developing calvaria did not impair cranial or skeletal bone growth when analyzed late gestation (e19.5) using x-ray, wholemount fluorescence microscopy (not shown) including bright field imaging. In the late stage Axin2+ embryonic calvaria, barring the mesenchyme of the midline sutures, the coronal and lambdoid sutures including the parietal bone fronts fluoresced red. By contrast, in the late-stage Gli1+ embryonic calvaria, only the lateral portions of the coronal sutures emitted the red fluorescence; none of the other sutures did, suggesting that stem cell populations other than Gli1 – such as Prx1 – may account for the growth and maintenance of the calvaria before birth, while in the postnatal period Gli1 may ramp up production to control bone growth through to adulthood. This may account for the absence of a calvarial phenotype in the Gli1 mutants. Because the combined ablation of ephrin-B1/B2 did not perturb cranial growth in the developing Gli1+ embryo, we did not generate Gli1cre/ ephrin-B1floxed allele embryos. Thus, further Gli1 conditional knockout studies were discontinued. Hence, colocalization analysis of ephrin-B2 with Gli1+ suture and periosteum in late-stage embryonic calvaria was not carried out. For similar reasons, colocalization of ephrin-B1 with Gli1 was not performed.

Next, we identified the requirement of ephrin-B signaling in the osteogenic niche of the developing calvaria. Knocking out ephrin-B2 alone in the Axin2+ suture mesenchyme and periosteum did not impair cranial growth when analyzed late gestation; 57% of the embryos were cre+ and the ratio of cre- to cre+ embryos was 2:3. All in all,

the lack of a cranial phenotype suggests possible functional redundancy between ephrin-B2 and ephrin-B1, with the latter compensating for ephrin-B2. Further analysis such as microCT and RT-PCR including Western blot is warranted to look for effects of ephrin-B2 ablation on ephrinB1 function in the skull cap/skeleton.

Because ephrin-B2 failed to perturb cranial bone growth following its ablation in the Axin2+ suture stem cells and periosteum, Axin2cre/EB1loxP embryos were generated to define the functional contribution of ephrin-B1 in calvarial growth and morphogenesis. Of the 81 late-stage embryos harvested, only 1 male embryo exhibited considerable facial dysmorphogenesis sparing the frontal bones and the rest of the cranial vault, with the remainder of the skeleton appearing unaffected. There were significant differences in height and weight between the ephrin-B1 knockout and control embryos, suggesting decreased skeletal bone mass as result of loss of ephrin-B1. MicroCT is warranted to further assess differences in skeletal bone volume and bone mineral density between the mutant and control littermates. Again, in those embryos where ephrin-B1 was knocked out, there was no observable phenotypic differences in the cranial vault, suggesting possible functional redundancy between ephrin-B1 and ephrin-B2 in Axin2 stem cell niche maintenance. Further analysis such as microCT and RT-PCR including Western blot is warranted to look for effects of ephrin-B1 ablation on ephrin-B2 function in the skull cap/skeleton.

However, the ablation of both ephrin-B1/B2 in the Axin2+ stem cells resulted in significant perturbation of calvarial bone growth resulting in exencephaly that was accompanied by varying degrees of facial dysmorphogenesis with foreshortening of the

cranial base and cervical spine disruption, while the remainder of skeleton appeared normal on x-ray. Forty percent of the double knockout embryos were cre+; of these, 15 embryos exhibited exencephaly at a 20% penetrance with females being more frequently affected than males in the ratio of ~3:1. Though there was a significant difference in weight, there was no significant difference in height between the knockout and control embryos. Though height was not greatly affected, the exencephalic embryos had significantly lower body weight, when compared to the non-knockouts. This could be due to an actual decrease in body weight without any effect on body length (height) in each of the affected pups. Interestingly, 59 non-phenotypic pups were also cre+ but did not exhibit exencephaly, suggesting a threshold for site-specific recombination in this proportion of knockouts, while in those with exencephaly the threshold for such recombination was achieved in the Axin2+ suture stem cell niche. Since knocking out both ephrin-B1/B2 adversely impairs ephrin-B signaling in the Axin2 osteogenic suture niche, it may be suggested that not only do these ephrins work in tandem in establishing and maintaining the osteogenic niche but also jointly influence stem cell behavior in terms of migration, proliferation, apoptosis and differentiation during calvarial growth and development. It may further be hypothesized that calvarial agenesis may be the direct result of failure of migration of stem cell precursors from the cranial neural crest in a caudal-to-rostral direction from e11.5 to e13.5 to form the frontal bone primordia (Jiang et al., 2019), including those from the paraxial mesoderm that form the parietal bones. This failure of migration may occur in conjunction with increased apoptosis

(Tonna et al., 2014) of mesenchymal precursors from both the neural crest and mesoderm.

The failure of the calvarial bones to form following ablation of ephrin-B1/B2 in the Axin2 suture stem cell population may be more attributable to a failure in stem cell migration than a decrease in cell proliferation, as Ki67+/Axin2+ cells were seen to aggregate at the edge of the posterior calvarial defect (Fig. 25A&B, C-F). However, the effect of this combined ephrin-B ablation on Axin2 stem cell apoptosis or differentiation to form the frontal and parietal bone primordia cannot be ruled out. Moreover, earlier serial induction-harvest timepoints are warranted i.e., induce pregnant female mice at e13.5 and harvest at e14.5, this being repeated through to e18.5/e19.5 and this would provide a more informative picture of the effect of combined ephrin-B ablation on Axin2 suture stem cell migration, proliferation, apoptosis and differentiation, rather than harvesting the embryos directly at e19.5 after the consecutive 3-day induction timepoint for calvarial phenotypic analysis. Hence, more experiments are warranted to confirm these.

Further, we wanted to analyze the effect of combined ablation of these ephrins on postnatal calvarial and skeletal bone growth, using the same prenatal induction protocol (e13.5 -e15.5). Initially, we allowed two induced pregnant dams to deliver their babies at full term, but on both the occasions we lost the dams to respiratory distress following extreme labor. To overcome this, we decided to surgically harvest the pups at e20.5 and surrogate them to another nursing/ lactating dam belonging to the same line. Unfortunately, the surrogated pups did not survive for more than a day either because the

induced pups were not functionally viable as they acquired a bluish tinge, or the nursing dam may have inherently rejected them. This procedure was repeated at least 8 times and all the occasions we failed to obtain a post-natal skeletal phenotype for analysis.

Stochastic events, possibly arising from epigenetic factors, gene pleiotropism or teratogenesis, occurred in three late-stage embryos – two that exhibited exencephaly following the combined ablation of ephrin-B1/B2 in the Axin2 stem cell population, and one embryo that exhibited anencephaly following ablation of only ephrin-B1 from this stem cell population. To that end, it is possible that one of the double knockout embryos exhibited exencephaly through Axin2cre-mediated excision of the cre-coding domain of the genomic DNA (called gene auto-excision or self-excision), as the embryo typed negative for the Axin2cre allele; in the other embryo, the phenotype was clearly a consequence of Axin2cre homozygosity, as the embryo typed positive for an extra copy of the Axin2cre knock-in allele. The anencephalic phenotype in the ephrin-B1 single knockout embryo may also be the result of gene auto-excision, because it typed negative for both Axin2cre and Ephrin-B1 'del' alleles, or the phenotype could be the consequence of drug-induced teratogenesis. For a craniofacial phenotype to manifest in the embryo, only one copy of the native Axin2 gene should be replaced by the Axin2cre knock-in allele i.e., the embryo must be heterozygous only: not wild type or homozygous. Therefore, these embryos were not included in the analysis. Further, in generating late-stage embryos for ephrin-B1/Axin2 colocalization analysis we obtained two embryos with exencephaly, but both the embryos typed positive for the EB1rtta and

cre alleles, implying that this phenotypic consequence may be the result of drug-induced teratogenesis and not cre-mediated gene auto excision.

To summarize, removing ephrin-B1/B2 in the Axin2 stem cell population dramatically impairs growth of the skull bones from both the cranial neural crest and paraxial mesoderm. There were no observable phenotypic differences in the Gli1 mutants, following the individual or combined ablation ephrin-B1 and/or ephrin-B2 in this stem cell population. This suggests that Gli1 and Axin2 are not identical stem cell populations in the developing embryo; further, ephrin-B signaling may be more important in the Axin2 than in the Gli1 suture stem cell population in the cranial vault. Thus, from evidence, ephrin-B1 and ephrin-B2 appear to function coordinately in establishing and maintaining the Axin2 osteogenic niche in the cranial sutures and periosteum of the developing embryo.

4.1 REFERENCES

1. Benson, M.D., and Opperman, L.A. (2011). Regulation of Calvarial Bone Growth by Molecules Involved in the Craniosynostoses.
2. Benson, M.D., Opperman, L.A., Westerlund, J., Fernandez, C.R., San Miguel, S., Henkemeyer, M., and Chenaux, G. (2012). Ephrin-B stimulation of calvarial bone formation. Dev Dyn *241*, 1901-1910.
3. Hirai, H., Maru, Y., Hagiwara, K., Nishida, J., and Takaku, F. (1987). A novel putative tyrosine kinase receptor encoded by the eph gene. Science *238*, 1717-1720.

4. Jiang, Y., Zhang, S., Mao, C., Lai, Y., Wu, D., Zhao, H., Liao, C., and Chen, W. (2019). Defining a critical period in calvarial development for Hedgehog pathway antagonist-induced frontal bone dysplasia in mice. Int J Oral Sci *11*, 3.

5. Maruyama, T., Jeong, J., Sheu, T.J., and Hsu, W. (2016). Stem cells of the suture mesenchyme in craniofacial bone development, repair and regeneration. Nat Commun *7*, 10526.

6. Niethamer, T.K., Teng, T., Franco, M., Du, Y.X., Percival, C.J., and Bush, J.O. (2020). Aberrant cell segregation in the craniofacial primordium and the emergence of facial dysmorphology in craniofrontonasal syndrome. PLoS Genet *16*, e1008300.

7. Rundle, C.H., Xing, W., Lau, K.-H.W., and Mohan, S. (2016). Bidirectional ephrin signaling in bone. Osteoporosis and Sarcopenia *2*, 65-76.

8. Shi, Y., He, G., Lee, W.-C., McKenzie, J.A., Silva, M.J., and Long, F. (2017). Gli1 identifies osteogenic progenitors for bone formation and fracture repair. Nature Communications *8*, 2043.

9. Tonna, S., Takyar, F.M., Vrahnas, C., Crimeen-Irwin, B., Ho, P.W., Poulton, I.J., Brennan, H.J., McGregor, N.E., Allan, E.H., Nguyen, H.*, et al.* (2014). Ephrin-B2 signaling in osteoblasts promotes bone mineralization by preventing apoptosis. Faseb j *28*, 4482-4496.

10. Twigg, S.R., Kan, R., Babbs, C., Bochukova, E.G., Robertson, S.P., Wall, S.A., Morriss-Kay, G.M., and Wilkie, A.O. (2004). Mutations of ephrin-B1 (EFNB1),

a marker of tissue boundary formation, cause craniofrontonasal syndrome. Proc Natl Acad Sci U S A *101*, 8652-8657.

11. Williams, S.A., Chastek, B., Sundquist, K., Barrera-Sierra, S., Leader, D., Jr., Weiss, R.J., Wang, Y., and Curtis, J.R. (2020). Economic burden of osteoporotic fractures in US managed care enrollees. Am J Manag Care *26*, e142-e149.

12. Xing, W., Kim, J., Wergedal, J., Chen, S.T., and Mohan, S. (2010). Ephrin B1 regulates bone marrow stromal cell differentiation and bone formation by influencing TAZ transactivation via complex formation with NHERF1. Mol Cell Biol *30*, 711-721.

13. Yu, H.M., Jerchow, B., Sheu, T.J., Liu, B., Costantini, F., Puzas, J.E., Birchmeier, W., and Hsu, W. (2005). The role of Axin2 in calvarial morphogenesis and craniosynostosis. Development *132*, 1995-2005.

14. Zhao, C., Irie, N., Takada, Y., Shimoda, K., Miyamoto, T., Nishiwaki, T., Suda, T., and Matsuo, K. (2006). Bidirectional ephrin-B2-EphB4 signaling controls bone homeostasis. Cell Metab *4*, 111-121.

15. Zhao, H., Feng, J., Ho, T.V., Grimes, W., Urata, M., and Chai, Y. (2015). The suture provides a niche for mesenchymal stem cells of craniofacial bones. Nat Cell Biol *17*, 386-396.

CHAPTER V

CONCLUSIONS

In summary, Axin2 stem cells are one of two major stem cell populations that reside in the calvarial suture midline and contribute to bone regeneration in a cell autonomous fashion. Both ephrin-B1 and ephrin-B2 colocalize with the Axin2 suture stem cell population in the coronal and lambdoid sutures of the developing calvaria. In the midline sutures, however, both ephrin-B1 and ephrin-B2 do not colocalize with the Axin2 stem cells, though ephrin-B2 did overlap with these stem cells in the parietal bone fronts flanking the midline suture mesenchyme. This varied expression patten may be attributable to the dual origin of the midline sutures as well as to differences in the rates of stem cell division i.e., the presence of slow cycling versus fast cycling cells in different portions of these sutures. Temporal and spatial patterns of expression may also influence the extent of colocalization of ephrin-B1/B2 with Axin2 in the midline sutures.

In defining the functional requirement for ephrin-B signaling in the Axin2 osteogenic suture niche of the developing calvaria, the individual ablations of ephrin-B1 or ephrin-B2 did not impair Axin2 osteoblastic stem cell function in the suture niche. This suggests possible functional redundancy among the two B-ephrins in regulating the developing niche. However, ablating ephrin-B1/B2 in the Axin2 stem cell population dramatically impaired growth of the skull bones from both the cranial neural crest and paraxial mesoderm, resulting in exencephaly that may or may not be associated with a range of facial dysmorphogenic phenotypes. But analysis at e19.5 would only give the

‘end point’ phenotype when much of stem cell function dysregulation – in terms of migration, proliferation, differentiation and apoptosis – would have already occurred. On the other hand, serial induction-harvest timepoints would catch the ‘live picture’ as and when and the extent to which stem cell function dysregulation occurs. Additionally, mutations in ephrin-B1 result in human CFNS, the manifestations of which range from mild to severe without loss of functional viability. However, the combined ablation of ephrin-B1/B2 results in dramatic phenotypic consequences with loss of functional viability.

Similarly, Gli1 identifies the major skeletal stem cell population and is central to calvarial bone growth and homeostasis. They are highly injury responsive and contribute to skeletal/calvarial bone regeneration. There were no observable phenotypic differences in the Gli1+ embryonic calvaria, following individual or combined ablation of ephrin-B1 and/or ephrin-B2 in this stem cell population. This may be attributed to the expression pattern of Gli1+ stem cells which is quite distinct from that of Axin2+ stem cells in the embryonic sutures. Failure to obtain a phenotype in the Gli1 mutants may be also ascribed to the presence of stem cell populations other than Gli1, such as Prx1, as well as to temporal and spatial patterns of expression of these B-ephrins in relation to Gli1 in the embryonic sutures. These therefore suggest that Gli1 and Axin2 are not identical suture stem cell populations of the calvaria in the developing embryo.

Taken together, ephrin-B signaling may be more important in the Axin2 than in the Gli1 stem cell population in the cranial vault. Thus, from evidence, ephrin-B1 and

ephrin-B2 appear to function coordinately in establishing and maintaining the Axin2 osteogenic niche in the cranial sutures and periosteum of the developing embryo.